THE EFFECT OF SMALL ADDITIONS OF RUTHENIUM ON THE PITTING CORROSION RESISTANCE OF LDX2101 DUPLEX STAINLESS STEEL

Shem Chiliungu Kandodo Banda

A Dissertation submitted to the Faculty of Engineering and the Built Environment, University of the Witwatersrand, in fulfilment of the requirement of the degree of Master of Science in Engineering.

Johannesburg 2013

DECLARATION

I declare that this dissertation is my own, unaided work. It is being submitted for the Degree of Masters of Science (MSc) in Engineering, in the Faculty of Engineering, University of the Witwatersrand, Johannesburg. It has not been submitted before for any degree or examination in any other university.

Shem Chiliungu Kandodo Banda

22 MAY 2013

ABSTRACT

This dissertation is a study of the effect of small additions of ruthenium on pitting corrosion resistance of LDX2101 duplex stainless steel. Four stainless steel alloys with incremental ruthenium (wt %) as per Table I were produced from pieces cut from commercial LDX2101 duplex stainless steel plate with the manufacturer's composition of 0.03C, 0.22N, 21.5Cr, 1.5Ni, 0.3Mo and 5.0Mn plus, pressed ruthenium powder with purity of 99.8%. After solution annealing the samples, the actual chemical composition was analysed using XRF analysis and then, ASTM A923 (01.03) Test method A – Sodium Hydroxide etch test for classification of etch structures of duplex stainless steel was used to analyse their microstructure.

Table I: Chemical composition (wt %) of alloys which were produced.

Alloy Designation	Targeted Composition (wt %)
A	*0.03C, 0.22N*, 22.26Cr, 1.58Ni, 0.25Mo and 4.99Mn + 0.13Ru
B	*0.03C, 0.22N*, 22.46Cr, 1.50Ni, 0.29Mo and 5.14Mn + 0.20Ru
C	*0.03C, 0.22N*, 22.31Cr, 1.60Ni, 0.26Mo and 4.84Mn + 0.31Ru
D	*0.03C, 0.22N*, 20.10Cr, 1.37Ni, 0.30Mo and 4.32Mn + 0.66Ru

NOTE: C and N shown in italics were not measured.

Corrosion potentials and pitting potentials of these samples were evaluated using a potentiodynamic polarisation technique and the results were compared to corrosion potentials and pitting potentials of control alloys: LDX2101, 304L and 904L. The tests for both produced and control alloys were carried out in naturally aerated 3.56% sodium chloride (NaCl) aqueous solution at 25^{o}C±2^{o}C. The results indicated that small additions of ruthenium slightly improved the corrosion potential of the resulting alloys. However, there was a significant improvement on the pitting potential of the resulting alloys compared to LDX2101 and 304L stainless steels. Exposed to the same experimental environment, 904L stainless steel did not experience pitting corrosion. Potentiodynamic polarisation evaluation of LDX2101 with 0.66%Ru samples in de-aerated 3.56% NaCl showed a decrease in both pitting and corrosion potentials with the decrease in oxygen content in the NaCl aqueous solution. Microstructural analysis results indicated that ruthenium addition has no detrimental

effect to the microstructure of the resulting alloys. However, alloys containing ruthenium were not commercially viable as the pitting corrosion resistance benefit ruthenium brought did not offset the cost of adding the ruthenium to LDX2101 stainless steel.

ACKNOWLEDGEMENTS

First, I would like to thank the Lord God Almighty for the grace He afforded me to complete these studies. You have been my source of encouragement and hope.

Secondly my appreciation goes to my Supervisor, Mr. Josias van der Merwe. Without his guidance, advice and patience this day would not have arrived.

Thirdly, I would like to thank Edson Muhuma (MINTEK) for sharing his technical knowledge on melting and Brayner (WITS) for sharing his experience on preparing and examining of samples.

The following very important people also deserve my appreciation: my wife Nandi Nyingi Ngosi-Banda, your love, understanding and forbearing cannot be matched, especially when it was necessary to work long hours and my daughter Nzeru-Bohlale Banda born, at the climax of my studies.

Last but not least, my appreciation goes to MSA Africa for sponsoring my studies, The School of Chemical and Metallurgical Engineering at the University of the Witwatersrand for allowing me to conduct my studies there and providing all necessary equipment and materials and, MINTEK for allowing me to use their equipment.

Table of contents

LIST OF FIGURES

LIST OF TABLES

1. INTRODUCTION

1.1 BACKGROUND AND MOTIVATION

Failure of stainless steel structures or components due to corrosion is still prevailing in various industries. Such failures have both economic implications and significant safety issues (Jones 1992, p. 1-4). Stainless steel manufacturer, Outokumpu Stainless AB, (OUTOKUMPU 2009) defined corrosion as the physiochemical interaction between a metal and its environment that results in changes in the properties of the metal, and which may lead to significant impairment of the function of the metal, the environment, or technical system, of which these form a part. Corrosion does not refer to deterioration caused by physical causes (Uhlig 1971). Since stainless steels are not fundamentally noble materials in the same way as gold or platinum, their corrosion resistance rely mainly on surface passivity. Thus, the resistance to corrosion of stainless steels results from the presence of a thin oxide or hydrate film on the surface of the metal, which is considered insoluble, nonporous and self-healing (Lyman 1984). If the film is broken, it will repair itself when re-exposed to an oxidising agent. However, under certain environments, permanent breakdown of the film can take place i.e. the passive layer cannot be rebuilt hence, corrosion occurs on the unprotected surface (OUTOKUMPU 2004). Depending on the environment or media, the corrosion of stainless steels can take any of the following forms: general corrosion, pitting corrosion, crevice corrosion, stress corrosion cracking, sulphide stress corrosion cracking, intergranular corrosion, galvanic corrosion and contact corrosion (Jones 1992; Kadry 2008).

This research focuses on pitting corrosion. The research was triggered by the pitting corrosion on a mining safety equipment enclosure/casing made from type 316 stainless steel shown in Figure 1.1. As noted by Outokumpu Stainless AB (OUTOKUMPU 2009, p. I:3) in many practical situations, corrosion failure of stainless steel often occurs as a result of a localized attack rather than uniform corrosion. Equipment fails because of perforation with only a small percentage weight loss of the entire structure (Fontana 1986, p. 63).

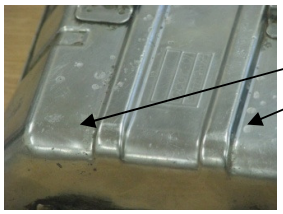

Figure 1.1 Pits developing on casing/enclosure for mine application safety equipment.

Different measures have been taken to combat pitting corrosion in stainless steels, which involve either decreasing the aggressiveness of the environment, or increasing the pitting corrosion resistance of materials. Decreasing the aggressiveness of the environment is not always practical in most applications and a significant number of studies have been performed to increase the pitting corrosion resistance of materials. Such efforts includes: evaluating the effect of the surface condition, the effect of the microstructure of the stainless steels and the effect of the composition of stainless steels (Sedriks 1979, p. 70-86). In order to quantify the influence of alloying elements the Pitting Resistance Equivalent number, PREN, was developed for stainless steels. This uses the concentrations of chromium, molybdenum and nitrogen as the beneficial elements to increase the pitting corrosion resistance of stainless steels. The PRE number is calculated using the equation (1) below (OUTOKUMPU 2004, p. I:96):

$$PREN = \%Cr + 3.3\%Mo + 16\%N \quad \ldots\ldots (1)$$

A higher PRE number represents a higher pitting corrosion resistance. The Table 1.1 gives an indication of PRE numbers for various stainless steels.

Table 1.1 Chemical composition and PRE number of some stainless steels (OUTOKUMPU 2009, p. I:48).

Steel Grade	Chemical Composition, %	PRE Number $= \%Cr + 3.3\%Mo + 16\%N$
LDX2101	0.03C, 0.22N, 21Cr, 1.5Ni, 0.3Mo, 5Mn	26
4404 (304L)	0.02C, 17Cr, 11Ni, 2.1Mo	24
2205 (904L)	0.02C, 0.17N, 22Cr, 5.7Ni, 3.1Mo	35

From Table 1.1, LDX2101 having a higher PER number than 4404 (304L) and should have a higher pitting corrosion resistance. However, practically as shown from experimental data in Figure 1.2, 4404 has a higher pitting corrosion resistance than LDX2101.

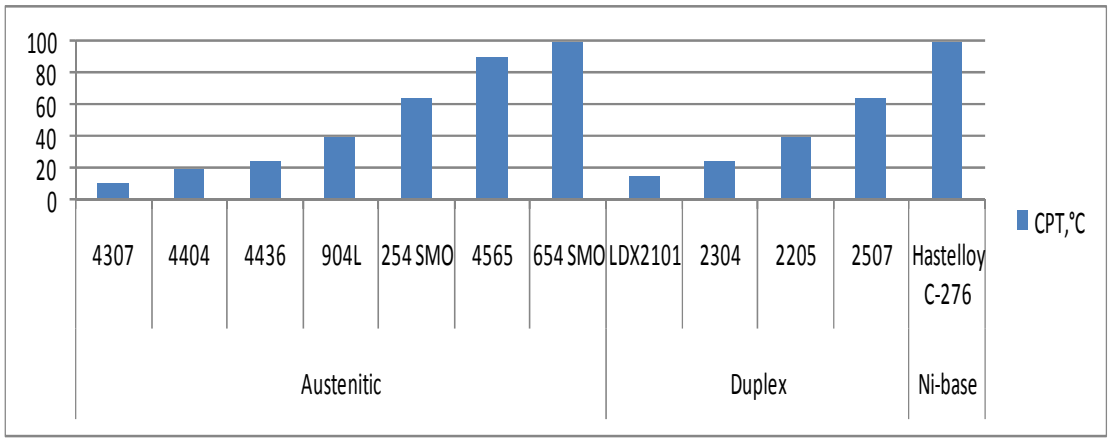

Figure 1.2 Typical critical pitting corrosion temperatures (CPT) determined according to ASTM G 48 Method E (OUTOKUMPU 2009).

This shows that the PRE number equation (equation 1) has limitations as it only considers the effect of molybdenum, nitrogen and chromium on the pitting resistance of stainless steel, and does not take the effect of other alloying elements into consideration which can have a significant effect (Sedriks 1979, p. 72).

One such alloying element is ruthenium (Ru), with atomic number 44, a rare transition metal of the platinum group metals. Ruthenium is associated with platinum ores and forms as a by-product during the extraction of platinum. It is used as a catalyst in some platinum alloys (Streicher 1977, p. 51-55). Ruthenium is readily available in South Africa, as the country meets as much as 95% of global demand (Wolff 1999).

The properties of duplex stainless steels alloyed with ruthenium have been studied previously by others and include the following:

a) Effects of minor additions of ruthenium on the passivation of duplex stainless-steel corrosion in concentrated hydrochloric acid solutions (El-Sayed et al. 2009).
b) Corrosion behaviour of duplex stainless steels containing minor ruthenium additions in reducing acid media (Potgieter et al. 1996).

These investigations and others have yielded positive results for the inhibition of corrosion of stainless steels by alloying with ruthenium.

1.2 PROJECT DESCRIPTION

Various studies on adding platinum group metals (PGM) to stainless steels by different groups and individuals resulted in producing spontaneous passivated alloys with consequent decreased corrosion rate (Higginson 1989; Mcgill 1990; Streicher 1977, p. 51-55; Wolff 1999). While there is agreement in literature that small additions of PGMs to stainless steels brings about cathodic modification which improves general corrosion in reducing acidic environments, pitting corrosion evaluation of such alloys has not produced encouraging results (Mcgill 1990; Higginson 1989). Mcgill (1990) reviewing various studies, concluded that only ruthenium, iridium and osmium can be added to stainless steel alloys without adversely affecting their pitting corrosion resistance. However, a recent study by El-Sayed et al. (2009), found that small additions of ruthenium to a duplex stainless steel did not only improved the alloy's passivation, but also shifted the corrosion and pitting potentials to higher noble values. Another factor that hindered researches on cathodic modification is cost. Higginson argued that 'even 0.2% weight of the alloy, PGMs would account for the major component of material cost of the cathodically modified alloy' rendering the alloy commercially unviable (Higginson 1989). Higginson even recommended future studies to aim at alloys containing less than 0.2% alloy weight of PGMs (Higginson 1989). However, El-Sayed et al. suggested a prospect of commercially viable stainless steel alloyed with ruthenium, since ruthenium is the least expensive of the PGMs (El-Sayed et al. 2009). Another point of consideration is the readily availability of PGMs in South Africa, as the country meets as much as 95% of global demand of PGMs (Wolff 1999). Therefore, contextually, it remains important to focus research on stainless steels alloyed with PGMs. It should also be noted that LDX2101 is a new low cost stainless steel grade developed by Outokumpu Stainless and less work has been done in this regard (OUTOKUMPU 2004, p. I:96 – I:97). It is therefore the objective of this research to evaluate the effect of small additions of ruthenium on pitting corrosion resistance of LDX2101 duplex stainless steel alloyed with up to 0.6%wt Ru.

1.3 OTHER OBJECTIVES

Other objectives of this research includes: (a) compare the pitting corrosion resistance of LDX2101 stainless steel alloyed with ruthenium to pitting corrosion resistance of commercial grade 304L and grade 904L; (b) evaluate the general corrosion of LDX2101 stainless steel alloyed with ruthenium and compare the results with the general corrosion of commercial grades 304L and 904L; (c) evaluate the effect of ruthenium addition to LDX2101 stainless steel on the microstructure of the resulting alloys; (d) evaluate the effect of oxygen on pitting corrosion resistance of LDX2010 stainless steel alloyed with ruthenium; and (e) evaluate the commercial viability of LDX2101 stainless steel alloyed with ruthenium up to 0.6%wt Ru.

1.4 METHODOLOGY

Potentiodynamic polarisation technique will be adopted for this research work in order to evaluate both general and pitting corrosion. Scanning electron microscopy will be adopted for microstructure evaluation and any surface imaging requirements. X-ray Fluorescence Spectroscopy (XRF) technique will be used to verify the composition of the alloys.

1.5 HYPOTHESIS

Since investigations on other duplex stainless steels alloyed with a small percentage of ruthenium yielded positive results for the inhibition of pitting corrosion, it is therefore much anticipated that alloying LDX2101 duplex stainless steel with a small percentage of ruthenium leads to significant pitting corrosion reduction.

1.6 RESEARCH QUESTIONS

This research work will answer the following questions:

(a) Will the small additions of ruthenium to LDX2101 stainless steel have beneficial effects on general and pitting corrosion of the resulting alloy?

(b) Will the small addictions of ruthenium to LDX2101 stainless steel have detrimental effect to the microstructure of the resulting alloy?

(c) How will the resulting alloys from alloying LDX2101 stainless steel with ruthenium perform in oxygen deprived environment?

(d) Even if the results in (a) to (c) are positive, will the resulting alloy be commercially viable?

1.7 EXPECTED CONTRIBUTION TO KNOWLEDGE

The research study on the effect of small additions of ruthenium on the pitting corrosion resistance of LDX2101 duplex stainless steel is expected to provide information on:

- Comparative general and pitting corrosion behaviour of stainless steels LDX2101, 304L and 904L to alloys resulting from alloying LDX2101 stainless steel with ruthenium up to 0.6%wt Ru.
- Performance of LDX2101 stainless steel alloyed with ruthenium up to 0.6%wt Ru in oxygen deprived environment.
- The commercial viability of LDX2101 stainless steel alloyed with ruthenium up to 0.6%wt Ru.

2. LITERATURE REVIEW

As pointed out in the project description, this research project is looking at the effect of small ruthenium additions on the pitting corrosion resistance of duplex stainless steel LDX2101. This literature survey provides information on: (a) the background history of iron and steel development. The brief history shows that most inventions were chance discoveries hence, emphasizing the importance of open minded in research work to be able to observe any trends in experiments; (b) the general properties of stainless steels based on microstructure, with more details on stainless steel grades 304L, 904L and LDX2101 which forms the reference point/control alloys of this research work; (c) corrosion of stainless steels, with more details provided on pitting corrosion and internal and external factors affecting pitting; (d) passivity and its influence on pitting corrosion; (e) the effect of alloying elements (chromium, molybdenum, nickel, manganese, nitrogen and copper) which are found in the control alloys (304L, 316L, 904L and 2101) on pitting corrosion of steels. The effect of alloying stainless steels with platinum group metals on pitting corrosion of such alloys has also been discussed with more details provided on stainless steels alloyed with ruthenium; (f) methods available to determine an alloy's susceptibility to pitting corrosion and their limitations; and (g) methods available to analyse an alloy's microstructure and composition of oxide films formed during corrosion

2.1 IRON AND STEEL BACKGROUND

Since the beginning of smelting iron in the early centres of civilization (Egypt, Chaldea, Babylonia, Assyria and China) which dates back as far as 4000BC (Fisher 1963), man has put considerable effort to improve iron properties to make iron suitable for different applications. The earliest improvement was the production of steel. Historians and archaeologists trace back the origin of relatively high quality steel to India, referred to as wootz steel (Fisher 1963; McGannon 1971). The advancement in smelting skills such as the invention of the Bessemer process, the open hearth process (Rollason 1973) in the middle of the nineteenth century eased and increased the production of steel and hence its applications. This, in turn, triggered further investigations aimed at improving the properties of steel.

Amongst others, these investigation lead to the development of steels grouped in certain categories as discussed in the following sections.

2.1.1 Tungsten Steel

High speed machine tools require hard end steels with a sharp cutting edge that will not blunt quickly. This resulted in alloying steel with titanium, chromium and tungsten. Tungsten alloyed steel succeeded considerably in this application, and it is credited to an Austrian chemist, Franz Koller who inverted it in 1855 (Fisher 1963). Present standard of which, contain 70% to 80% of tungsten and a maximum of 0.6% carbon (McGannon 1971, p. 258).

2.1.2 Manganese Steel

Machinery which must withstand severe knocks and abrasive action like power shovels, bulldozers, dipper dredges, ore crushers and similar earth-moving and mining equipment have their jaws made of manganese steel. In 1882 Hadfield discovered that whereas 1% to 1.5% manganese made a good grade of ordinary steel and 3% to 7% made the steel too brittle to be of any use, 10% to 15% manganese steel possesses the peculiar property of acquiring hardness under repeated impact. Robert made this discovery while experimenting with the objective of producing a hard steel for tramway wheels, and also as a substitute for emery in grinding wheels (Fisher 1963).

2.1.3 Silicon Steel

In the same search for a hard material to substitute for emery grinding wheels, in 1886 Robert Hadfield invented a low carbon steel containing from about 1.5% to 5% silicon which found its use in the cores of transformers and generators of the electricity industry (Fisher 1963).

2.1.4 Steel for Military Application

Between 1877 and 1886, a Frenchman, A. Brustlein advanced the use of chromium steel for armaments. In 1885, steels alloyed with chromium and nickel, were used for guns, armour and projectiles in Europe with nickel favoured in guns of heavy calibre (Fisher 1963).

A good observation is that most of these inventions were chance discoveries hence, emphasizing the importance of open minded in research work to be able to observe any trends in experiments. Streicher (American Society for Metals 1979) observed the following three requirements which must be met if a chance observation is to lead to the actual use of

the new material of construction, a new phenomenon, or a new substance: a) the alertness of mind to recognize a new phenomenon or effect when it occurs as an unexpected result; b) the concept or idea for applying this observation for the solution of at least one concrete problem and; c) the will, opportunity, and skill to apply the new solution in practice within the available economic framework or the ability and opportunity to find others who will do this.

2.2 STAINLESS STEELS

Stainless steel, as the name implies, are more resistant to rusting and staining than are plain carbon and low alloy steels (McGannon 1971, p. 1163). Stainless steel was discovered more or less contemporaneously around 1913 by researchers in Britain and Germany from an early research, which was originally intended to enable the development of gun barrels for the military powers (OUTOKUMPU 2008). Stainless steels are ferrous alloys which contain a minimum of 12% chromium for corrosion and oxidation resistance (Sheir 1976). In stainless steel development studies, it is important to understand the microstructure and main alloying composition of the stainless steels as these have a direct influence on pitting corrosion resistance of the stainless steels. Based on chemical composition and response to heat treatment, hence the microstructure, there are four major types of stainless steels namely: martensitic, austenic, ferritic and austenitic-ferritic (duplex) stainless steels (OUTOKUMPU 2008). Figure 2.1 (a) shows the phase transformations that are possible at certain temperatures and Fe-Cr compositions for the Fe-Cr system without considering the influence of other alloying elements like nickel and molybdenum (Kovach 2011, p. 11). This helps to illustrate the effect of temperature on regions of phase stability for the ferritic (γ), austenitic (α) and duplex ($\gamma + \alpha$) stainless steel alloys. Hence, further illustrating the effect of heat processes like welding, annealing and including high temperature applications of stainless steels, will have on these phases. Figure 2.1 (b) shows the phase transformations that are possible at certain temperatures and 60% iron, illustrating the effect of small changes in nickel and chromium on regions of phase stability for the ferritic (γ), austenitic (α) and duplex ($\gamma + \alpha$) stainless steel alloys for the Fe-Cr-Ni system (Kovach 2011, p. 11). Hence, other alloying elements like molybdenum and ruthenium will also have an effect of altering these phases.

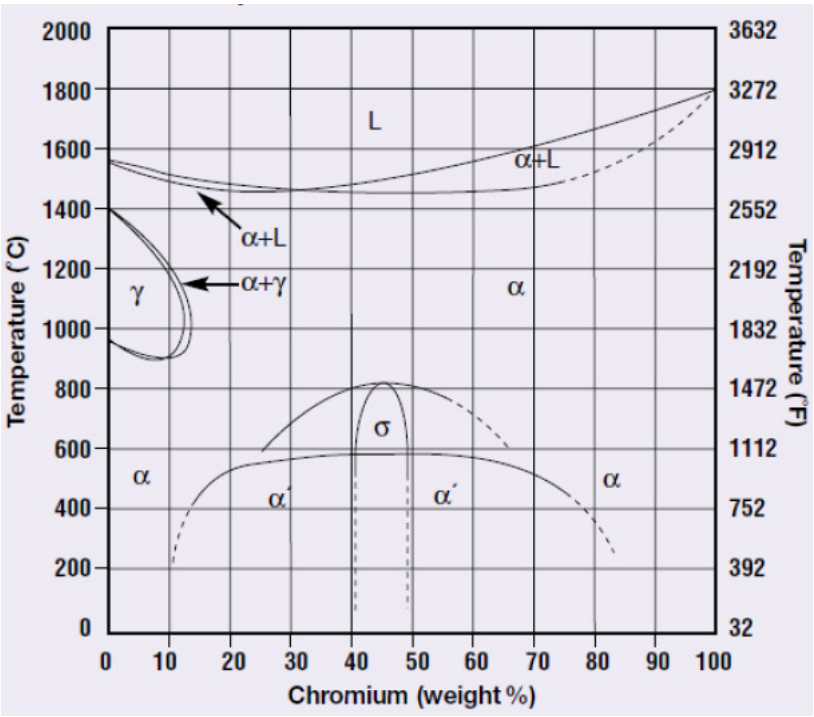

(a) Fe-Cr phase diagram

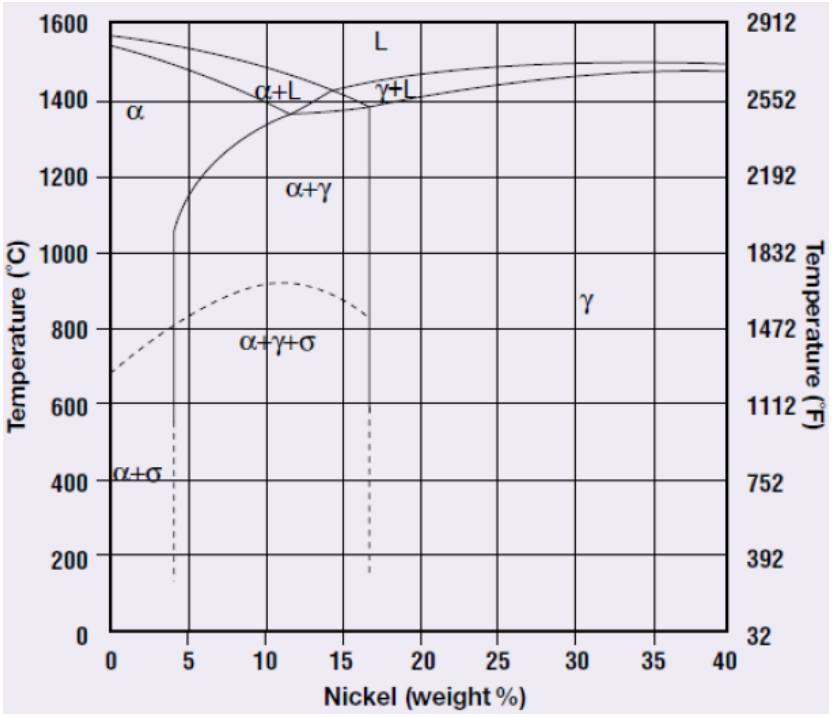

(b) Fe-Cr-Ni phase diagram at 60% Fe

Figure 2.1 Fe-Cr and Fe-Cr-Ni phase diagrams (Kovach 2011, p. 11).

2.2.1 Austenitic Stainless Steels

Austenite or gamma phase (γ) in Figure 2.1, exists between 910°C and 1400°C where iron is face-centred cubic (fcc) (Peckner & Bernstein 1977). Austenitic stainless steels are therefore produced when this structure (fcc) is maintained to lower temperatures hence rendering them paramagnetic properties. This type of stainless steel is dominant in the market. Examples include grade 302, 303, 304 and 316 stainless steels. Austenitic steels are characterized by their high content of austenite-formers, especially nickel. They are also alloyed with chromium, molybdenum and sometimes with copper, titanium, niobium and nitrogen. Alloying with nitrogen raises the yield strength of the steels (OUTOKUMPU 2008). Typical applications of austenitic stainless steels include: chemical industry and the food processing industry. The molybdenum-free austenite stainless steels have very good high-temperature properties, and are therefore used in furnaces and heat exchangers (OUTOKUMPU 2008). Their good impact strength at low temperatures is often exploited in apparatus such as vessels for cryogenic liquids. Austenitic steels cannot be hardened by heat treatment. They are normally quench-annealed, which means that they are soft and highly formable. Cold working increases their hardness and strength (OUTOKUMPU 2008). Figure 2.2 is a microstructure image of an austenitic stainless steel produced by Outokumpu.

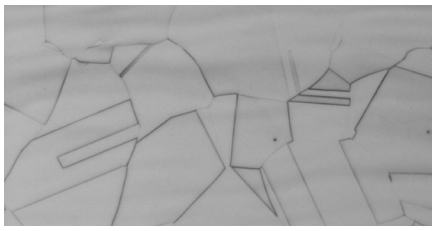

Figure 2.2 Microstructure image of an austenitic stainless steel (OUTOKUMPU 2008).

Mechanical/physical properties and typical chemical compositions of the following specific austenitic steel grades 304L, and 904L, which are control alloys in this research, will be discussed in detail in section 2.2.5.

2.2.2 Ferritic Stainless Steels

Ferritic stainless steels, consisting of Cr-Fe alpha (α) in Figure 2.1, are in principle ferritic at room temperature. They have a body-centred cubic (bcc) structure (Peckner &

Bernstein 1977). This is achieved by a low content of austenite forming elements, mainly nickel, and a high content of ferrite forming elements, mainly chromium. Typical applications of ferritic stainless steels include: application in household utensils, catering equipment and other purposes where corrosion conditions are not particularly demanding. Ferritic stainless steels with high chromium content, such as 4762 with 24% chromium, are used at high temperatures where their resistance to sulphurous flue gages is an advantage. Ferritic steels, such as 4521 with extremely low carbon and nitrogen contents, find greatest use where there is a risk of stress-corrosion cracking (OUTOKUMPU 2008). Figure 2.3 shows the microstructure of a ferritic stainless steel produced by Outokumpu.

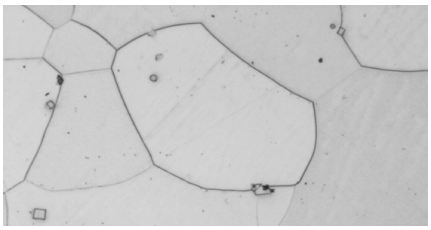

Figure 2.3 Microstructure image of ferritic stainless steel (OUTOKUMPU 2008).

2.2.3 Martensitic Stainless Steels

Martensitic stainless steels are primarily chromium steels which can be hardened by heat treatment (Lyman 1984). They mostly contain 12% to 13% chromium and are both strong and hard with moderate corrosion resistance. Figure 2.4 is a microstructure image of a martensitic stainless steel produced by Outokumpu.

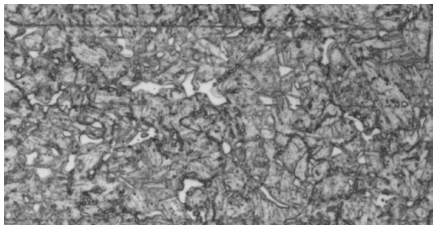

Figure 2.4 Microstructure image of a martensitic stainless steel (OUTOKUMPU 2008).

Brearly was the first to see clearly the commercial possibility of the 12% - 13% Cr martensitic steel introduced to the public in the form of stainless cutlery over the period 1912-1915 (Monypenny 1951; Sheir 1976). Martensitic steels have the highest strength, but

also the lowest corrosion resistance of the stainless steels. Martensitic steels with high carbon contents are used for tool steels (OUTOKUMPU 2008). Due to their high strength in combination with some corrosion resistance, martensitic steels are suitable for applications where the material is subjected to both corrosion and wear like in hydroelectric turbines.

2.2.4 Austenitic-Ferritic Stainless Steels

Commonly known as duplex stainless steels, this group of steels is intermediate in terms of structure and alloy content between ferritic and austenitic stainless steels (Alvarez-Armas 2007). Duplex stainless steels are popularly increasing in their application due to their excellent combined ferritic and austenic steels properties (Alvarez-Armas 2007; Zhang et al. 2009). Factors which have advanced the development and use of duplex alloys include: (a) high demand of nickel as an alloying element that pushed up the price of austenitic steels; (b) increasing activity in the offshore oil industry, an aggressive environment which demands stainless steels with combined good strength and corrosion properties; (c) the great improvement in steel production techniques with the introduction of the vacuum and argon oxygen decarburization practices and; (d) the introduction of continuous casting in stainless steel production which has contributed to lower production costs and higher quality (Alvarez-Armas 2007). The main characteristic that differentiates austenitic-ferritic stainless steels from austenitic and ferritic stainless steels is that they have a higher yield strength and tensile strength. They are therefore often used in dynamically stressed machine parts, e.g. suction rolls for paper machines. As already pointed out, new areas of application are within the oil, gas and petrochemical sector, seawater-bearing systems and the offshore industry (OUTOKUMPU 2008). Figure 2.5 is a microstructure image of a duplex stainless steel produced by Outokumpu.

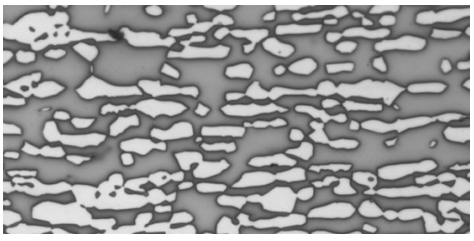

Figure 2.5 Duplex (austenitic-ferritic) well balanced two-phase structure with ferrite content between 30-50% (OUTOKUMPU 2008).

Mechanical/physical properties and chemical composition of lean duplex stainless steel LDX2101 which is also control alloys in this research will be discussed in detail in section 2.2.5.

2.2.5 Control Alloys

Stainless steel grades 304L, 904L and LDX2101 forms the reference point/control alloys of this research work. Details of their chemical composition, mechanical/physical properties and their suggested applications which have a bearing on pitting corrosion have been discussed in sections 2.2.5.1, 2.2.5.2 and 2.2.5.3. The critical pitting temperature and the relative pitting corrosion resistance of all the control alloys are shown in Figure 1.2.

2.2.5.1 304L Stainless Steel

The 304L stainless steel is a low carbon version of the austenitic 304 stainless steel grade and is normally used in heavy gauge components for improved weldability. Type 304 stainless steel is the most versatile and widely used stainless steel. It is still sometimes referred to by its old name 18/8, which is derived from the nominal composition of type 304 stainless steel being 18% chromium and 8% nickel (OUTOKUMPU 2008). Type 304 stainless steel is an austenitic grade that can be severely deep drawn. This property has resulted in 304 stainless steel being the dominant grade used in applications like sinks and saucepans. Tables 2.1 and 2.2 show the standard chemical composition and mechanical properties for 304L stainless steel respectively.

Table 2.1 Standard chemical composition limits for stainless steel grade 304L (OUTOKUMPU 2008).

Chemistry	**C**	**Si**	**Mn**	**P**	**S**	**Cr**	**Ni**	**N**
Min						17.5	8.0	
Max	0.030	1.0	2.0	0.045	0.030	21.0	10.0	0.11
Target	0.020					18.3	9.2	0.06

Table 2.2 Standard mechanical and physical properties of stainless steel grade 304L (OUTOKUMPU 2008).

Property	**Value**
Density	7.9 kg/dm^3
Modulus of Elasticity	200 GPa
Ultimate Tensile Strength (UTS)	600 MPa

2.2.5.2 904L Stainless Steel

904L stainless steel is a high-alloyed austenitic grade with a significant resistance to uniform corrosion and to pitting and crevice corrosion. It has a high resistance to stress corrosion cracking and was originally developed to resist uniform corrosion in dilute sulphuric acid (OUTOKUMPU 2008). This grade has also good formability and weldability properties. Tables 2.3 and 2.4 show the standard chemical composition and mechanical properties for 904L stainless steel respectively.

Table 2.3 Standard chemical composition limits for stainless steel grade 904L (OUTOKUMPU 2008).

Chemistry	**C**	**Si**	**Mn**	**P**	**S**	**Cr**	**Ni**	**Mo**	**Cu**	**N**
Min						19.0	23.0	4.0	1.2	
Max	0.020	1.0	2.0	0.045	0.015	23.0	28.0	5.0	2.0	0.15
Target	0.010					20.0	25.0	4.3	1.5	0.06

Table 2.4 Standard mechanical and physical properties of stainless steel grade 904L (OUTOKUMPU 2008).

Property	**Value**
Density	8.0 kg/dm^3
Modulus of Elasticity	195 GPa
Ultimate Tensile Strength (UTS)	600 MPa

2.2.5.3 LDX2101 Stainless Steel

LDX2101 stainless steel is a low-alloyed, general-purpose duplex stainless steel. Its high mechanical strength is similar to that of other duplex grades, and its good corrosion resistance is on par with that of most standard stainless steel grades (OUTOKUMPU 2008). Tables 2.5 and 2.6 show the standard chemical composition and mechanical properties for LDX2101 stainless steel respectively.

Table 2.5 Standard chemical composition limits for stainless steel grade LDX2101 (OUTOKUMPU 2008).

Chemistry	**C**	**Si**	**Mn**	**P**	**S**	**Cr**	**Ni**	**Mo**	**Cu**	**N**
Min			4.0			21.0	1.35	0.10	0.10	0.20
Max	0.040	1.0	6.0	0.040	0.030	22.0	1.70	0.80	0.80	0.25
Target	0.030		5.0			21.5	1.50	0.30		0.22

Table 2.6 Standard mechanical and physical properties of stainless steel grade LDX2101 (OUTOKUMPU 2008).

Property	**Value**
Density	7.8 kg/dm^3
Modulus of Elasticity	200 GPa
Ultimate Tensile Strength (UTS)	700 MPa

Table 2.7 is a comparison of chromium, nickel and molybdenum content in these control alloys while Table 2.8 is a comparison of their standard mechanical and physical properties. From the comparisons, 904L stainless steel, having high content of nickel, will be more expensive followed by 304L. Also, it is observed that both 904L and 304L will be bulky to achieve the same strength provided by LDX2101 stainless steel as their densities are comparable to LDX2101 stainless steel while their strength is relatively lower than LDX2101 stainless steel.

Table 2.7 Comparison of the targeted chromium, nickel and molybdenum content in control alloys.

Property	904L	304L	LDX2101
Chromium	20	18.3	21.5
Nickel	25	9.2	1.5
Molybdenum	4.3	0	0.3

Table 2.8 Comparison of the standard mechanical and physical properties of control alloys.

Property	904L	304L	LDX2101
Density (kg/dm^3)	7.9	8	7.8
Modulus of elasticity (GPa)	200	195	200
Ultimate Tensile Strength (MPa)	600	600	700

2.3 PITTING CORROSION AND PITTING CORROSION RESISTANCE OF STAINLESS STEELS

Pitting corrosion is a localized form of corrosion that leads to the creation of small holes of varying shapes and sizes on the metal surface that can penetrate the wall thickness of a vessel (Fontana 1986). The driving force for pitting corrosion is the deprivation of oxygen around a small area that becomes anodic while the surrounding area exposed to an excess of dissolved oxygen becomes cathodic; leading to very localized galvanic corrosion attack. The corrosion penetrates the mass of the metal, with limited diffusion of ions, further pronouncing the localized lack of oxygen and the increase of aggressive anions (Jones 1992). To therefore fully understand the pitting corrosion and pitting corrosion resistance of a metal, it is important to understand the surface passivity of the metal and under which conditions the surface film will experience permanent damage.

2.3.1 Surface passivity and pitting corrosion

Just like any other form of corrosion of stainless steels, the resistance to pitting corrosion of stainless steels rely on surface passivity i.e. it results from the presence of a thin oxide or hydrate film on the surface of the metal, which is considered insoluble and nonporous. Hence, the chemical composition of the passive film, its structure, chemical and physical

properties, coherence, and thickness are of important in the initiation and propagation of pitting corrosion although there is still considerable controversy in literature regarding its nature (Szklarska-Smialowska 1986; Yang 2008). It can therefore be deduced that any alloying element introduced to a stainless steel which will improve these characteristics of the passive film would also improve the resistance of the steel to corrosion including pitting.

The composition of the oxide film or corrosion inhibiters can be evaluated using the Raman Spectroscopy. Raman spectroscopy is a powerful surface analysis technique to study the film that forms on a metal surface during its corrosion or corrosion inhibition in an aggressive environment (Sherifa, Erasmus & Comins 2010).

To further understand the phenomenon of passivity and the breakdown of the passive film of stainless steels, consider a schematic illustration of an electrochemical polarisation curve of stainless steel in an aqueous solution, Figure 2.6, where the cathodic curve can be assumed to be the reduction of hydrogen ions or oxygen reduction (Sedriks 1979).

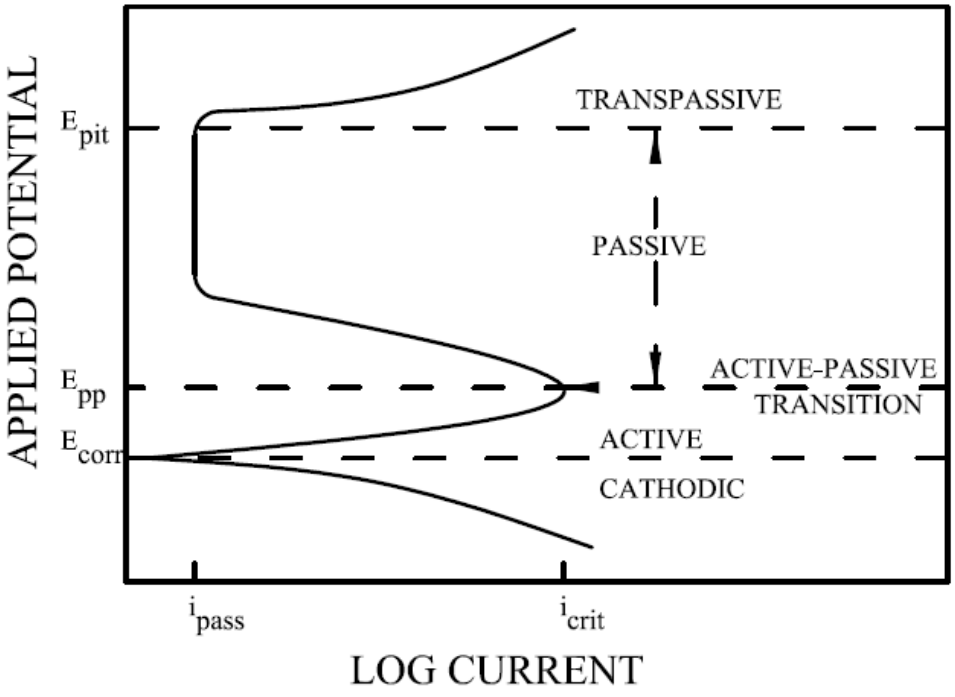

Figure 2.6 A schematic of typical electrochemical polarization curve of stainless steel in an aqueous solution (Sedriks 1979).

When the applied potential is increased in the noble direction from the corrosion potential (E_{corr}), the measured current density first ceases to increase with the applied potential at a potential usually referred to as the primary passivation potential (E_{pp}) (Sedriks 1979; Yang 2008). From E_{corr} to E_{pp} (active region) the stainless steel will experience active dissolution and it is normally susceptible to general corrosion (Wrisley et al. 1990). The current density corresponding to E_{pp} is referred to as critical current density i_{crit}. When the potential is increased further, the current density will decrease significantly to a current referred to as the passivation current (i_{pass}) due to the formation of a passive layer on the stainless steel which prohibits further active dissolution hence, bringing the stainless steel into a passive state (passivity) (Frankenthal & Kruger 1978). E_{pp} is therefore a demarcation between the active region and the passive region hence, it also corresponds to the active-passive transition. When the applied potential is increased further, the current density or i_{pass} remains constant. The potential range corresponding to i_{pass}, called the passive potential range, defines passivity of a given stainless steel/environment combination (Sedriks 1979) and, most of the literature attributes this to the energy being used to improve the characteristics of the passive film (Frankenthal & Kruger 1978; Yang 2008) which agrees with the law of conservation of energy. At high enough potentials the current density would experience a spontaneous increase with a small increase in applied potential. This sudden current density increase is mostly associated with localized corrosion, generally pitting corrosion. This passive film breakdown potential, where sudden current density increases starts, is referred to as pitting potential (E_{pit}) i.e. the potential where pits are initiated (Frankenthal & Kruger 1978; Sedriks 1979; Yang 2008; Wrisley et al. 1990).

2.3.2 Pitting corrosion propagation mechanism

The mechanism of pitting corrosion of stainless steel can be divided into three consecutive steps as follows: initiation, metastable propagation and stable propagation (Qvarfort 1998; Szklarska-Smialowska 1986). The initiation step is a local breakdown of the passivating oxide layer by aggressive ions in the environment. The corrosion process can then continue in the unprotected metal revealed by the initiation step. The corrosion rate is increased by the fact that an even more aggressive environment is produced by the corrosion reaction itself. However, at the earlier stages of pit propagation, when the pits are still very small, the pits can repassivate spontaneously. This stage is often referred to as metastable pit growth. The

stage of stable propagation is reached when spontaneous repassivation is no longer possible hence pitting corrosion takes place.

Figure 2.7 is an illustration of the relatively wide accepted mechanism of propagation of the pitting process (Key to metals 1999; Sedriks 1979). This illustration does not include the metal oxide cap that form on top of the pit and further inhibits the diffusion of oxygen into the pit. Up to recently, there is no consensus on mechanism of pit initiation. However, the initiation of pitting has long been associated with the presence of manganese sulphides (MnS) inclusions which are difficult to avoid in the steel making process (Key to metals 1999; Matter-University of Liverpool 2000 ; Schmuki et al. 2004).

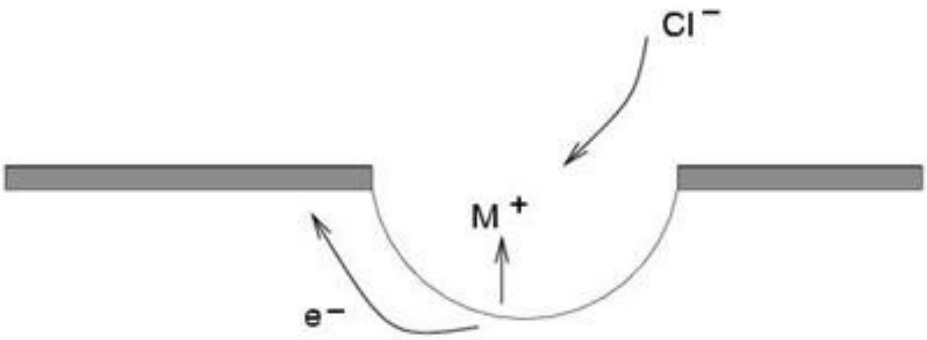

Figure 2.7 Schematic illustration of pitting corrosion (Key to metals 1999).

The anodic dissolution of the steel leads to introduction of M^+ in solution within the pit. The increased concentration of these M^+ within the pit causes migration of Cl^- ions in order to maintain neutrality. In turn, metal chloride formed M^+Cl^- is hydrolysed by water to the hydroxide and free acid:

$M + Cl^- + H_2O \Rightarrow MOH + H^+ Cl^-$ (Sedriks 1979)

The generation of the acid causes the drop of pH. The cathodic reaction, on the surface near the pit follows:

$O_2 + 2H_2O + 4e \Rightarrow MOH + 4OH^-$ (Sedriks 1979)

Hydrogen (H^+) and Chloride (Cl^-) ions stimulate the dissolution of the metal and the entire process accelerate with time. Since the solubility of oxygen is virtually zero in concentrated solutions, no oxygen reduction occurs within a pit thus, the cathodic oxygen reduction on the surface adjacent to the pit tend to suppress corrosion of the rest of the metal surface (Fontana 1986) hence, the preferential corrosion.

The growth of the pit will depend on: concentration of aggressive ions in the solution (Cl^- in this case), presence of nonaggressive anions in the solution, temperature, potential, properties of the passive film and crystal orientation of the metal grain on which pitting occurs (Szklarska-Smialowska 1986).

2.3.3 Susceptibility to pitting

There are different ways of estimating the alloy's susceptibility to pitting, amongst which, are listed below (Szklarska-Smialowska 1986):

- by determining the alloy's PRE number
- by determining the characteristics of the metal's or alloy's pitting potentials
- by determining the metal's or alloy's critical pitting temperature
- by measuring the number of pits per unit area, weight loss, and if possible, the size and depth of pits formed in the standard solution and,
- by determining the lowest concentration of aggressive ions causing the pitting

The PRE number method has already been discussed in the introduction. The remaining methods will be discussed in detail in the following sections.

2.3.3.1 Characterisation of pitting potentials

Different electrochemical polarisation techniques are used to determine the characteristics of the alloy's pitting potentials. The basis of electrochemical corrosion testing is derived from the potential theory which separates the oxidation and reduction reactions of corrosion and postulates that the total rates of all oxidation reactions equal the total rates of all reduction reactions on the corroding surface (Sedriks 1979). Table 2.9 is a summary of some common techniques, and the relevant information they give.

Table 2.9 Summary of electrochemical polarisation techniques for estimating the metal's or alloy's susceptibility to pitting (Yang 2008).

Polarisation Technique	Typical measurement	Information obtained	Relevant Standard
Cyclic potentiodynamic polarisation	Application of overpotential from corrosion potential towards noble direction to a potential at which current is 5 mA, where the potential is reversed and scanned until hysteresis loop is completed or until corrosion potential is reached	Critical pitting potential; Passive current; Transpassive region;	ASTM G5 ASTM G61 ASTM G102
Potentiostatic polarisation	Application of potential step to a more positive potential (above breakpoint potential) and stepping it down to a less positive potential (below breakdown potential)	Pitting potential; Protection potential;	ASTM F746

The protection potential is obtained at the point where the reverse scan polarisation curve intersects the forward scan else, if the reverse polarisation scan does not intersect the forward scan, then the protection potential is estimated using a threshold current density. Potentiostatic polarisation potential is favourable when more information (such as localised initiation time, stability and propagation) is needed as opposed to cyclic potentiodynamic polarisation (Yang 2008). When pitting potential is used, a critical aspect of pitting resistance is the magnitude of the difference between the critical pitting potential (E_{pit}) and the corrosion potential (E_{corr}), as illustrated schematically by Figure 2.6. Generally, pitting should not occur in situations where E_{corr} remains negative to E_{pit} and vice versa (Hartt et al. 2004).

2.3.3.2 Critical pitting temperature

A potentiostatic polarisation where a single potential step is applied (typically to 700mV vs SCE) according to ASTM G150 result in obtaining the alloy's critical pitting temperature (Yang L, 2008). The Critical Pitting Temperature (CPT) defines the lowest potential - independent temperature, below which pitting does not occur (Eghbali et al. 2010; Yang 2008).

2.3.3.3 Other methods

Pitting corrosion can also be estimated by measuring the number of pits per unit area, weight loss, and if possible, the size and depth of pits formed in the standard solution and, by determining the lowest concentration of aggressive ions causing the pitting.

In their study, Berner, Liu and Olsson (2008), recommended potentiodynamic polarisation method for ranking the relative corrosion resistance of lean duplex stainless steel. This is the method which will be adopted for this research to rank the relative corrosion resistance of LDX 2101 stainless steel alloyed with ruthenium compared to the control alloys.

2.3.4 Factors affecting pitting corrosion

Both external and internal factors affect pitting corrosion. Hence, combat pitting corrosion in stainless steels is targeted at addressing these factors by either decreasing the aggressiveness of the environment (external factors) or increasing the pitting corrosion resistance of the materials (internal factors). Decreasing the aggressiveness of the environment is not always practical in some applications, and hence a significant number of studies have been developed focusing on increasing the pitting corrosion resistance of stainless steel alloys. However, understanding of the environment is important in order to develop a solution to any corrosion problem. Hence, efforts to combat pitting corrosion in stainless steels includes evaluating the effect of both external (environment composition, temperature, electrode potential) and internal parameters (alloy composition, heat treatment, microstructure and surface preparation) among others (Sedriks 1979; Szklarska-Smialowska 1986). The following paragraphs will discuss these factors affecting pitting corrosion in detail.

2.3.4.1 Effects of external factors on pitting corrosion

These are mostly environmental factors which affects pitting corrosion of stainless steels. They include: temperature, pH and, availability of aggressive ions and their concentration in the electrolyte and oxygen content in the electrolyte. These factors are discussed in detail in the following sections.

2.3.4.1.1 Effect of pH

According to Szklarska-Smialowska (1986), the most available literature indicates that pitting corrosion is much less dependent on pH values. However, in their recent studies, Trepanier and Pelton (2006) found that corrosion test results for stainless steel tested at pH of 1.0, 7.4 and 9.0 indicated both general and pitting corrosion resistance are negatively affected by a decrease in pH. They also found that although the general and pitting corrosion resistance of the stainless steel severely deteriorated by exposure to low pH solution, repassivation of the stainless steel was possible. However, repassivation of the stainless steel at a pH of 7.4 and 9.0 was not observed. They concluded that repassivation may have been possible at low pH because the samples in this group were polarized to low potentials. Trepanier and Pelton (2006) further found that increase in the pH from 7.4 to 9.0 did not affect the corrosion resistance of the stainless steel. This suggests that there is a pH threshold above which general and pitting corrosion resistance of stainless steel is less dependent on pH. Trepanier and Pelton (2006) results and observations agrees with research study results by Malik et al. (1990) where they found that low pH and stagnancy provided most favourable conditions for pit growth. Under conditions of 4-5 ppm dissolved oxygen and 25° C, Malik et al. (1990) observed that pits grew between 450 and 325 microns at pH 4 under static and dynamic conditions, when 316L stainless steel specimens were immersed in 300 ppm chloride solutions for 4 months. At higher pH's (7 and 10), and the same conditions, the depth rarely exceeded 70 microns.

2.3.4.1.2 Electrolyte Composition

As discussed, pitting corrosion is caused by aggressive ions present in the electrolyte. The most common aggressive ion which attacks stainless steels is chloride (British Stainless Steel Association 2007 – 2012). Figure 2.8 (a) shows the effect of chloride concentration on pitting corrosion (Hartt et al. 2004). Szklarska-Smialowska (1986) found that the majority of construction materials suffer from pitting corrosion only in solutions containing Cl^- or other halogen ions. Three main reasons are given for the specific effects of chloride and its ability to produce pitting as follows: (i) chloride forming a complex with cation and hydroxide (ii) its ability to increase the activity of hydrogen ions in the pit electrolyte and, (iii) forming a salt layer at the bottom of pits. The third factor appears to explain the specific role of halides in pitting attack. It is suggested that transmission from passivity to pitting condition can be

explained by competitive adsorption mechanism in which chloride ions move into the double layer (oxide/liquid interface) of the electrode surface, eventually reaching at a critical potential (E pit), corresponding to the Cl^- concentration required to displace adsorbed oxygen species (Uhlig 1971). The presence of adsorbed Cl^- increases the potential difference across the passive film thereby enhancing the rate of metal ion diffusion from the metal/film interface to film/solution interface. This leads to the formation of cation vacancies at the metal/film interface which normally disappear into the bulk of the metal. When the Cl^- concentration is such that the rate of cation diffusion, and thus the formation of cation vacancies, is greater than the rate of disappearance of cation vacancies, voids develop at the metal/film interface. Continued growth of a void results in the localized collapse of the passive film, which will subsequently dissolve faster than other regions of the passive film leading to pit growth and ultimately substrate alloy dissolution. Anions such as BO_3^{-2}, SO_4^{-2} and ClO_4^{-2} also have the same effect. An increase in chloride concentration thus results in an increase in the stainless steel's susceptibility to pitting corrosion. Asaduzzaman, Mustafa and Islam (2011) in their studies on "Effects of Concentration of Sodium Chloride Solution on the Pitting Corrosion Behaviour of AISI-304L Austenitic Stainless Steel" agrees with this phenomenon as they observed that pitting corrosion resistance of AISI-304L stainless steel reduced with the increase in NaCl concentration from 0.5%NaCl to 4.5%NaCl in aqueous media. This is in agreement with research study results by Malika et al. (1990) where they observed that pitting behaviour of 316L in Cl^- containing solutions is greatly influenced by the variation in Cl^- concentration where higher Cl^- concentration in the electrolyte increased the steels susceptibility to pitting. Szklarska-Smialowska (1986) even observed that for each alloy/environment condition, there exist a minimum concentration of the aggressive ions below which pitting will not occur.

2.3.4.1.3 Temperature

Generally high temperature is a catalyst for chemical reactions, hence, increases corrosion rates and an increase temperature changes may move a metal form passive to active state (Sheir 1976; Souzaa, Rossitti & Rolloa 2009). Figure 2.8 (b) shows effect of temperature on pitting corrosion (Hartt et al. 2004). This is in agreement with the study results by Trepanier and Pelton (2006), where they found out that as the temperature was increased from 10°C and 80°C, a shift in the polarization curve towards lower potentials was observed. However, in their research, Laycock and Newman (1998) found that pitting potentials of austenitic

stainless steels decreased slowly with increasing temperature above the critical pitting temperature. Laycock and Newman (1998) also found that at temperatures much higher than the critical pitting temperatures, the pitting potential becomes less dependent upon temperature. Szklarska-Smialowska (1986), explained this phenomenon as resulting from interrelated process that occurs simultaneously with pitting such as growth of oxide films, diffusion of ions into and out of the pit and, formation of a salt layer on the bottom of the pit which will counter act the pitting process.

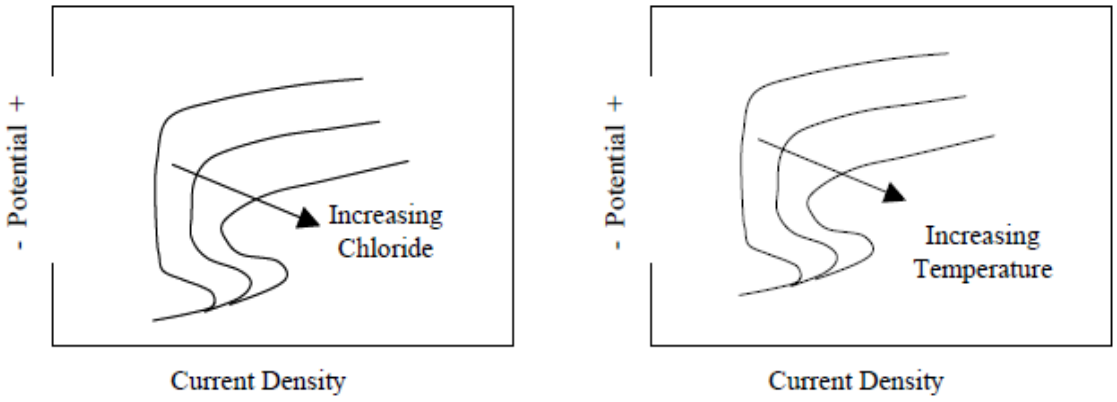

(a) (b)

Figure 2.8 An illustration on how a stainless steel's susceptibility to pitting increases with an increase in temperature and chloride concentration (Hartt et al. 2004).

2.3.4.1.4 Oxygen

Stainless steels rely on a source of oxygen to maintain their passive condition (Jones 1992; Szklarska-Smialowska 1986). This implies that a good supply of oxygen will improve stainless steels susceptibility to corrosion including pitting. For general corrosion, this theory is supported by the research study on "Effect of Oxygen Concentration on Corrosion Rates of Steel and Composition of Corrosion Products Formed in Oxygenated Water" done by Cox and Roetheli (1931) where they found that the corrosion rates of steel in oxygenated water are approximately proportional to the oxygen concentration below concentrations of *5.5* cc. per litre (7.865 ppm), while at higher concentrations the rates of corrosion are considerably lower than those demanded by a strict adherence to the linear relationship. They attributed the decrease in the differential corrosion rate as oxygen concentrations increased due to the gradual formation of corrosion products to a type which exhibits a greater resistance to the

transfer of oxygen. At low oxygen concentrations the corrosion product formed consists largely of a granular black magnetic oxide of iron which is not resistant to the transfer of the oxygen, while at higher oxygen concentrations the protective gelatinous ferric hydroxide is formed. At low oxygen concentrations the rate of oxidation of ferrous ions to form ferric hydroxide is slow enough to permit the precipitation of both the ferrous and ferric hydroxides with the subsequent formation of magnetic oxide. On the other hand at high oxygen concentrations the rate of oxidation of ferrous ions to ferric is high enough to prevent the accumulation of ferrous ions so that only the protective ferric hydroxide is precipitated. Aerated seawater however can be more corrosive than de-aerated seawater. It has been found that very low levels of oxygen, such as those found at sea depths of around 200 metres, make seawater less aggressive. This is associated with the slowing down of pitting corrosion rates (British Stainless Steel Association 2007 – 2012) The observations by the British Stainless Steel Association is also backed by the research study results by Vasilenko (2007) on "The Effect of Oxygen Concentration on the Corrosion of Heat Supply Networks and Heat Exchangers" where he observed that higher oxygen concentrations in the heating network water resulted in higher pitting corrosion experienced by the tubes during down time. This disagreement in literature confirms the complexity of the pitting corrosion process which is dependent on more than one variable hence, the need to consider an alloy/environment combination in corrosion evaluations.

2.3.4.2 Effects of internal factors on pitting corrosion of Stainless Steels

These are factors inhibited by the stainless steel alloy which includes composition, microstructure, and surface conditions. These are normally directly linked to the stainless steel production processes. The following sections will discuss these factors in detail.

2.3.4.2.1 Effects of stainless steel production processes

Processes used in the production of stainless steels have a direct influence on microstructure and hence pitting corrosion of the steel. It has already been shown in Section 2.2 that not only based on composition, but also at different heat treatment procedures how ferritic, austenitic, martensitic and duplex stainless steels are produced. It is therefore important to verify that the processes adopted in the production of stainless steels achieve the intended alloy to be

produced. The following are some other processes in steel production and their effect on pitting corrosion:

2.3.4.2.1.1 Cold working

In their study, Peguet, Malki and Baroux (2006) showed that altering the metal shape by plastic deformation (cold working) generally increased the stainless steel susceptibility to pitting. This is due to the fact that both thickness and composition of passive films are likely to be modified in many ways by cold working. However, the transfer resistance and interfacial capacitance do not appear to change linearly as a function of cold reduction. Although there is no agreement in literature that cold working reduces the alloys pitting potential, Szklarska-Smialowska (1986) agrees with the findings of Peguet, Malki and Baroux (2006) that the density of pits distribution was likely substantially increased on cold worked samples.

2.3.4.2.1.2 Sensitisation

If a stainless steel is heat-treated to exhibit the susceptibility of intergranular corrosion in an aqueous media, it is referred to as sensitization. Generally, sensitization has an adverse influence on pitting corrosion resistance stainless steels (Ebrahimi et al. 2010; Torres et al. 1998). This is due to the depletion of Cr along the stainless steel grain boundaries hence, rendering the passive film less protective along these regions (Szklarska-Smialowska 1986).

2.3.4.2.2 The effect of the surface condition

As discussed, corrosion of stainless steels, including pitting corrosion, starts form the surface of the metal. As such, the surface finish of the stainless steel alloy plays a major role in preventing or enhancing pitting. Sedriks (1979) pointed that it is meaningless to compare the pitting tendencies of different alloys having different surface finishes. Generally, pitting corrosion resistance increases with improved surface conditions both chemically and physically (Szklarska-Smialowska 1986). Such surface conditions include surface roughness and chemical surface treatment like pickling and passivation and they have been discussed further in the following sections.

2.3.4.2.2.1 Surface Roughness

Surface roughness is the finish on the stainless steel which results from different mechanical processes used in production of stainless steel and stainless steel products such as milling. A research study by Mathiesen, Nielsen and Frantsen (2006) on the "Influence of Various Surface Conditions on Pitting Corrosion Resistance of Stainless Steel Tubes Type EN 1.4404" showed improvement on critical pitting temperature and fewer pits on the surface of the tested specimen on electro-polished finish samples as compared to ground finish samples. This is in agreement with the research study results by Zatkalikova and Liptakova (2011) on "Pitting Corrosion of Stainless Steel at the Various Surface Treatment" where they found that the size and the shape of pits formed on their test samples were evidently related to the form of mechanical finishing (blasting and turning).This is why when ranking pitting corrosion resistance of different alloys, it is important to ensure that the samples being compared have the same surface finish.

2.3.4.2.2.2 Chemical surface treatment (Pickling and Passivation)

Pickling is the removal of any high temperature scale and any adjacent low chromium layer of metal from the surface of stainless steel by chemical means (ASSDA 2010). Where the steel has been heated by welding, heat treatments or other means, to the point where a coloured oxide layer can be seen, there is a chromium depleted layer on the surface of the steel underneath the oxide layer. The lower chromium content gives lower corrosion resistance. To restore the best corrosion resistant performance, the damaged metal layer must be removed, exposing a fully alloyed stainless steel surface. Mechanical removal may leave abrasive or other particles embedded (interfering with corrosion performance) or may be impractical, so chemical means are usually employed. Procedures incorporating pickling solutions of nitric (HNO_3) and hydrofluoric (HF) acids remove the scale and the underlying chromium depleted layer and restore the corrosion resistance. Pickling solutions also remove contaminants such as ferrous and ferric oxide particles. Pickling solutions other than mixtures of nitric and hydrofluoric acids exist and can be used for specialized applications. Pickling pastes, where the solution is mixed with an inert carrier, are commonly used to treat selected areas such as welds. Pickling involves metal removal and a change or dulling in the visual brightness of the metal. Electro-polishing is a useful alternative to pickling.

Passivation is the treatment of the surface of stainless steels, often with acid solutions or pastes, to remove contaminants and promote the formation of the passive film on a freshly created surface through grinding, machining or mechanical damage (ASSDA 2010). Common passivation treatments include nitric acid (HNO_3) solutions or pastes which will clean the steel surface of free iron contaminants. Care must be taken in selecting and using passivation treatments to ensure the selected treatment will target the contaminant. Passivation will also aid in the rapid development of the passive oxide film on the steel's surface. Passivation does not usually result in a marked change in appearance of the steel surface.

Pickling and passivation are both acid treatments and neither will remove grease or oil. If the fabrication is dirty, it may be necessary to use a detergent or alkaline clean before pickling or passivation. Also, both pickling and passivation solutions can employ dangerous acids that can damage both the operator and the environment if not handled correctly. Stainless pickling acids are highly corrosive to carbon steel. It is essential that all acids are thoroughly removed by rinsing the component after completing the process. Residual hydrofluoric acid will initiate pitting corrosion. It may be advantageous to neutralize the acid with an alkali before the rinsing step. *ASTM A380 Standard Practice for Cleaning, De-scaling and Passivation of Stainless Steel Parts, Equipment and Systems* is a valuable source of information on pickling and passivation treatments.

In their research, Zatkalikova and Liptakova (2011) also found that chemical surface treatment (pickling and passivation) improved the protective passive film of stainless steels. Pickling and passivation transformed the roughness and segmentation of variously mechanically treated surfaces, thereby creating the capillary effect in close crevices which changed kinetics of the pitting corrosion.

2.3.4.2.3 The effect of the microstructure

How stainless steels are structured on a microscopic level plays an important part in determining pitting resistance of an alloy. Stainless steel microstructures are influenced by composition and, processes/methods used to produce and treat stainless steels. The effect of composition, which in turn also influences the microstructure, will be discussed separately. Studies have shown that secondary phases, such as sulphides, delta ferrite, sigma and

sensitised grain boundaries, amongst others, have an effect on pitting resistance of stainless steel alloys (Sedriks 1979). Table 2.10 summarises the effects of these phases. In duplex stainless steels, the alloying elements must be in solid solution and homogeneously distributed in order to maintain the high resistance to localized corrosion (Cvijovic´ & Radenkovic´ 2006). Because of the two phases system and the availability of both ferrite and austenite formers, the PRE value and the associated resistance to pitting may become notably different in the two phases. This can be overcome by selecting a diffusion annealing temperature such that the concentration of alloying elements corresponds to equal pitting resistance in ferrite and austenite (Cvijovic´ & Radenkovic´ 2006).

Table 2.10 Summary of the effect secondary phases (Sedriks 1979).

PHASE	EFFECT
Sulphides	Sulphide composition in stainless steels reduces its pitting corrosion resistance
Delta ferrite	Delta ferrite in stainless steels is generally considered detrimental to pitting corrosion resistance
Sigma	Sigma is also detrimental to pitting resistance of stainless steels
Sensitisation	Sensitised grain boundaries act as preferred sites for pit initiation

2.3.4.2.4 Alloying Elements/Composition

Many studies have been undertaken to analyse the effects of various alloying elements, and hence composition, on pitting corrosion susceptibility of stainless steels. Commonly evaluated are the influences of the alloying elements on the pitting potential, and critical pitting temperature (Szklarska-Smialowska 1986). Different alloying elements have different effects on pitting corrosion resistance depending on whether they will improve the characteristics of the passive film or not. Some alloying elements improves the susceptibility to pitting corrosion of stainless steels, others have a detrimental effect while others may have both beneficial and detrimental effects depending on the added content. The following paragraphs will discuss in detail the effect of alloying elements found in control alloys and,

platinum group metals, ruthenium in particular which will be used to modify LDX2101 stainless steel. It should be noted however, that general trends will be discussed, and the exact effect of the alloying elements on pitting corrosion resistance depends on the alloy composition/environment combination.

2.3.4.2.4.1 Chromium

As already defined, stainless steels are chromium containing steel alloys. Chromium makes the steel 'stainless' this means improved corrosion resistance. Chromium has a favourable effect on the pitting corrosion resistance of steels (Szklarska-Smialowska 1986; Uhlig 1971). Figure 2.9 (a) shows how a higher chromium content will increase the pitting potential to more noble values (Hartt et al. 2004).

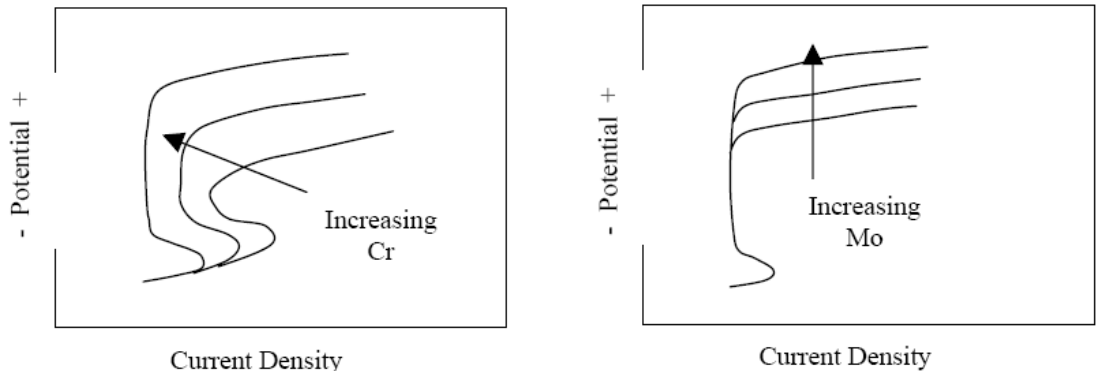

Figure 2.9 Schematic polarisation diagram illustrating the influence of (a) Cr and (b) Mo on the pitting corrosion resistance of stainless steel (Hartt et al. 2004).

2.3.4.2.4.2 Molybdenum

Although there is no agreement in literature on the mechanism on how molybdenum enhances pitting corrosion of stainless steels, just like chromium, molybdenum (Mo), when used as an alloying element in stainless steels enhances their pitting corrosion resistance (Hartt et al. 2004; Ilevbare & Burstein 2001; Szklarska-Smialowska 1986; Uhlig 1971). Ilevbare and Burstein (2001), outlined the following as some of the many suggestions offered as to how Mo enhances pitting corrosion resistance in stainless steels: improving of the bonds in the oxide film, elimination of active sites by the formation of molybdates or Mo

oxyhyroxides, changing of the ion selectivity at the oxide film surface in Mo containing alloys through the formation of molybdates and increasing the thickness of the passive film. Figure 2.9 (b) illustrates how an increase in molybdenum content in a steel alloy will push the pitting potential to more noble values thereby increasing the passive region (Hartt et al. 2004).

2.3.4.2.4.3 Nickel

Alloying stainless steels with nickel, which is a austenite former, improves the alloys pitting corrosion resistance (Potgieter et al. 2008). However, the high and fluctuating price of nickel has led to research on alternative elements. Figure 2.10 is summary of nickel prices fluctuations from the London Metal Exchange in year 2010 (London Metal Exchange 2003 - 2011).

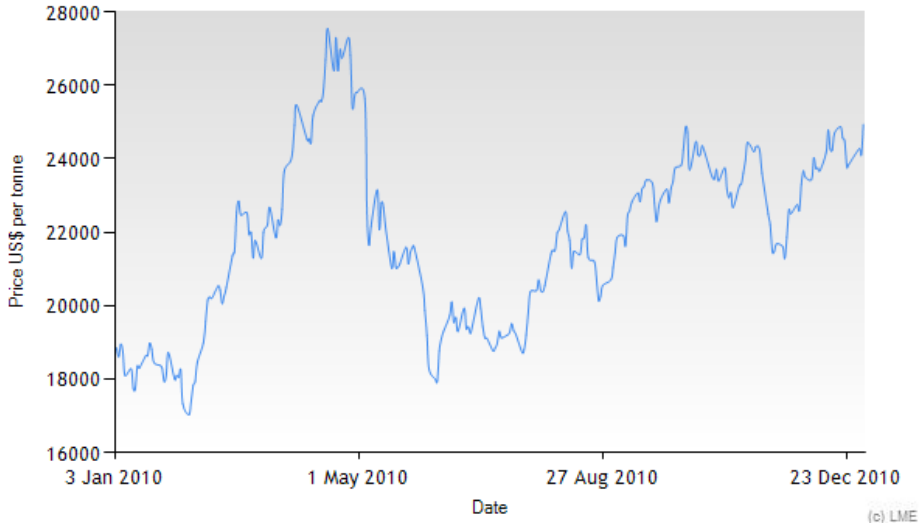

Figure 2.10 Summary of nickel prices in USD/Tonne (cash buyer) for the year 2010 (London Metal Exchange 2003 - 2011).

2.3.4.2.4.4 Manganese

As already discussed, manganese, through the formation manganese sulphide inclusions, is detrimental to stainless steels pitting corrosion resistance. As a result, reducing Mn content in stainless steels has proven to be a successful strategy for increasing the pitting corrosion resistance of stainless steels (Fredriksson, Edström & Olsson 2010; Szummer & Janik-Czachor 1993). However, manganese is still added in some stainless steel alloys to increase

the solubility of nitrogen (Pardo et al. 2008) which result in production of improved pitting corrosion resistance alloys due to the influence of nitrogen.

2.3.4.2.4.5 Nitrogen

Many investigations have shown that when stainless steels are alloyed with nitrogen, their susceptibility to pitting corrosion decreases (Lothongkum et al. 2004). To explain the effect of nitrogen on corrosion resistance, the ammonium formation is an applicable consideration in increasing pitting corrosion in acid, neutral and basic solutions. The nitrogen enrichment at the interface metal/passive film and adsorption mechanism is also an applicable consideration in increasing the pitting corrosion resistance (Lothongkum et al. 2004). This is achieved by nitrogen's ability to promote passivity and widening the passive range in which pitting is less probable (Mudali et al. 2002). Even after the passive film is mechanically damaged, Baba, Kodama & Katada (2002), in their research on 'Role of Nitrogen on the Corrosion Behaviour of Austenitic Stainless Steels', found that nitrogen facilitated the steel's repassivation.

2.3.4.2.4.6 Copper

Although Cu has a beneficial effect on general corrosion through the suppression of anodic dissolution by the noble metallic copper (Cu) enriched on the surface film of stainless steels, it has a detrimental effect on the localised corrosion resistance in noble potential range (Ujiroet al. 2000). The detrimental effect is emphatic in ferrite containing stainless steels (ferritic and duplex) since the solubility of copper in ferrite is lower than in austenite leading to the formation of the ε-phase. The ε-phase, like copper, is not resistant to pitting corrosion in chloride containing solutions (Banas & Mazurkiewicz 2000). However, recent investigations by Jeon et al. (2011), argued otherwise. In their study research on "Effects of Copper Addition on the Formation of Inclusions and the Resistance to Pitting Corrosion of High Performance Duplex Stainless Steels", Jeon et al. (2011), found than the addition of copper to duplex stainless steel increased the number and area of numerous (Mn, Cr, (Al), (Fe)) oxides and oxy-sulphides due to an increase in the activity of chromium and resulted in decreased pitting resistance.

2.3.4.2.4.7 Platinum Group Metals (PGM) - Cathodic Modification

The commonly known effect of alloying stainless steels with platinum group metals (Ruthenium - Ru, Rhodium - Rh, Palladium - Pd, Osmium - Os, Iridium - Ir, and Platinum - Pt) is cathodic modification. This is the retardation of the anodic reaction as a result of an increase in the ability of a metal/alloy to be passivated by further alloying with a metal that greatly increases the rate of the cathodic process (Potgieter, Heyns & Skinner 1990; Higginson 1989). Figure 2.11 is a schematic of a typical electrochemical polarization curve of stainless steel in aqueous solution, showing the effect of cathodic modification (Wolff 1999).

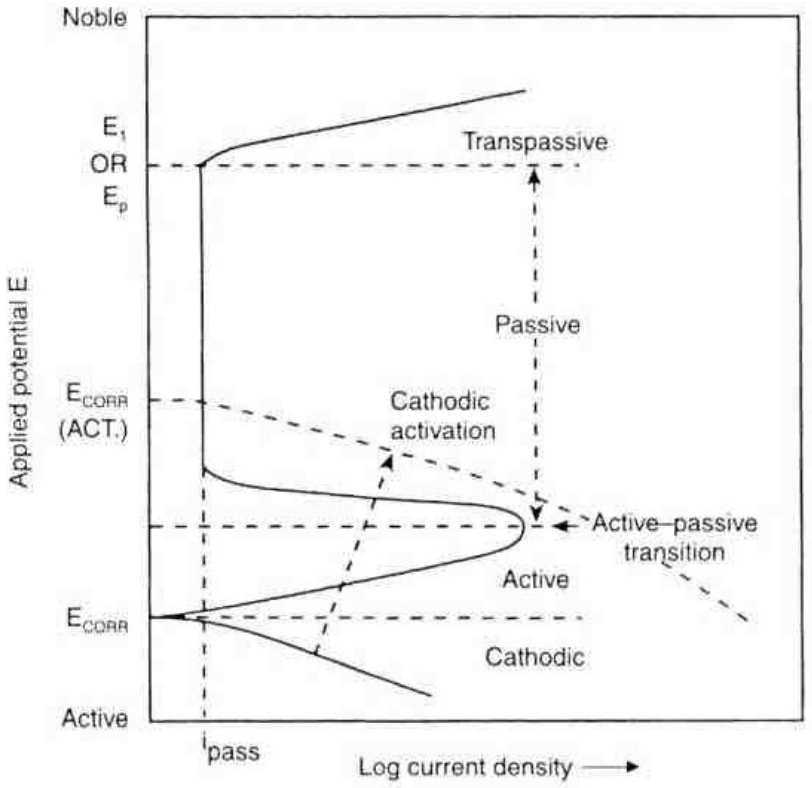

Figure 2.11 A schematic of typical electrochemical polarization curve of stainless steel in aqueous solution, showing the effect of cathodic modification (Wolff 1999)

Basic conditions required for successful cathodic alloying were fully explained by Potgieter, Heyn and Skinner (1990). These include: (a) the base alloy must have a small critical current density (the corresponding current density value at the active-passive transition in Figure 2.11) that will be easily exceeded by the current of the hydrogen cathodic reaction on the added noble metal at the given passive potential. (b) The passive potential of the base metal

must be sufficiently negative to allow the cathodic component that has been introduced to change the corrosion potential of the alloy to a value in the passive range that is more positive than pitting potential but less positive than the potential associated with the onset of the transpassive processes. (c) the transpassive potential of the base alloy should be sufficiently electropositive to allow a wide passive range. Further to this, Potgieter, Heyn and Skinner (1990) also noted that the cathodic alloying component needs to have a higher exchange current density (and a lower overvoltage) for the cathodic process of hydrogen evolution than the base metal or the alloy, and it should be corrosion resistant under the given conditions.

In addition to cathodic modification, as already pointed out in the introduction, a recent study by El-Sayed et al. (2009), found that small additions of ruthenium to a duplex stainless steel did not only improved the alloy's passivation, but also shifted the corrosion and pitting potentials to higher noble values. Also of importance to note is that literature indicates that alloying stainless steels with platinum group metals does not affect their mechanical properties. Actually, in some instances, it was observed that PGMs enhance the mechanical properties of the resulting stainless steel alloys (Higginson 1989).

3. PROCEDURES AND METHODOLOGIES

3.1 ALLOYS PRODUCTION

The production of alloys was aimed at producing alloys with the same carbon, nitrogen, chromium, molybdenum and manganese content as that of LDX2101 duplex stainless steel but having 0.10% by weight incremental composition of ruthenium from 0.10% to 0.30% and then doubles the last amount (0.60%). The aim was to eliminate the influence of these chemical compositions on pitting corrosion of stainless steels as discussed in Chapter 2 hence, establishing a platform to only evaluate the effect of the added ruthenium. The recommendation by Higginson (1989), where he recommended using less than 2% of PGM in order to develop an economically viable alloy, was used as guideline in choosing the percentage range of ruthenium to be added to the produced sample. Using the processes and ingredients explained in this chapter, four stainless steel alloys with different targeted compositions as per Table 3.1 were produced.

Table 3.1 Targeted composition (wt %) of alloys which were produced.

Alloys Designation	***Targeted Composition (wt %)***						
	C	***N***	***Cr***	***Ni***	***Mo***	***Mn***	***Ru***
A	0.3	0.22	21.5	1.5	0.3	5	0.1
B	0.3	0.22	21.5	1.5	0.3	5	0.2
C	0.3	0.22	21.5	1.5	0.3	5	0.3
D	0.3	0.22	21.5	1.5	0.3	5	0.6

3.2 MATERIALS USED TO PRODUCE THE ALLOYS

The following two ingredients were used for the production of the alloys:

- Pressed ruthenium powder with purity of 99.8%, and
- Pieces cut from commercial LDX2101 duplex stainless steel plate with the manufacturer's composition as shown in Table 3.2

Table 3.2 Typical manufacturer's composition of LDX2101 stainless steel.

Alloy	*Composition (wt %)*					
	C	***N***	***Cr***	***Ni***	***Mo***	***Mn***
LDX2101	0.3	0.22	21.5	1.5	0.3	5

Prior to melting, all four sides of the cut pieces from LDX2101 duplex stainless steel plate were wet ground, water washed and air dried in order to remove any impurity arising from either prior natural oxidation or the cutting process. The aim was to eliminate inclusions and impurities which are a major concern in stainless steels corrosion resistance. Table 3.3 provides the exact calculated and weighed quantities of LDX2101 duplex stainless steel and ruthenium used for the samples production in order to achieve the targeted composition. These quantities were based on the mass of small pieces of LDX2101 stainless steel (Mass LDX2101 in the table) which were cut from a large commercial LDX2101 duplex stainless steel plate.

Table 3.3 LDX2101 stainless steel and ruthenium used for samples production.

Sample designation	*Mass LDX2101 (g)*	*Weight percentage LDX2101*	*Mass Ru (g)*	*Weight percentage Ru*	*Total mass (g)*	*Total weight percentage*	*No. of samples produce*
A	17.9327	99.9	0.01795	0.1	17.9507	100	3
B	16.3448	99.8	0.03276	0.2	16.3776	100	3
C	17.7724	99.7	0.05348	0.3	17.8259	100	3
D	17.2563	99.4	0.10416	0.6	17.3605	100	3

3.3 MELTING PROCEDURE

The four samples were melted in an argon atmosphere. Also, as a measure to eliminate inclusions and impurities, the furnace was first flushed with argon three times to remove oxygen before filling it with argon. Pure Ti was melted prior to melting the samples to ensure the removal of any residual oxygen. The samples were turned and re-melted three times to ensure proper solution of ruthenium in LDX2101 duplex stainless steel with the flushing of the furnace with argon and melting of pure Ti repeated each time.

3.4 HEAT TREATMENT PROCEDURE

The produced samples (Table 3.3) were solution annealed at 1050^{o}C for 1 hour and water quenched. The heat treatment was based on the recommended solution annealing temperature (1050^{o}C) by the LDX2101 duplex stainless steel manufacturer Outokumpu in order to achieve a balanced chemical composition and a microstructure containing a fair ferrite-austenite solution and, thermal calculations which showed that such small additions of ruthenium has no effect on the solution annealing temperature of the resulting alloy (Outokumpu, 2004).

3.5 CHEMICAL COMPOSITION ANALYSIS PROCEDURE

Chemical composition analysis was performed in order to verify the targeted chemical compositions shown in Table 3.3.

3.5.1 Specimen preparation

A small section was cut from each stainless steel alloy sample and mounted in bakelite leaving only one side exposed as shown in Figure 3.1. The exposed surface was wet ground to 1200 grit before polishing with a 1 µm Emily cloth removing 150 µm/min for 2 minutes. The exposed surface was then thoroughly clean with water and air dried.

Figure 3.1 A small section of stainless steel alloy mounted in bakelite.

3.5.2 Analysis

The specimen in section 3.5.1 were analysed as is, the metal bits were loaded in sample cup holders and covered with cellulose backing. A sample of just the cellulose baking and

bakelite were analysed separately and the results were used to make background corrections for the samples analysed. The instrumentation used is an ARL 9400XP+Wavelength dispersive XRF Spectrometer with a Rliodium tube, LÍF200, LÍF220, GER. AXO6 (a 50Â synthetic multilayer) and PKT analysing crystals, with a flow proportional and scintÜlation detector and Uniquant software was used for analyses (Loubser & Verryn 2008). The software enables the qualitative and quantitative analysis of an unknown sample with or without sample preparation. Elements from fluorine to uranium in the periodic table can be analysed with detection limits varying from 0.5 ppm for heavier elements like Mo to 100 ppm for the lightest element F. With the fundamental parameter approach, everything in the sample is analysed to enable accurate matrix corrections. The software allows for manual input of elements not determinable by XRF, like carbon, oxygen and hydrogen in different compounds and this data is then used in the matrix correction model. For higher accuracy, matrix matched calibration curves can be set up for specific matrices with specific sample preparation protocols followed. Only elements found above the detection limits were reported. The values were normalised, as no percentage loss on ignition (LOI) was done to determine crystal water and oxidation state changes. All elements were expressed as oxides.

3.6 MICROSTRUCTURAL ANALYSIS PROCEDURE

The microstructural analysis was performed in order to verify that the small addition of ruthenium to LDX2101 and the samples melting procedure did not have any negative effect on the resulting alloys. ASTM A923 Test method A – Sodium Hydroxide etch test for classification of etch structures of duplex stainless steel was used to analyse the microstructure for acceptance of the samples (ASTM Standard A923 2008).

3.6.1 Specimen preparation

Specimen for microstructural analysis were prepared using the procedure in section 3.5.1

3.6.2 Analysis

The specimen as in section 3.6.1 were etched at 3 V dc for 30 seconds in a 40% sodium hydroxide solution which was prepared by adding 40 g of sodium hydroxide in 100 ml of distilled water. Following etching, samples were thoroughly rinsed in hot water and air dried. The etched surfaces were examined on a metallurgical microscope at 500X magnification.

During etching, any intermetallic phase is revealed by yellow, then brown staining followed by staining of the ferrite.

3.7 POTENTIODYNAMIC POLARISATION PROCEDURE

Potentiodynamic tests were performed to determine the corrosion potentials, pitting potentials and corrosion currents for both control and produced samples. The tests were repeated for each alloy in order to verify accuracy of the results.

3.7.1 Specimen preparation

A small section was cut from each stainless steel alloy sample and connected to a copper wire before being mounted in thermosetting plastic leaving only one side exposed as shown in Figure 3.2.

Figure 3.2 Mounting of sample for potentiodynamic polarisation measurements

The exposed surface areas of these samples were measured. After the thermosetting plastic dried, the exposed area was wet abraded using silicon carbide (SiC) paper to a 600 grit finish until all previous course scratches were removed. Then, the samples exposed areas were rinsed and dried. The selection of the thermosetting plastic used ensured elimination of gaps between the metal and thermosetting plastic interface hence, elimination of crevice corrosion.

Before each test, the testing surface was wet abraded again with a 600 silicon carbide grit paper, rinsed and dried.

3.7.2 Potentiodynamic test

The potentiodynamic tests were conducted mostly by following ASTM G61-86 (ASTM Standard G61 1986 -1998), using the cyclic voltammetry potentiostatic technique of Metrohm Autolab Nova software in a naturally aerated 3.56% NaCl aqueous solution at a controlled temperature of 25°C±2°C. A glassy carbon counter electrode and silver/silver chloride [Ag/AgCl, KCl (3M)] reference electrode were used as in the testing cell. The specimens in section 5.1.1 were connected to the working electrode of the cell. The open circuit potential for each scan was determined 1hour after immersing the sample in the solution. Each sample was anodically polarized separately at a scan rate of 0.000167 mV/s from 200 mV below its open circuit potential/corrosion potential, passing through the corrosion potential to more noble values. For each scan, the scan was reversed at 1 mA/cm^2 and, where applicable, the repassivation potentials of the alloys were determined accordingly. Fresh solution was used for each scan.

3.7.3 Solution Purging Procedure

For the experiments where it was necessary to remove oxygen from the prepared 3.5% NaCl aqueous solution, the solution was purged with nitrogen gas for 1 hour and the oxygen content in the solution was measured before and after purging. On all experiments requiring solution purging, air tightness was ensured on the test cell.

3.8 Corrosion rate calculations

Corrosion rate was determined using the Faraday's Law (Metrohm Autolab 2011), Equation (2).

$$R_M = \frac{M}{nF\rho} i_{corr} \quad \text{..... (2)}$$

Where R_M is the corrosion rate, M is the atomic weight of the metal, ρ is the density, n is the valance electrons and F is the Faraday constant (96.485 C/mol). The ratio M/n is also referred to as equivalent weight.

For an alloy like LDX2101, the equivalent was calculated by the equation (3), disregarding all elements below 1 mass percentage in the alloy.

$$\text{Equivalent weight} = 1 \Big/ \sum \frac{n_i f_i}{W_i} \qquad \text{.......... (3)}$$

Where f_i is the mass fraction of the i^{th} element in the alloy, W_i is the atomic weight of the i^{th} element in the alloy, and n_i is the valence of the i^{th} element in the alloy.
Applying equation (2) and obtaining the valence electrons for stable phases as a function of corrosion potential (E_{corr}) and p-H of 8 for elements Fe, Cr, Mn and Ni in the Atlas of Eh-pH diagrams [(13)] the equivalent weight of LDX2101 is **24.75**.

Using this equivalent weight, the exposed surface area of each sample and the density of LDX2101 (7.8 kg/dm^3), the corrosion current I_{corr}, corrosion potential E_{corr}, and corrosion rate as presented in Table 4.2 were directly extracted from the Metrohm Autolab Nova software for each potentiodynamic curve. Correct estimates of the Tafel slopes was possible by choosing two point on the linear Tafel region of each slop which were at least a decade in current apart.

4. RESULTS

This chapter provides and discusses the results on produced alloys, their composition analysis, microstructural analysis and potentiodynamic polarisation of both control and produced samples.

4.1 PRODUCED ALLOYS

Following procedures described in section 4.1 to section 4.4, twelve samples were produced, three samples per each targeted chemical composition. Figure 5.1 below is the representation of the samples which were produced.

Figure 4.1 A representation of the produced samples

4.2 CHEMICAL COMPOSITION ANALYSIS RESULTS

The chemical compositions of all twelve produced samples were analysed following the procedure discussed in section 3.5. The results of the chemical composition analysis are provided in Table 4.1. The results showed that the samples production process was not very accurate especially for very small targeted ruthenium composition. Some of the ruthenium which was added to the LDX2101 stainless might have been blown away during the melting procedure. This resulted in all three samples with the targeted 0.1%wt Ru plus one sample with targeted 0.2%wt Ru having the actual ruthenium composition of less than 0.01%wt. Only four samples (S.B 05, S.B 06, S.B 09 and S.B 11 in Table 4.1) closely matched the targeted ruthenium composition in the alloys as intended in Table 3.1. Although much effort was undertaken to exclude oxygen in the alloys production procedure (section 3.1), the results showed samples S.B 02 and S.B 11 had high content of oxygen further indicating the inadequacy of the alloy production process.

Table 4.1 Summary of XRF composition analysis results of the produced samples.

Element	Samples composition (wt %)											
	S.B 01	**S.B 02**	**S.B 03**	**S.B 04**	**S.B 05**	**S.B 06**	**S.B 07**	**S.B 08**	**S.B 09**	**S.B 10**	**S.B 11**	**S.B 12**
Fe	70.48	62.86	70.60	70.50	69.92	70.46	70.14	70.29	70.36	69.83	61.83	70.07
Mn	4.97	4.50	4.96	5.05	5.14	4.99	4.90	4.96	4.84	4.91	4.42	4.73
Cr	22.45	20.21	22.22	22.38	22.46	22.26	22.51	22.22	22.31	22.27	20.10	22.38
Ni	1.50	1.35	1.57	1.55	1.50	1.58	1.52	1.60	1.60	1.56	1.37	1.52
V	0.06	0.05	0.06	0.06	0.06	0.06	0.06	0.06	0.05	0.06	0.05	0.06
Cu	0.22	0.30	0.21	0.19	0.21	0.21	0.22	0.22	0.20	0.21	0.17	0.16
Co	0.08	0.08	0.07	0.07	0.07	0.08	0.06	0.08	0.08	0.04	0.06	0.08
Ce	*<0.01*	*<0.01*	*<0.01*	*<0.01*	0.05	*<0.01*	*<0.01*	*<0.01*	*<0.01*	*<0.01*	*<0.01*	*<0.01*
Mo	0.25	0.31	0.29	0.21	0.29	0.25	0.23	0.20	0.26	0.28	0.30	0.26
O	*<0.01*	10.12*	*<0.01*	*<0.01*	*<0.01*	*<0.01*	*<0.01*	*<0.01*	*<0.01*	*<0.01*	11.04*	*<0.01*
Pt	*<0.01*	0.13	*<0.01*	*<0.01*	*<0.01*	*<0.01*	*<0.01*	*<0.01*	*<0.01*	*<0.01*	*<0.01*	*<0.01*
Pr	*<0.01*	0.09	*<0.01*	*<0.01*	0.07	*<0.01*	*<0.01*	*<0.01*	*<0.01*	*<0.01*	0.06	*<0.01*
Nd	*<0.01*	*<0.01*	0.02	*<0.01*	*<0.01*	*<0.01*	*<0.01*	*<0.01*	0.02	0.02	*<0.01*	*<0.01*
Ru	*<0.01*	*<0.01*	*<0.01*	*<0.01*	0.20	0.13	0.35	0.34	0.31	0.83	0.66	0.74
Totals	**100.00**	**99.99**	**100.00**	**100.01**	**99.97**	**100.00**	**99.99**	**99.97**	**100.02**	**100.00**	**100.06**	**100.00**

4.3 MICROSTRUCTURAL ANALYSIS RESULTS

Only the microstructures of produced alloys which closely matched the targeted ruthenium composition in Table 4.1 discussed above were analysed. Also, for comparison, the microstructure of LDX2101 which was used as feed for the sample production and, as a control alloy in this research, was analysed. Although primarily the technique used to evaluate the microstructure, ASTMA923, is used to determine detrimental phases in duplex stainless steels, in this application it was used to confirm a balanced solution of ferrite in austenite for the produced samples.

4.3.1 Microstructure results for LDX2101 Stainless steel

The transverse microstructure of LDX2101 was examined as shown in Figure 4.2. The examined specimen revealed that the LDX2101 stainless steel sample contained

approximately 65% Ferrite (α) and 35% Austenite (γ), the ferrite being the darker staining in Figure 4.2.

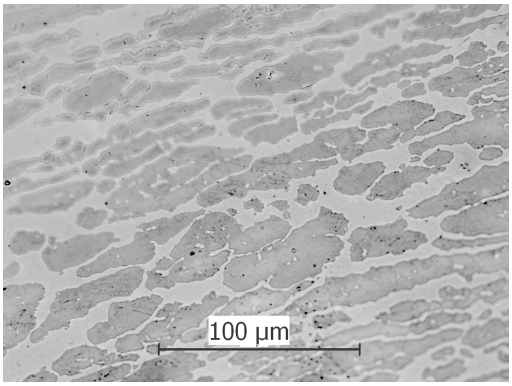

Transverse

Figure 4.2 Transverse microstructure of LDX2101 as examined at 500X magnification.

4.3.2 Microstructure results for LDX2101+0.13%wt Ru

The microstructure of LDX2101 with 0.13%wt Ru alloy samples were examined as shown in Figure 4.3. The examined specimens revealed that the alloy samples contained approximately 20% Ferrite (α) and 80% Austenite (γ), the ferrite being the darker staining in Figure 4.3.

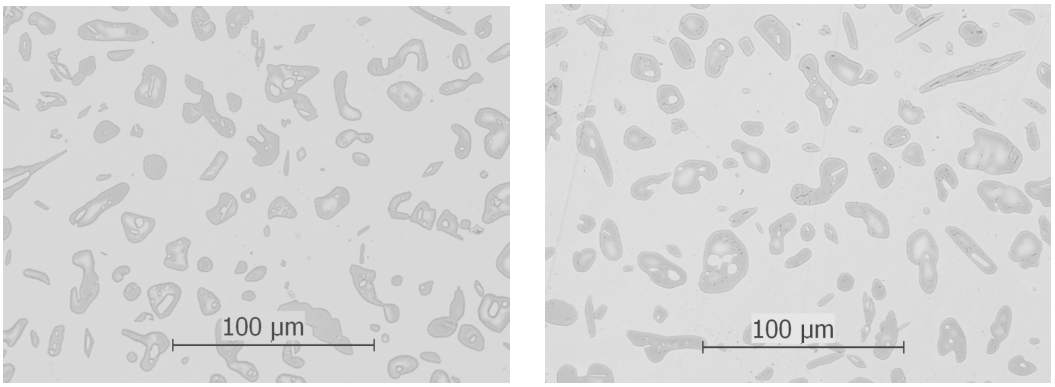

Figure 4.3 Microstructure of LDX2101 with 0.13% Ruthenium, obtained at different points on the same sample, as examined at 500X magnification.

4.3.3 Microstructure results for LDX2101+0.2%wt Ru

The microstructure of LDX2101 with 0.20%wt Ru alloy samples were examined as shown in Figure 4.4. The examined specimens revealed that the alloy samples contained approximately 80% Ferrite (α) and 20% Austenite (γ), the ferrite being the darker staining in Figure 4.3.

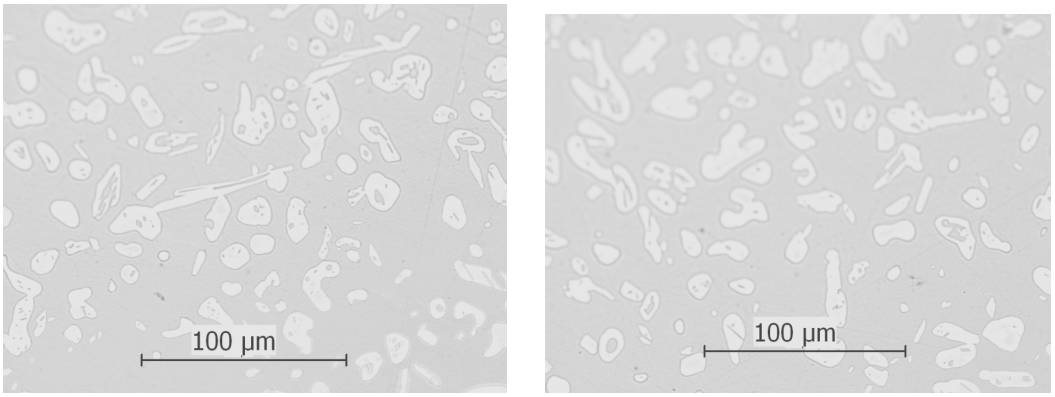

(b)

Figure 4.4 Microstructure of LDX2101 with 0.20% Ruthenium, obtained at different points on the same sample, as examined at 500X magnification.

4.3.4 Microstructure results for LDX2101+0.31%wt Ru

The microstructure of LDX2101 with 0.31%wt Ru alloy samples were examined as shown in Figure 4.4. The examined specimens revealed that the alloy samples contained approximately 60% Ferrite (α) and 40% Austenite (γ), the ferrite being the darker staining in Figure 4.5.

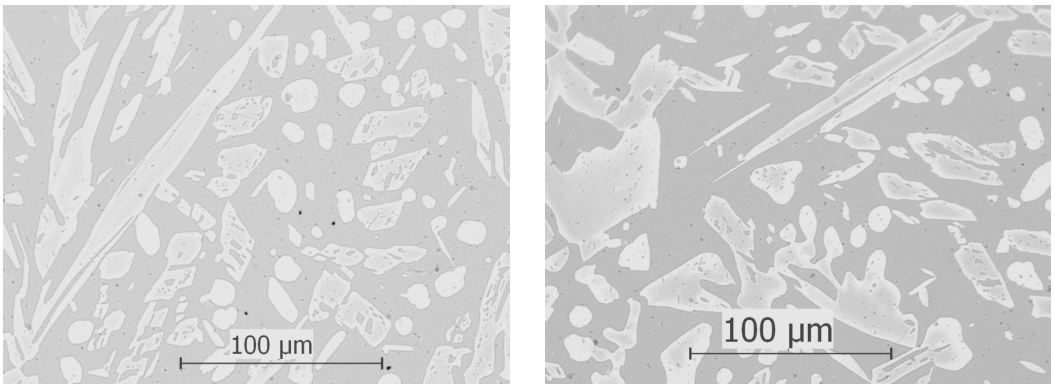

Figure 4.5 Microstructure of LDX2101 with 0.31% Ruthenium, obtained at different points on the same sample, as examined at 500X magnification.

4.3.5 Microstructure results for LDX2101+0.66%wt Ru

The microstructure of LDX2101 with 0.66%wt Ru alloy samples were examined as shown in Figure 4.4. The examined specimens revealed that the alloy samples contained approximately 60% Ferrite (α) and 40% Austenite (γ), the ferrite being the darker staining in Figure 4.6.

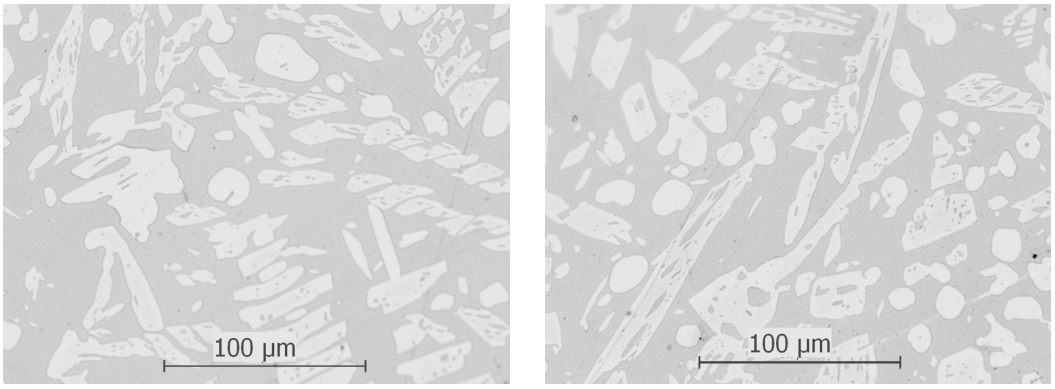

Figure 4.6 Microstructure of LDX2101 with 0.66% Ruthenium, obtained at different points on the same sample, as examined at 500X magnification.

4.4 POTENTIODYNAMIC POLARISATION RESULTS

Potentiodynamic polarisation tests were conducted on control alloys (stainless steel grades 304L, 904L and LDX2101), and on all produced alloys which closely matched the targeted composition (samples S.B 05, S.B 06, S.B 09 and S.B 11 in Table 4.1). Detailed results of these tests have been discussed in the following sections. The AUT22771 in the legends of all polarisation curve figures is a default setting for the equipment which was used.

4.4.1 Potentiodynamic Polarisation results of 304L Stainless Steel

Figures 4.7 (a) and (b) are potentiodynamic polarisation curves obtained when 304L stainless steel samples were anodically polarised in 3.5% NaCl aerated solution at 25^{o}C ±1^{o}C following the procedure discussed in section 3.7. Sample X-1 was scanned from -370 mV, passing through the observed corrosion potential of -170 mV. At 152 mV a drastic increase in current density was observed, suggesting the point of pit initiation. The sample recovered slightly before experiencing stable pit growth at 187 mV. At this potential (187 mV), current density increased with little or no increase in polarisation potential. After reverse scanning,

the sample re-passivated at a repassivation potential of -100 mV. Sample X-2 was scanned from -357 mV, passing through the observed corrosion potential of -157 mV. At 290 mV a drastic increase in current density was observed, suggesting the point of pit initiation. The sample recovered slightly before experiencing stable pit growth at 321 mV. At this potential (321 mV), current density increased with no increase in polarisation potential. After reverse scanning, the sample re-passivated at a repassivation potential of -85 mV.

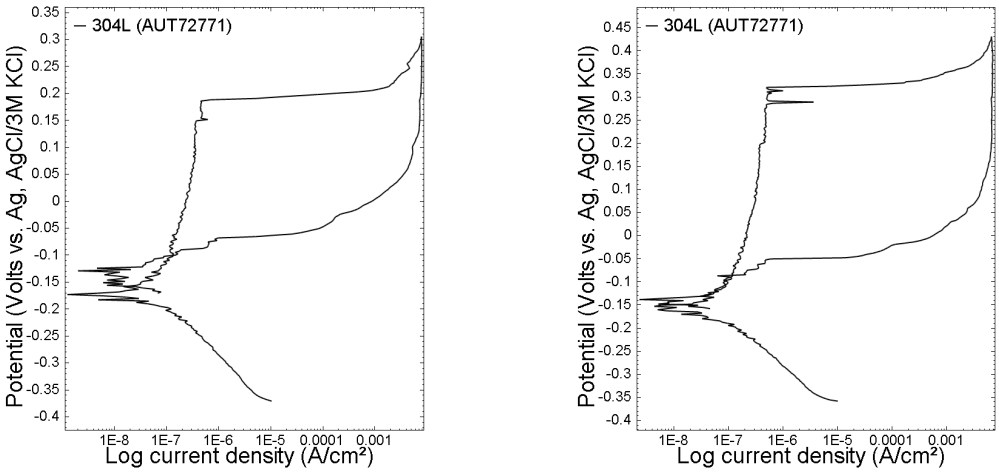

(a) Sample X-1 (b) Sample X-2

Figure 4.7 Potentiodynamic polarisation curves of 304L stainless steel samples in 3.5% NaCl aerated solution at 25°C ±1°C.

4.4.2 Potentiodynamic Polarisation Results of 904L Stainless Steel

Figures 4.8 (a) and (b) are potentiodynamic polarisation curves obtained when 904L stainless steel samples were anodically polarised in 3.5% NaCl aerated solution at 25°C ±1°C following the procedure discussed in section 3.7. Sample Y-1 was scanned from -292 mV, passing through the observed corrosion potential of -92 mV. At 721 mV and 843 mV a drastic increase in current density was observed, suggesting the points of pit initiation. The sample recovered slightly before experiencing stable pit growth at 887 mV. At this potential (887 mV), current density increased with a slight increase in polarisation potential. After reverse scanning, the sample re-passivated at a repassivation potential of 82 mV. Sample Y-2 was scanned from -321 mV, passing through the observed corrosion potential of -121 mV. Between 290 mV and 279 mV a spike increase in current density were observed, suggesting points of pit initiation. The sample fully recovered before experiencing stable pit growth at

951 mV. At this potential (951 mV), current density increased with a slight increase in polarisation potential. After reverse scanning, the sample did not repassivate.

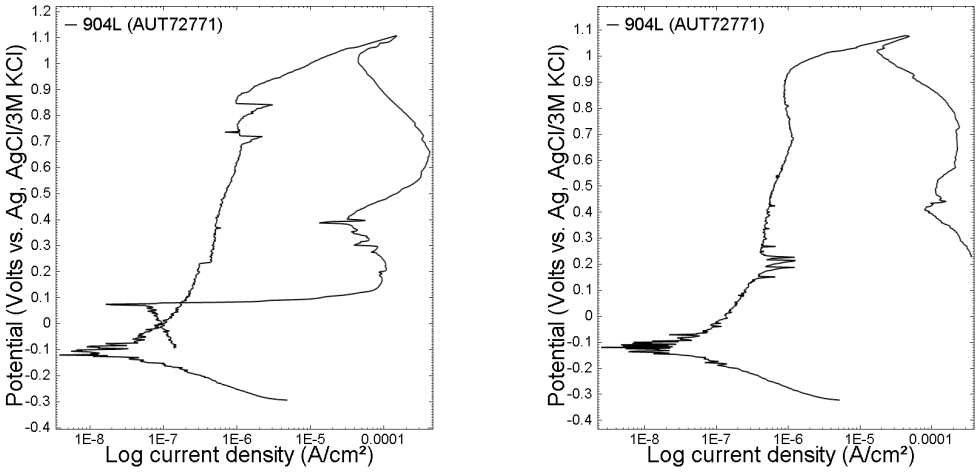

(a) Sample Y-1 (b) Sample Y-2

Figure 4.8 Potentiodynamic polarisation curves of 904L stainless steel samples in 3.5% NaCl aerated solution at 25°C ±1°C.

4.4.3 Potentiodynamic Polarisation Results of LDX2101 Stainless Steel

Figures 4.9 (a) and (b) are potentiodynamic polarisation curves obtained when LDX2101 stainless steel samples were anodically polarised in 3.5% NaCl aerated solution at 25°C ±1°C following the procedure discussed in section 3.7.

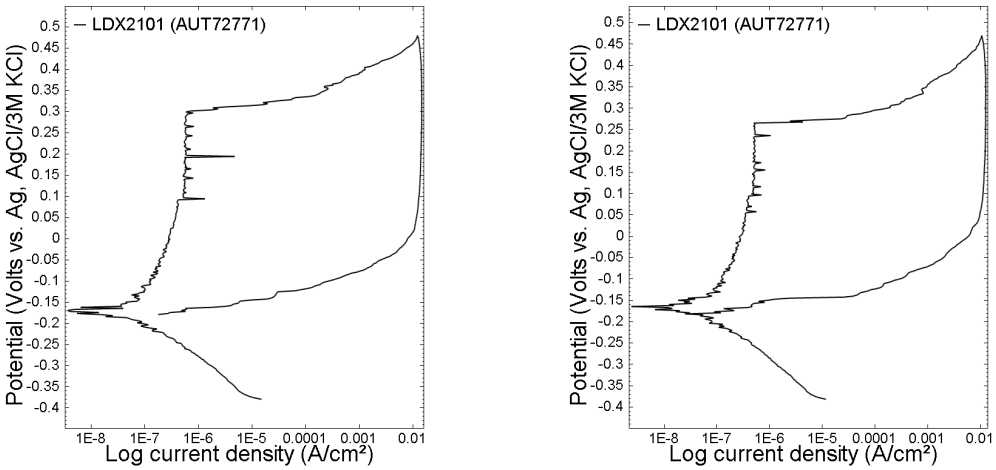

(a) Sample Z-1 (b) Sample Z-2

Figure 4.9 Potentiodynamic polarisation curves of LDX2101 stainless steel samples in 3.5% NaCl aerated solution at 25°C ±1°C.

Sample Z-1 was scanned from -379 mV, passing through the observed corrosion potential of -179 mV. Between 95 mV and 266 mV spike increases in current density were observed, suggesting pit initiation and propagation. The sample recovered slightly before experiencing stable pit growth at 300 mV. At this potential (300 mV), current density increased with no increase in polarisation potential. After reverse scanning, the sample did not repassivate. Sample Z-2 was scanned from -381 mV, passing through the observed corrosion potential of -181 mV. Between 58 mV and 237mV spike increases in current density were observed, suggesting pit initiation and propagation. The sample recovered slightly before experiencing stable pit growth at 266 mV. At this potential (266 mV), current density increased with no increase in polarisation potential. After reverse scanning, the sample re-passivated at a repassivation potential of -181 mV.

4.4.4 Potentiodynamic Polarisation Results of LDX2101+0.13%wt Ru Alloy

Figures 4.10 (a) and (b) are potentiodynamic polarisation curves obtained when LDX2101+0.13%wt Ru alloy samples were anodically polarised in 3.5% NaCl aerated solution at 25^{o}C ±1^{o}C following the procedure discussed in section 3.7.

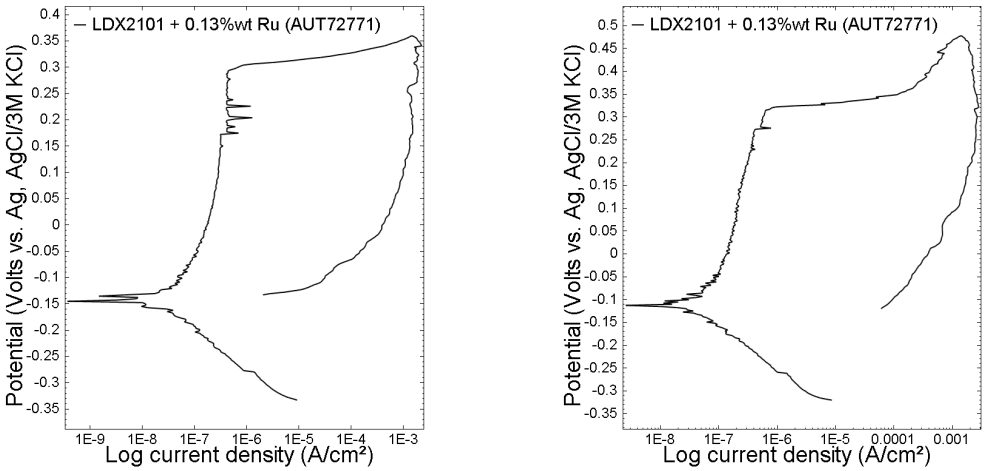

(a) Sample A-1 (b) Sample A-2

Figure 4.10 Potentiodynamic polarisation curves of LDX2101+0.13%wt Ru alloy samples in 3.5% NaCl aerated solution at 25^{o}C ±1^{o}C.

Sample A-1 was scanned from -332 mV, passing through the observed corrosion potential of -132 mV. Between 175 mV and 240 mV spike increases in current density were observed,

suggesting pit initiation and propagation. The sample recovered slightly before experiencing stable pit growth at 295 mV. At this potential (295 mV), current density increased with no increase in polarisation potential. After reverse scanning, the sample did not repassivate. Sample A-2 was scanned from -319 mV, passing through the observed corrosion potential of -119 mV. At 276 mV spike increase in current density was observed, suggesting the point of pit initiation. The sample recovered slightly before experiencing stable pit growth at 315 mV. At this potential (315 mV), current density increased with no increase in polarisation potential. After reverse scanning, the sample did not repassivate.

4.4.5 Potentiodynamic Polarisation Results of LDX2101+0.20%wt Ru Alloy

Figures 4.11 (a) and (b) are potentiodynamic polarisation curves obtained when LDX2101+0.20%wt Ru alloy samples were anodically polarised in 3.5% NaCl aerated solution at 25°C ±1°C following the procedure discussed in section 3.7.

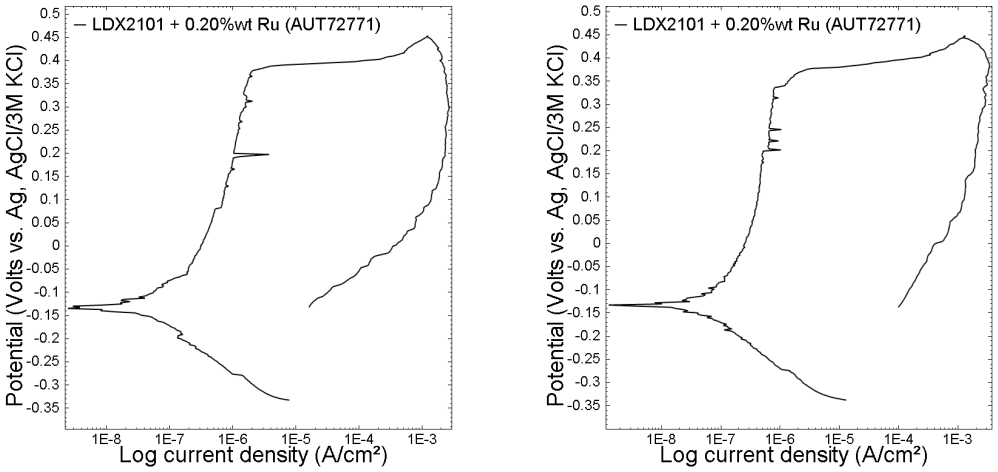

(a) Sample B-1 (b) Sample B-2

Figure 4.11 Potentiodynamic polarisation curves of LDX2101+0.20%wt Ru alloy samples in 3.5% NaCl aerated solution at 25°C ±1°C.

Sample B-1 was scanned from -332 mV, passing through the observed corrosion potential of -132 mV. Between 198 mV and 313 mV spike increases in current density were observed, suggesting pit initiation and propagation. The sample recovered slightly before experiencing stable pit growth at 379 mV. At this potential (379 mV), current density increased with no increase in polarisation potential. After reverse scanning, the sample did not repassivate.

Sample B-2 was scanned from -337 mV, passing through the observed corrosion potential of -137 mV. Between 203 mV and 315 mV spike increases in current density were observed, suggesting pit initiation and propagation. The sample recovered slightly before experiencing stable pit growth at 337 mV. At this potential (337 mV), current density increased with no increase in polarisation potential. After reverse scanning, the sample did not repassivate.

4.4.6 Potentiodynamic Polarisation Results of LDX2101+0.31%wt Ru Alloy

Figures 4.12 (a) and (b) are potentiodynamic polarisation curves obtained when LDX2101+0.31%wt Ru alloy samples were anodically polarised in 3.5% NaCl aerated solution at 25°C ±1°C following the procedure discussed in section 3.7. Sample C-1 was scanned from -335 mV, passing through the observed corrosion potential of -135 mV. At 420 mV a slight increase in current density was observed, suggesting the point of pit initiation. The sample fully recovered before experiencing stable pit growth at 592 mV. At this potential (592 mV), current density increased with no increase in polarisation potential. After reverse scanning, the sample did not repassivate.

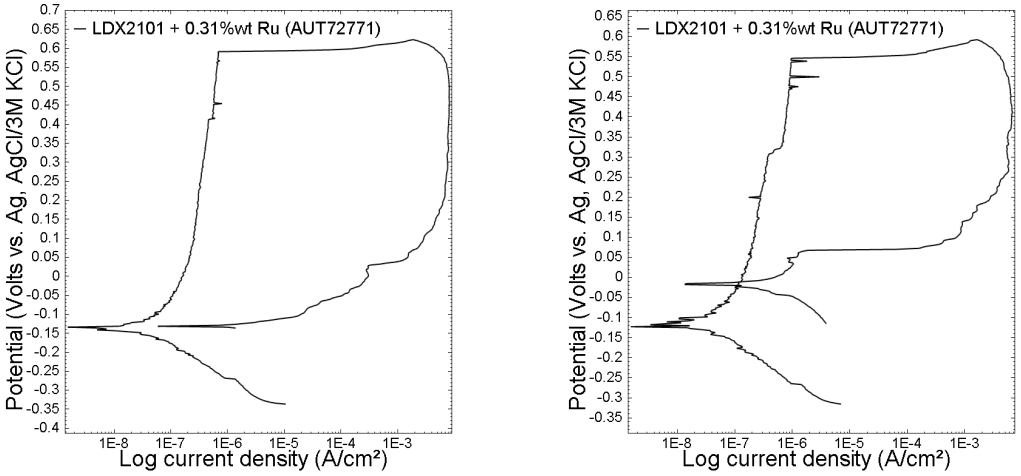

(a) Sample C-1 (b) Sample C-2

Figure 4.12 Potentiodynamic polarisation curves of LDX2101+0.31%wt Ru alloy samples in 3.5% NaCl aerated solution at 25°C ±1°C.

Sample C-2 was scanned from -315 mV, passing through the observed corrosion potential of -115 mV. At 310 mV a slight increase in current density was observed, suggesting the point of pit initiation. The sample fully recovered before experiencing stable pit growth at 547 mV. At this potential (547 mV), current density increased with no increase in polarisation

potential. After reverse scanning, the sample re-passivated at a repassivation potential of -10 mV.

4.4.7 Potentiodynamic Polarisation Results of LDX2101+0.66%wt Ru Alloy

Figures 4.13 (a) and (b) are potentiodynamic polarisation curves obtained when LDX2101+0.66%wt Ru alloy samples were anodically polarised in 3.5% NaCl aerated solution at 25°C ±1°C following the procedure discussed in section 3.7. Sample D-1 was scanned from -309 mV, passing through the observed corrosion potential of -109 mV. At 260 mV and 485 mV, slight increases in current density were observed, suggesting the points of pit initiation and propagation. The sample fully recovered before experiencing stable pit growth at 653 mV. At this potential (653 mV), current density increased with no increase in polarisation potential. After reverse scanning, the sample did not repassivate. Sample D-2 was scanned from -261 mV, passing through the observed corrosion potential of -61 mV. At 275 mV, 430 mV and 590 mV, spike increases in current density were observed, suggesting the points of pit initiation and propagation.

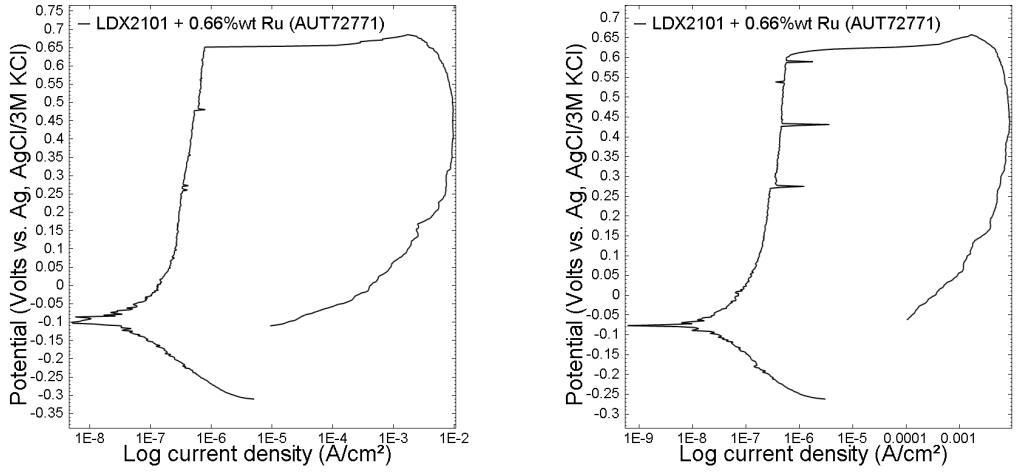

(a) Sample D-1 (b) Sample D-2

Figure 4.13 Potentiodynamic polarisation curves of LDX2101+0.66%wt Ru alloy samples in 3.5% NaCl aerated solution at 25°C ±1°C.

After the spike increase in current density at 590 mV, the sample recovered slightly before experiencing stable pit growth at 600 mV. At this potential (600 mV), current density increased with no increase in polarisation potential. After reverse scanning, the sample did not repassivate.

Figures 4.13 (a) and (b) are potentiodynamic polarisation curves obtained when LDX2101+0.66%wt Ru alloy samples were anodically polarised in 3.5% NaCl de-aerated solution at 25°C ±1°C following the procedure discussed in section 3.7. The solution was purged according to the procedure discussed in section 3.7.3.

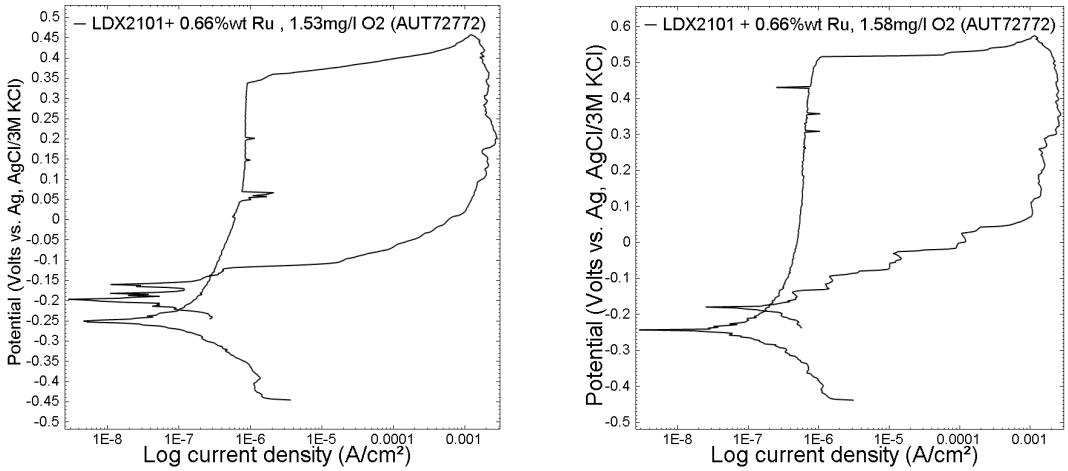

(a) Sample D-3 (b) Sample D-4

Figure 4.14 Potentiodynamic polarisation curves of LDX2101+0.66%wt Ru alloy samples in 3.5% NaCl de-aerated solution at 25°C ±1°C.

For sample D-3, the oxygen content in the solution was 1.53 mg/l after purging. The sample was then scanned from -309 mV, passing through the observed corrosion potential of -445 mV. Between 45 mV and 70 mV, slight increases in current density were observed, suggesting the points of pit initiation. At 150 mV and 200 mV further spike increases in current density were observed, suggesting pit propagation. After spike increases in current density at 200 mV, the sample fully recovered before experiencing stable pit growth at 339 mV. At this potential (339 mV), current density increased with no increase in polarisation potential. After reverse scanning, the sample re-passivated at a repassivation potential of -140 mV. For sample D-4, the oxygen content in the solution was 1.58 mg/l after purging. The sample was then scanned from -437 mV, passing through the observed corrosion potential of -237 mV. At 310 mV and 360 mV, spike increases in current density were observed, suggesting the points of pit initiation and propagation. After the spike increase in current density at 360 mV, the sample fully recovered before experiencing stable pit growth at 515 mV. At this potential (515 mV), current density increased with no increase

in polarisation potential. After reverse scanning, the sample re-passivated at a repassivation potential of -173 mV.

4.4.8 Summary of Potentiodynamic Polarisation Results

From the polarisation curves (section 4.4.1 to 4.4.7) corrosion rate, pitting potential and corrosion current were calculated and the results are summarised in Table 4.2 below. Table 4.3 show results of the oxygen content before and after purging for the potentiodynamic polarisation of samples D-3 and D4.

Table 4.2 Table of results for all potentiodynamic polarisation tests in 3.5%NaCl aqueous solution.

Sample Designation	Alloy Composition	Area (cm^2)	Corrosion Rate mm/yr	Observed E_{corr} (mV)	Calculated E_{corr} (mV)	I_{corr} $\eta A/cm^2$	Polarization Resistance (MΩ)	E_{pit} (mV)	Solution Purged
X-1	304L	0.7876	0.000228	-170	-169	19.64	0.89	187	No
X-2	304L	0.7760	0.000218	-157	-158	18.72	0.84	321	No
Y-1	904L	0.9316	0.000137	-92	-108	11.82	1.32	887	No
Y-2	904L	0.7045	0.000125	-121	-118	10.73	1.59	951	No
Z-1	LDX2101	0.7413	0.000185	-179	-154	17.78	1.09	300	No
Z-2	LDX2101	0.7523	0.000216	-181	-174	18.61	1.05	266	No
A-1	LDX2101 +0.13%wt Ru	0.5541	0.000181	-132	-144	17.45	0.84	295	No
A-2	LDX2101 +0.13%wt Ru	0.5860	0.000180	-119	-112	15.45	0.95	315	No
B-1	LDX2101 +0.20%wt Ru	0.5865	0.000177	-132	-134	17.05	0.76	379	No
B-2	LDX2101 +0.20%wt Ru	0.5807	0.000177	-137	-135	15.27	0.87	337	No
C-1	LDX2101 +0.31%wt Ru	0.6298	0.000173	-135	-133	16.71	1.12	592	No
C-2	LDX2101 +0.31%wt Ru	0.5947	0.000168	-165	-166	14.43	1.33	547	No
D-1	LDX2101 +0.66%wt Ru	0.4894	0.000152	-109	-101	14.65	1.47	653	No
D-2	LDX2101 +0.66%wt Ru	0.5567	0.000155	-61	-75	13.35	1.58	600	No
D-3	LDX2101 +0.66%wt Ru	0.4762	0.000198	-245	-250	17.05	0.81	339	Yes
D-4	LDX2101 +0.66%wt Ru	0.5036	0.000231	-237	-241	19.85	0.73	515	Yes

Where: E_{corr} = Corrosion potential

E_{pit} = Pitting potential

Table 4.3 Oxygen content before and after solution purging.

Sample Designation	O_2 Content (mg/l)	
	Before Purging	After Purging
D-3	7.14	1.53
D-4	7.24	1.58

4.5 MICROSCOPY OF CORRODED SURFACES AFTER POTENTIODYNAMIC POLARISATION

After potentiodynamic polarisation, the exposed surfaces were examined under a metallurgical microscope at 100X magnification for physical presence of pits. Pits were observed on the surface of all evaluated samples, but the frequency and size of the pits differed with 2101LDX without ruthenium suffering severe pits as compared to 2101LDX with 0.66%wt Ru. Detailed results of these evaluations are discussed in the following sections where, an area of 4 mm^2 was chosen as the best representation of the exposed surface area for the analysis for each sample. The summary of the results are shown in Table 4.4.

4.5.1 Pits observed on LDX2101 samples

Figure 4.15 shows the image of the pits that were observed on LDX2101 without ruthenium added to it after potentiodynamic polarisation of samples Z-1 and Z-2 in Table 4.2.

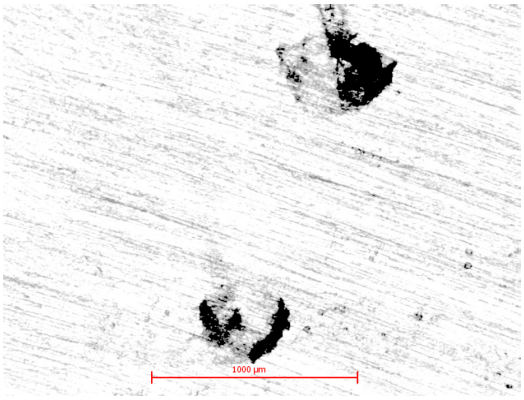

Figure 4.15 Pits observed on LDX2101 samples after potentiodynamic polarisation examined at 100X magnification.

The images in Figure 4.15 shows that two pits with an average diameter of 0.59 mm were observed in every 4 mm^2 of exposed surface area of the samples. This translated to a total area of 0.138 mm^2 suffering from pitting corrosion in every 1 mm^2 of exposed surface area during the samples potentiodynamic polarisation evaluation.

4.5.2 Pits observed on LDX2101+0.13%wt Ru samples

Figure 4.16 is a representation of the pits that were observed on LDX2101 with 0.13%wt Ru added to it after potentiodynamic polarisation of samples A-1 and A-2 in Table 4.2. The image in Figure 4.16 shows that one pit with an average diameter of 0.67 mm was observed in every 4 mm^2 of exposed surface area of the samples. This translated to a total area of 0.089 mm^2 suffering from pitting corrosion in every 1 mm^2 of exposed surface area during the samples potentiodynamic polarisation evaluation.

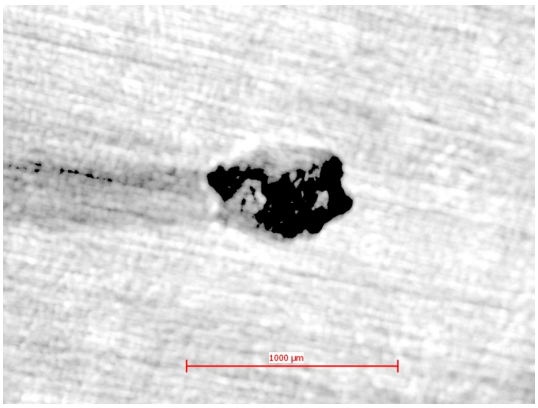

Figure 4.16 Pits observed on LDX2101 with 0.13% Ruthenium samples after potentiodynamic polarisation examined at 100X magnification.

4.5.3 Pits observed on LDX2101+0.20%wt Ru samples

Figure 4.17 is a representation of the pits that were observed on LDX2101 with 0.20%wt Ru added to it after potentiodynamic polarisation of samples B-1 and B-2 in Table 4.2. The image in Figure 4.17 shows that one pit with an average diameter of 0.59 mm was observed in every 4 mm^2 of exposed surface area of the samples. This translated to a total area of

0.067 mm^2 suffering from pitting corrosion in every 1 mm^2 of exposed surface area during the samples potentiodynamic polarisation evaluation.

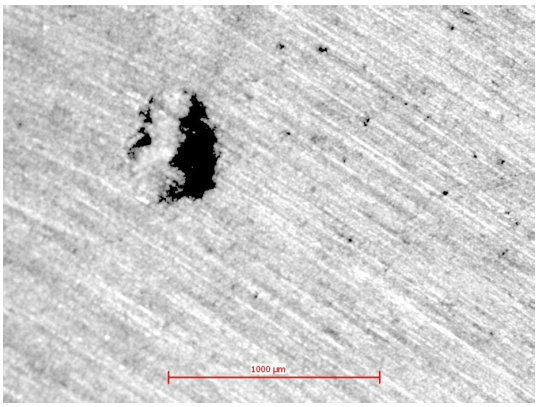

Figure 4.17 Pits observed on LDX2101 with 0.20% Ruthenium samples after potentiodynamic polarisation examined at 100X magnification.

4.5.4 Pits observed on LDX2101+0.31%wt Ru samples

Figure 4.18 is a representation of the pits that were observed on LDX2101 with 0.31%wt Ru added to it after potentiodynamic polarisation of samples C-1 and C-2 in Table 4.2. The image in Figure 4.18 shows that one pit with an average diameter of 0.31 mm was observed in every 4 mm^2 of exposed surface area of the samples. This translated to a total area of 0.019 mm^2 suffering from pitting corrosion in every 1 mm^2 of exposed surface area during the samples potentiodynamic polarisation evaluation.

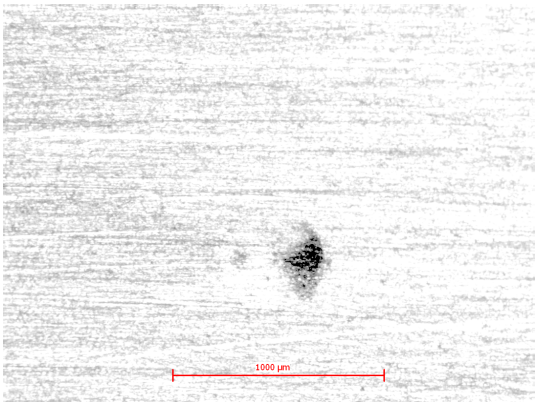

Figure 4.18 Pits observed on LDX2101 with 0.31% Ruthenium sample after potentiodynamic polarisation examined at 100X magnification.

4.5.5 Pits observed on LDX2101+0.66%wt Ru samples

Figure 4.19 is a representation of the pits that were observed on LDX2101 with 0.66%wt Ru added to it after potentiodynamic polarisation of samples D-1 and D-2 in Table 4.2. The image in Figure 4.19 shows that one pit with an average diameter of 0.18 mm was observed in every 4 mm^2 of exposed surface area of the samples. This translated to a total area of 0.007 mm^2 suffering from pitting corrosion in every 1 mm^2 of exposed surface area during the samples potentiodynamic polarisation evaluation.

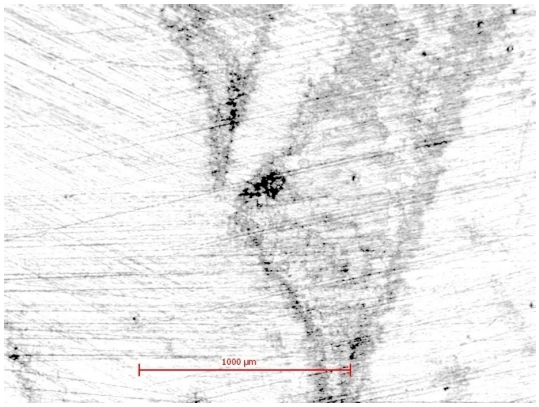

Figure 4.19 Pits observed on LDX2101 with 0.66% Ruthenium samples after potentiodynamic polarisation examined at 100X magnification.

4.5.6 Summary of microscopy results

Table 4.4 provide the summary of the results obtained from the microscopy of corroded surfaces after potentiodynamic polarisation (section 4.5.1 to 4.5.5). The area under consideration ($4mm^2$) is a close representation of the evaluated sample.

Table 4.4 Summary of results from microscopy of corroded surfaces.

	LDX2101	LDX2101+ 0.13%wt Ru	LDX2101+ 0.20%wt Ru	LDX2101+ 0.31%wt Ru	LDX2101+ 0.66%wt Ru
Pits frequency/4mm²	2	1	1	1	1
Average pit diameter (mm)	0.592	0.671	0.585	0.308	0.183
One pit average area (mm²)	0.275	0.354	0.269	0.075	0.026
Total area suffered pitting per 4mm²	0.550	0.354	0.269	0.075	0.026
Area suffered pitting per every mm²	0.138	0.088	0.067	0.019	0.007

Pit diameters were measured from the microscopic images (Figures 4.15 to 4.19). The results provided in Table 4.4 are based on having an integer number of pits in every 4 mm^2 as observed in the evaluated samples. Although the pit frequency is unlikely to be an integer for every 4 mm^2 area for a larger sample, the trend observed in the evaluated samples showed an almost inverse proportional relationship between the ruthenium added to LDX2101 stainless steel, and the frequency and severity of pits suffered by the samples. The results of the evaluated samples confirm that this trend will also apply to a larger sample.

4.6 PASSIVATION RESULTS OF LDX2101 STAINLESS STEEL AND LDX2101 WITH UP TO 0.66%WT RU

From the potentiodynamic polarisation curves, the passivation current density, passivation potential and passive potential range of LDX2101 samples and the produced alloys were recorded as presented in Table 4.5 below.

Table 4.5 Passivation current density, passivation potential and passive potential range of LDX2101 stainless steel and LDX2101 with up to 0.66%wt Ru obtained from potentiodynamic polarisation curves.

Sample Designation	Alloy Composition	Passivation I Density ηA/cm^2)	Passivation Potential (mV)	Pitting Potential (mV)	Passive potential range (mV)
Z-1	LDX2101	128	-108	300	408
Z-2	LDX2101	144	-108	266	374
A-1	LDX2101 +0.13%wt Ru	77	-69	295	364
A-2	LDX2101 +0.13%wt Ru	95	-41	315	356
B-1	LDX2101 +0.20%wt Ru	184	-61	379	440
B-2	LDX2101 +0.20%wt Ru	146	-59	337	396
C-1	LDX2101 +0.31%wt Ru	95	-67	592	659
C-2	LDX2101 +0.31%wt Ru	115	-27	547	574
D-1	LDX2101 +0.66%wt Ru	155	20	653	633
D-2	LDX2101 +0.66%wt Ru	102	24	600	576

5. DISCUSSIONS, CONCLUSIONS AND RECOMMENDATION

5.1 MICROSTRUCTURE

On all evaluated samples of LDX2101 stainless steel with small additions of ruthenium up to 0.66%wt Ru, the duplex stainless steel microstructure was maintained with a well-balanced solution of ferrite in austenite. There were also no any detrimental phases observed on the evaluated samples. The microstructures obtained from all produced alloys were also acceptable according to acceptable duplex stainless steel structures outlined in ASTM 932. This research therefore concluded that small additions of ruthenium of up to 0.66%wt Ru to LDX2101 stainless steel does not have any detrimental effect to the microstructure of the resulting alloy. Also, from the microstructural analysis results, it can also be concluded that as the % wt of ruthenium added to LDX2101 stainless steel was increased, the austenite-ferrite balance become more stable, and more resemblance to the microstructure of LDX2101 stainless steel without ruthenium as shown in Figure 5.1.

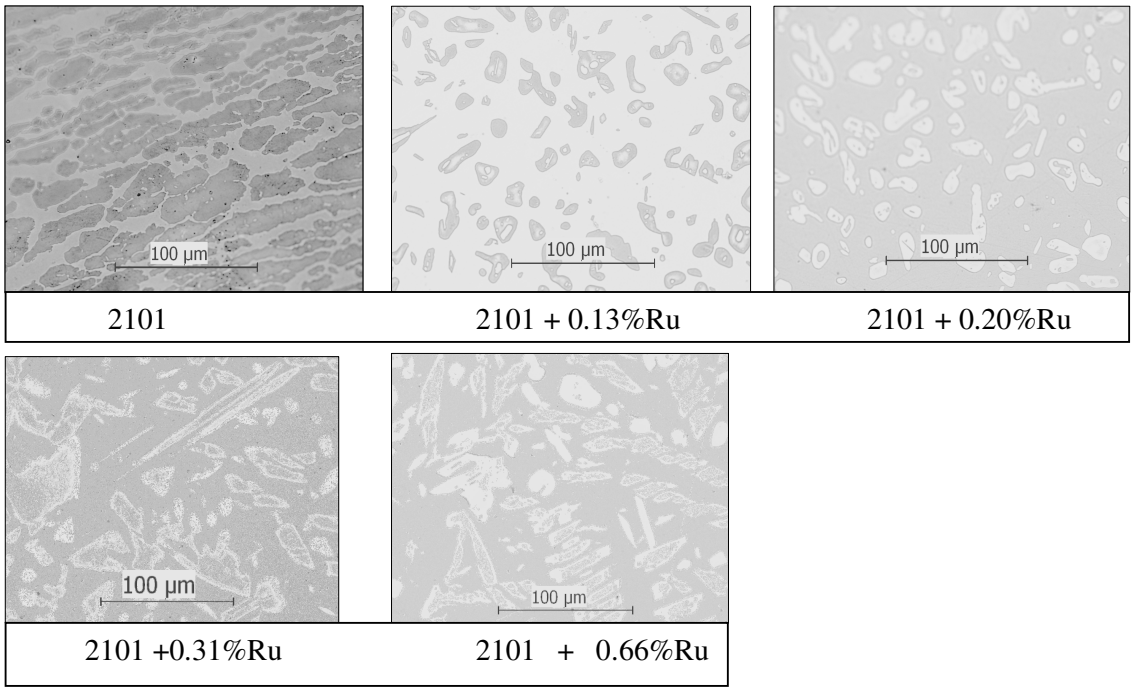

Figure 5.1 Comparison of microstructures obtained from analysing the alloys as examined at 500X magnification.

5.2 CORROSION RATE, CORROSION POTENTIAL & POLARISATION RESISTANCE

Adding platinum group metals to stainless steels has resulted in producing spontaneously passivated alloys with consequent decreasing corrosion rates (Higginson 1989; Mcgill 1990; Potgieter, Heyns & Skinner 1990; Streicher 1977, p. 51-55; Wolff 1999). The potentiodynamic polarisation results on all LDX2101 stainless steel alloys with small additions of ruthenium showed slight improvements in corrosion rate as compared to LDX2101 stainless steel alloy without any ruthenium added to it as shown in Table 4.2 and Figure 5.3. Also, both observed and calculated corrosion potentials (E_{corr}) results in the same Table 4.2, shows that the E_{corr} of the LDX2101 stainless steel alloy was shifted to more noble values from -179 mV and -181 mV (observed E_{corr}), -153 mV and -174 mV (calculated E_{corr}) for LDX2101 without Ruthenium to -60 mV and 109 mV (observed E_{corr}), -75 mV and -101 mV (calculated E_{corr}) for LDX2101 stainless steel alloy with 0.66%wt Ru. Figure 5.2 shows the trend on corrosion potential which was observed on the evaluated samples.

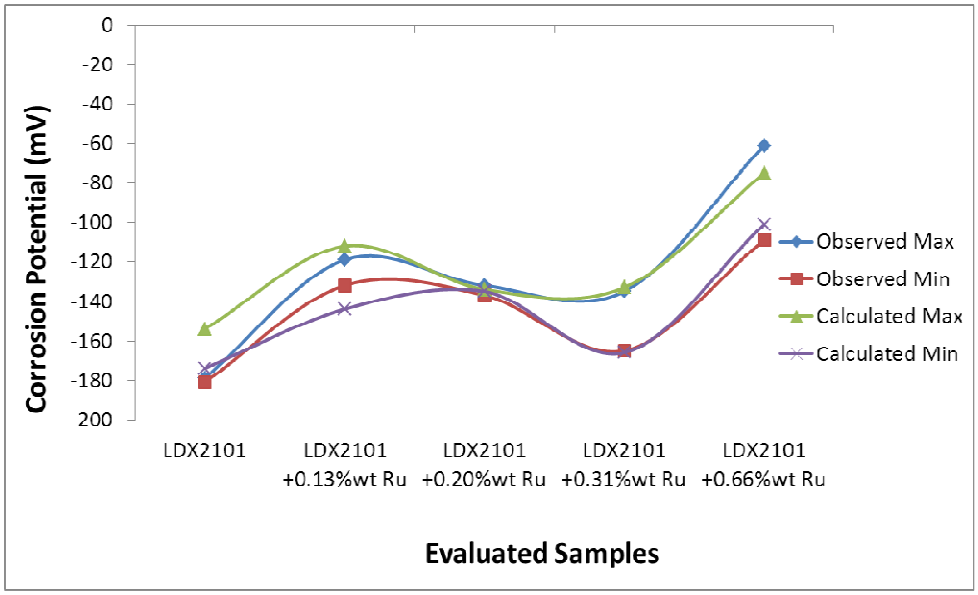

Figure 5.2 Comparison of corrosion potentials of LDX2101 without Ru to LDX2101 with up to 0.66%wt Ru.

The corrosion current density (I_{corr}) was also reduced from 17.78 ηA/cm^2 and 18.61 ηA/cm^2 on LDX2101 stainless steel alloy without ruthenium to 13.35 ηA/cm^2 and 14.65 ηA/cm^2 for

LDX2101 stainless steel alloy with 0.66%wt Ru which resulted in an improvement in polarisation resistance Figure 5.3 and 5.4.

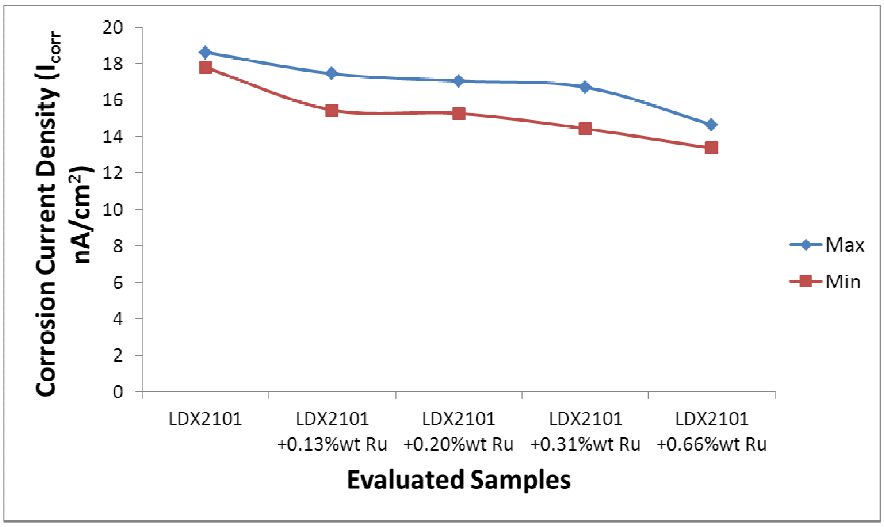

Figure 5.3 Comparison of corrosion current density of LDX2101 without Ru to LDX2101 with up to 0.66%wt Ru.

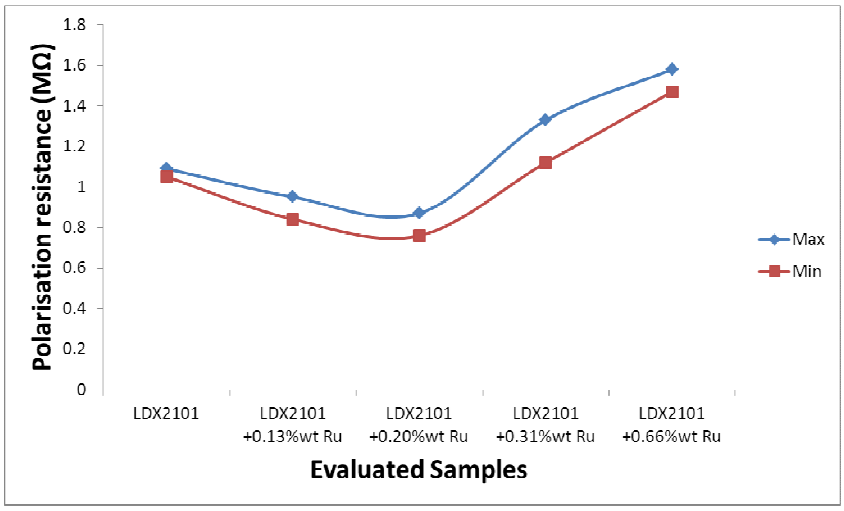

Figure 5.4 Comparison of polarisation resistance of LDX2101 without Ru to LDX2101 with up to 0.66%wt Ru.

Considering the Faraday's law equation (2) page 41, the reduction in corrosion current should result in reduction in corrosion rate (R_M) of these alloys since all other parameters are the

same. This is in agreement with the corrosion rate values directly extracted from the Metrohm Autolab Nova software results of the potentiodynamic polarisation curves which indicated a reduction in corrosion rate from 0.000185 mm/yr and 0.000216 mm/yr on LDX2101 stainless steel alloy without ruthenium to 0.000152 and 0.000155 mm/yr on LDX2101 stainless steel alloy with 0.66%wt Ru also shown in Figure 5.5.

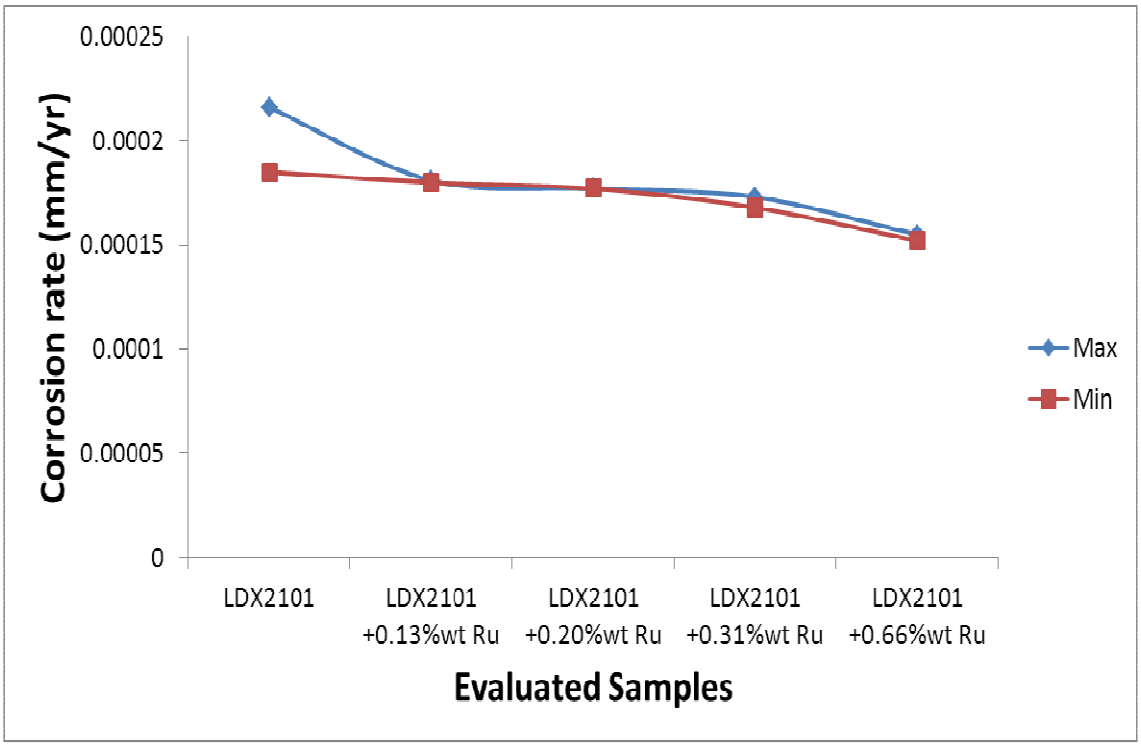

Figure 5.5 Comparison of corrosion rate of LDX2101 without Ru to LDX2101 with up to 0.66%wt Ru.

Although all the improvements in corrosion potential, corrosion current, polarisation resistance and corrosion rate were not significant, from the results of this experiment, it is concluded that small additions of ruthenium of up to 0.66%wt Ru to LDX2101 stainless steel, if it will not decrease the general corrosion behaviour of the resulting alloy; at least it will not have a detrimental effect on the resulting alloy.

5.1 PASSIVATION OF LDX2101 STAINLESS STEEL AND LDX2101 WITH UP TO 0.66%WT RU

The passivation electrochemical characteristics of LDX2101stainless steel were compared to the passivation electrochemical characteristics of LDX2101 with up to 0.66%wt Ru alloys as discussed in the following chapters.

5.1.1 Passivation current density

From the potentiodynamic polarisation results of LDX2101 stainless steel and all LDX2101 with up to 0.66%wt Ru alloys (section 4.4), it was observed that the passive current density corresponded to the critical current density. The current density did not decrease after the critical current density; it was just maintained for all these alloys. Figure 5.6 shows the comparison of the observed passive current density for these alloys. From Figure 5.6, it is observed that apart from LDX2101 with 0.2%wt Ru, all alloys with ruthenium up to 0.66%wt required less current to be passivated as compared to LDX2101 stainless steel without ruthenium.

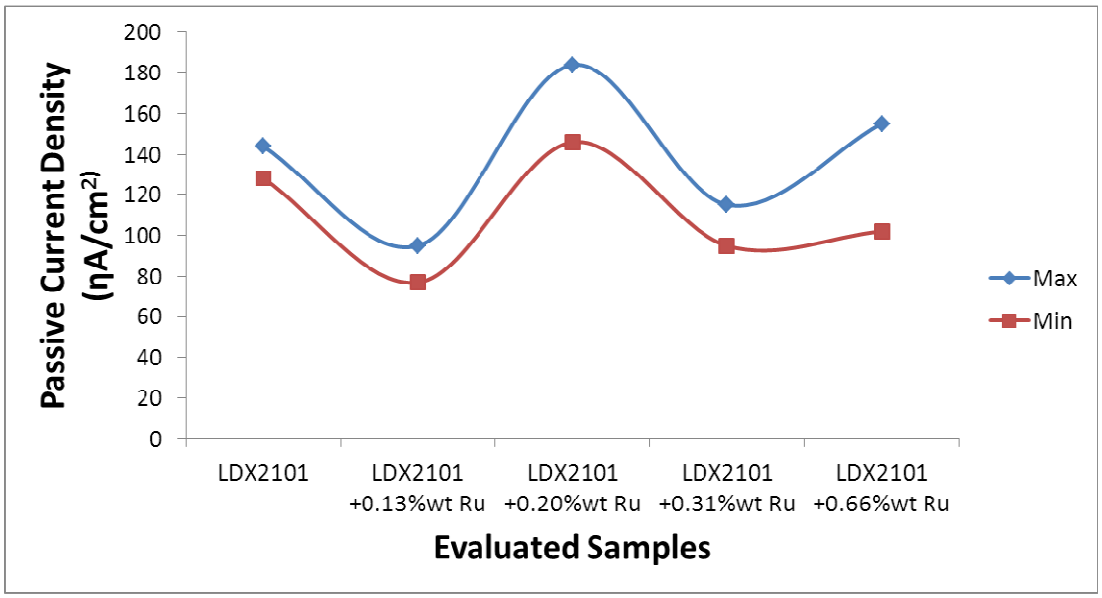

Figure 5.6 Comparison of passive current density of LDX2101 without Ru to LDX2101 with up to 0.66%wt Ru.

5.1.2 Passive potential range

The passive potential range was calculated as the difference between pitting potential and passive potential (Table 4.5) where, the passive potential is the potential corresponding to the critical current density. Figure 5.7 shows the comparison of the passive potential range of LDX2101 stainless steel without Ru to LDX2101 with up to 0.66%wt Ru. From Figure 5.7, it is observed that LDX2101 with up to 0.66%wt Ru alloys had significantly higher passive potential ranges compared to LDX2101 stainless steel without Ru apart from LDX2101 with 0.13%wt Ru. It was further observed that LDX2101 with 0.31%wt Ru had a higher passive potential range compared to LDX2101 with 0.66%wt Ru. It can therefore be concluded that adding ruthenium to LDX2101 stainless steel up to 0.66%wt Ru will increase the passive potential range of the alloy.

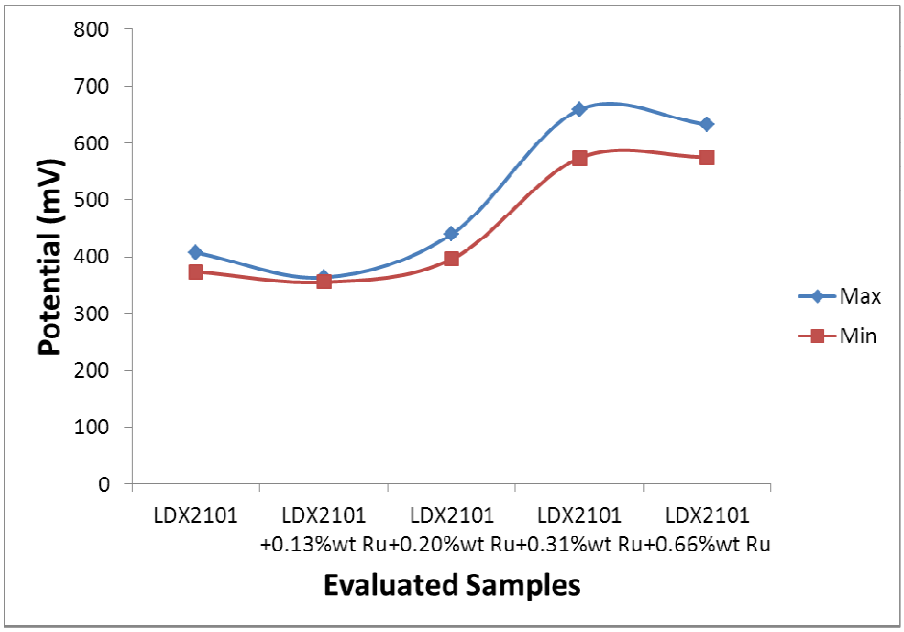

Figure 5.7 Comparison of passive potential range of LDX2101 without Ru to LDX2101 with up to 0.66%wt Ru.

5.2 PITTING CORROSION

Potentiodynamic polarisation results, summarised in Tables 4.2, indicated that the small addition of ruthenium of up to 0.66%wt Ru to LDX2101 stainless steel shifted the pitting potential (E_{pit}) to more noble values from 266 mV and 300 mV and for LDX2101 without

ruthenium up to 600 mV and 653 mV for LDX2101 stainless steel alloy with 0.66%wt Ru. This is also evident when the polarisation curves of LDX2101 without Ru is compared to polarisation curves of LDX2101 with incremental additions of ruthenium up to 0.66%wt Ru as shown in Figure 5.8.

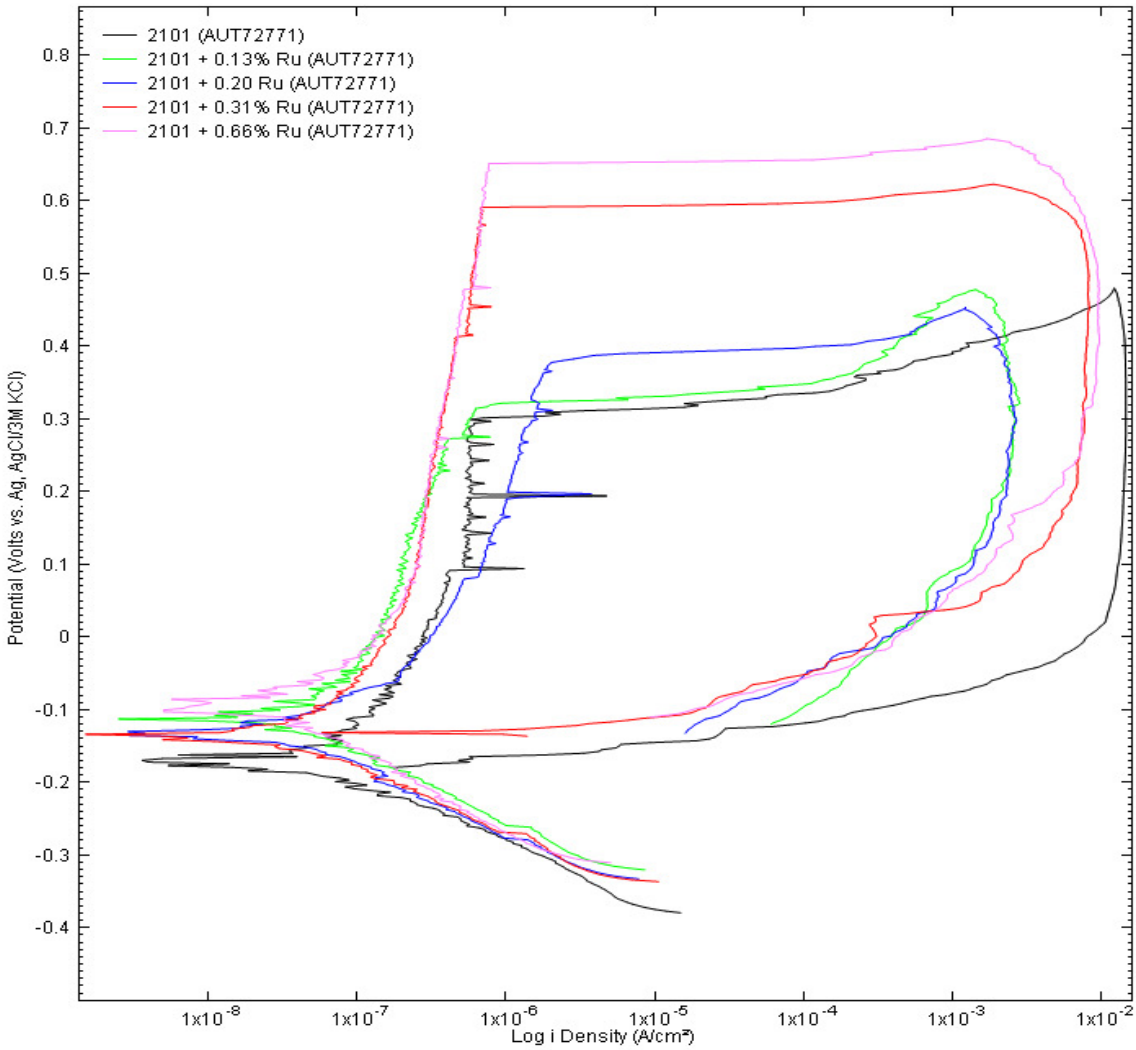

Figure 5.8 Potentiodynamic polarisation results of produced alloys and 2101LDX samples in 3.5% NaCl aerated solution at 25°C±1°C.

The shifting of the pitting potential was a steady incremental with every increase in the ruthenium percentage weight added to LDX2101 stainless steel up to 0.2%wt Ru, and then there was a significant jump when ruthenium content was increased from 0.2%wt Ru to

0.31%wt Ru. A steady incremental in pitting potential was also observed when ruthenium content was increased from 0.3%wt Ru to 0.6%wt Ru shown in Figure 5.9.

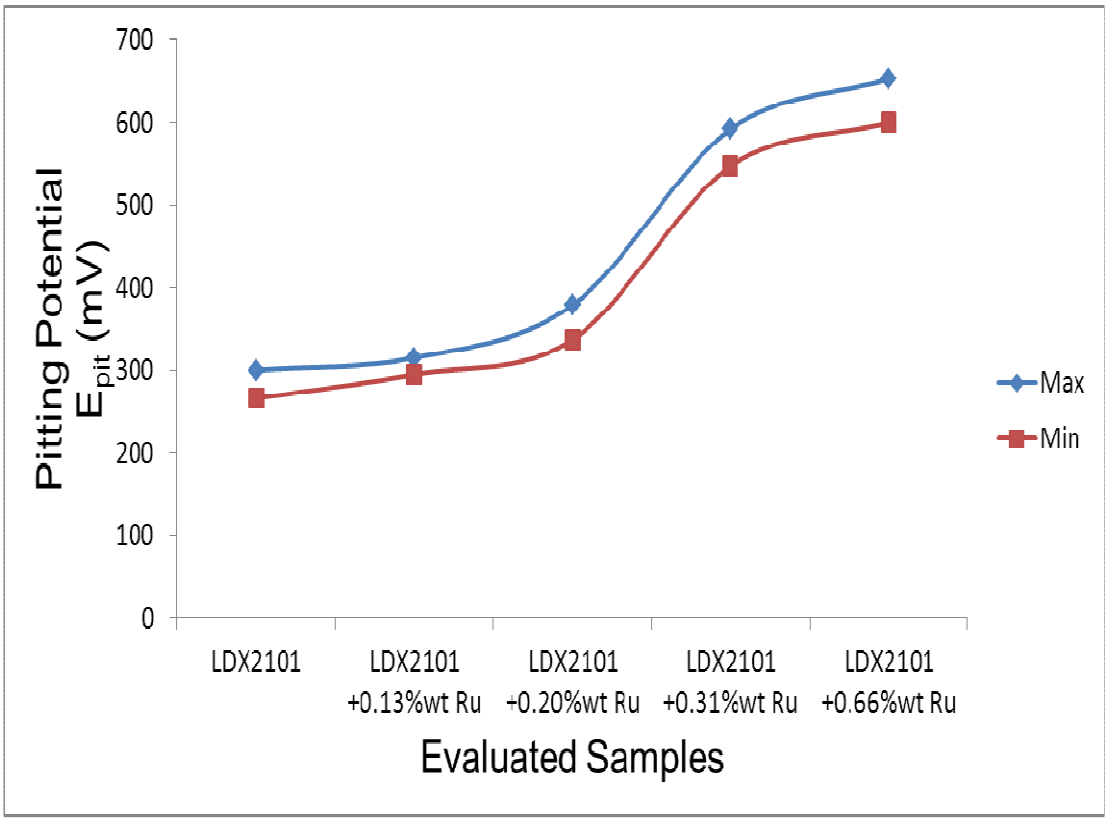

Figure 5.9 Comparison of pitting potentials of LDX2101 without Ru to LDX2101 with up to 0.66%wt Ru.

Since all experimental parameters were the same for the potentiodynamic polarisation test, including the surface finish of the evaluated samples, this improvement in E_{pit} is the direct effect of the addition of ruthenium. This also implies that small additions of ruthenium of up to 0.66%wt Ru to LDX2101 stainless steel has an effect that increases the strength of the thin protective layer formed on the surface of the resulting alloy when exposed to NaCl corrosive environments. This is in agreement with the work of El-Sayed et al. (2009) done on other duplex stainless steels with addition of ruthenium where, the presence of Ru, and its increasing content, enhance the passivation parameters on the duplex stainless steel surface against corrosion. It should also be noted that the improvements in pitting corrosion potentials observed in produced alloys containing 0.31%wt Ru and 0.66%wt Ru are well above any experimental margin of error. The potentiodynamic polarisation results were

further supported by the microscopy results of the corroded surface area as shown in Figure 5.10. The microscopy results of corroded surfaces showed a reduction in total corroded surface area with every increase in Ru added to the alloy. The images of samples of the alloy with 0.66%wt Ru as shown in Figure 4.19 also indicated that this alloy experienced the least pitting. Therefore, it can be concluded that small additions of ruthenium of up to 0.66%wt Ru to LDX2101 stainless steel will increase the pitting corrosion resistance of the resulting alloy.

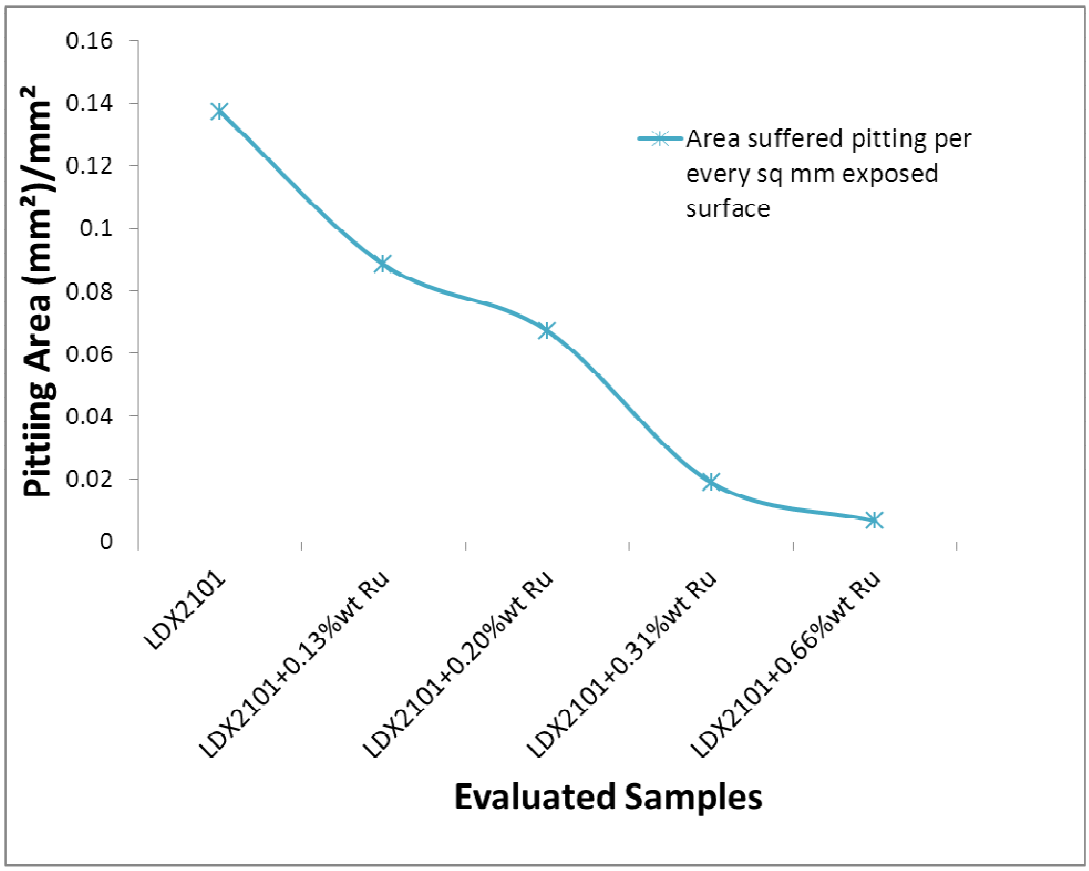

Figure 5.10 Results of microscopy of corroded surfaces showing the area that suffered pitting for every 1 mm^2 of the sample in consideration.

However, it was observed that with more than doubling the ruthenium content in the alloy from 0.31%wt Ru to 0.66%wt Ru, alloy C and D in Table 4.2 representing a 113% increase in ruthenium content by weight, there was a slight improvement in pitting corrosion resistance with pitting potential values indicating an increase from 592 mV to 652 mV representing a mere 10% increase. For economic viability, an alloy with 0.31%wt Ru would

be favourable as compare to an alloy with 0.66%wt Ru. However, the corrosive environment for the application will also determine which alloy to use.

5.3 COMPARISON WITH CONTROL ALLOY

For comparison sake, the performance of the alloy D in Table 4.2 with 66%wt Ru was compared to 304L, LDX2101 and 904L stainless steels as shown in Figures 5.11 and 5.12.

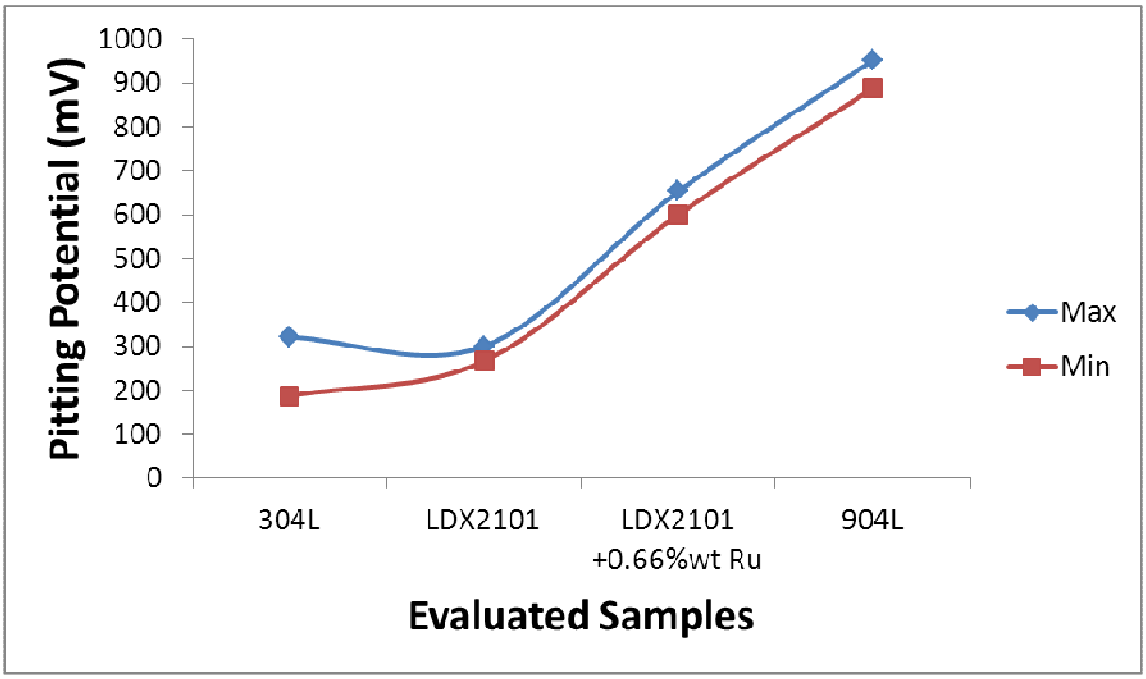

Figure 5.11 Comparison of pitting potentials of control alloys to LDX2101 with 0.66%wt Ru.

Under the experimental environment, 904L stainless steel experienced the least pitting corrosion. However, the LDX2101 stainless steel with 0.66%wt Ru alloy was more resistant to pitting corrosion compared to 304L stainless steel. The difference in pitting potentials observed in the potentiodynamic polarisation curves (Figure 5.1) between LDX2101 with 0.66%wt Ru alloy and 304L stainless steel was well above any experimental margin of error.

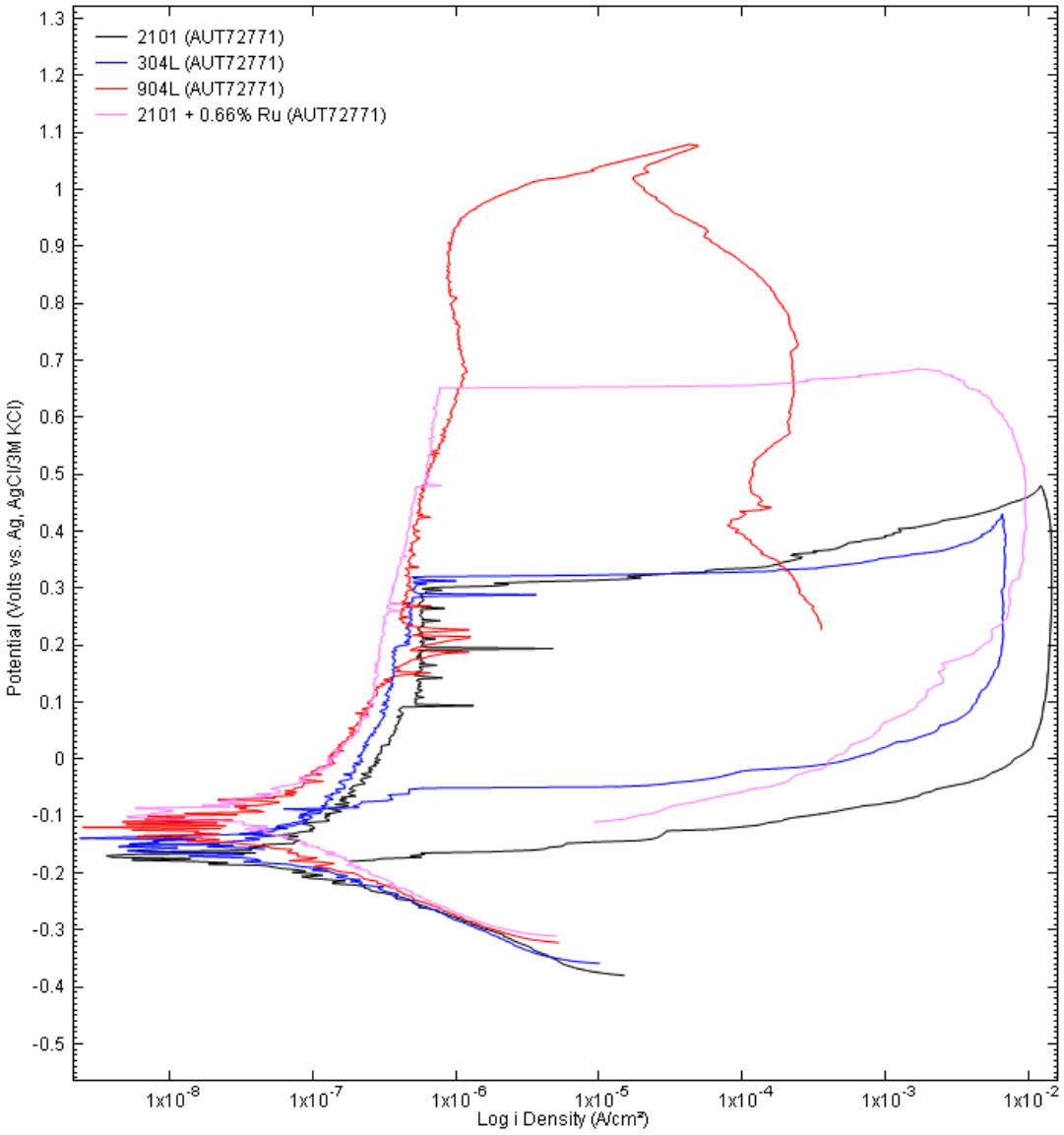

Figure 5.12 Potentiodynamic polarisation results of control alloys as compared to 2101LDX with 0.66% Ru in 3.5% NaCl aerated solution at 25°C±1°C

5.4 EFFECT OF OXYGEN CONTENT IN THE NaCl AQUEOUS SOLUTION

The potentiodynamic polarisation results for LDX2101 stainless steel with 0.66% ruthenium indicates that both pitting potential and corrosion potentials decreased with the reduction of oxygen in NaCl aqueous solution as shown in Figure 5.13 and 5.14. From Table 4.2, the

pitting potential reduced from 653 mV in aerated 3.56% NaCl solution to 515 mV and 339 mV when the oxygen content was reduced to 1.58 mg/l and 1.53 mg/l respectively in similar solution. This supports the notion that stainless steels rely on a source of oxygen to maintain their passive condition (Jones 1992; Szklarska-Smialowska 1986).

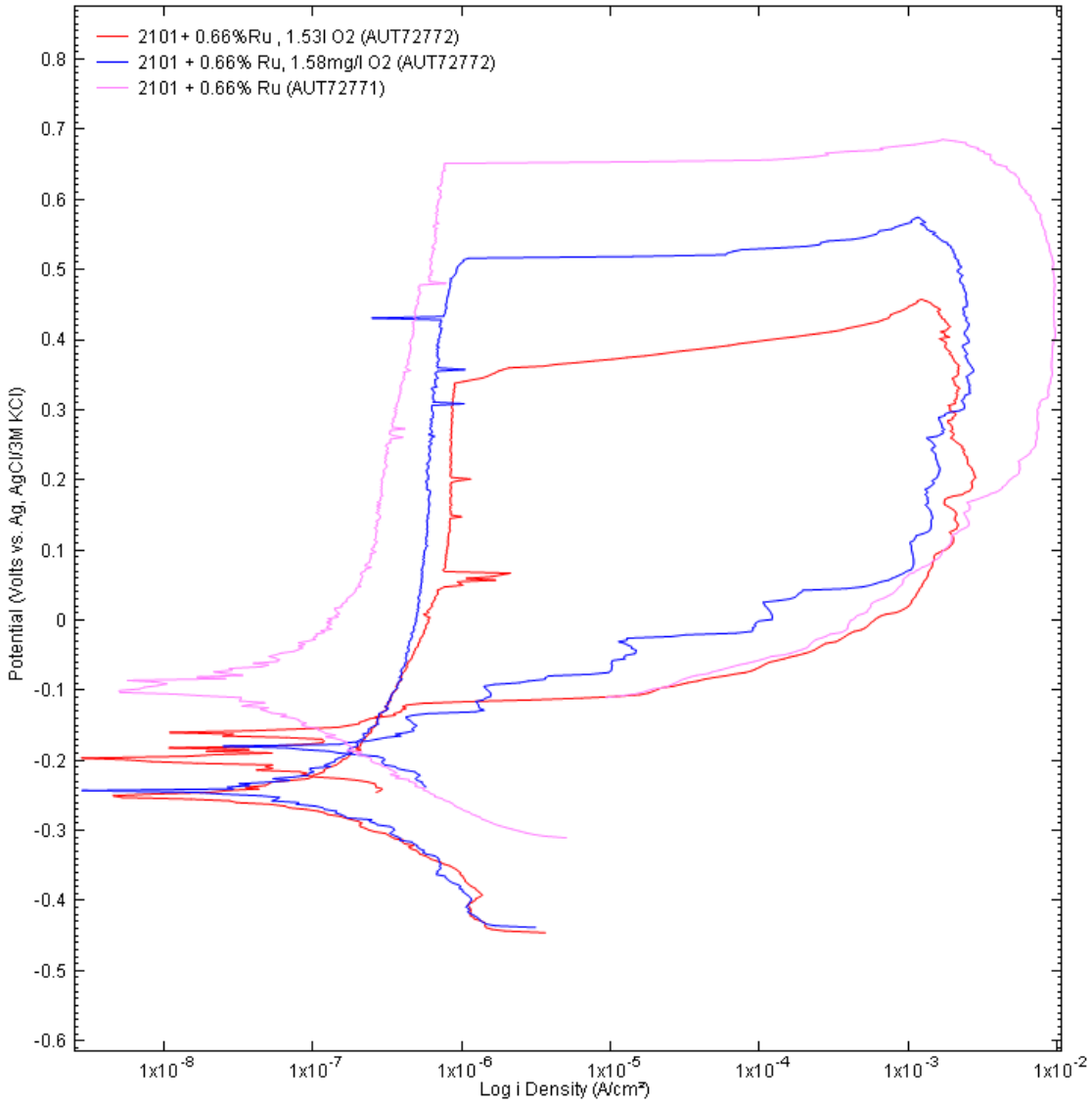

Figure 5.13 Performance of 2101LDX with 0.66% ruthenium performed in oxygen staved 3.56 NaCl aqueous solution in comparison to aerated 3.56% NaCl aqueous solution

Another observation was that while the potentiodynamic polarisation curves of LDX2101 with 0.66%wt Ru in an aerated solution indicated the alloy did not repassivate, the same alloy re-passivated when the solution was purged. This may be due to the fact that the alloy was

polarised to lower potentials in purged solution than in aerated solution as also observed by Trepanier and Pelton (2006).

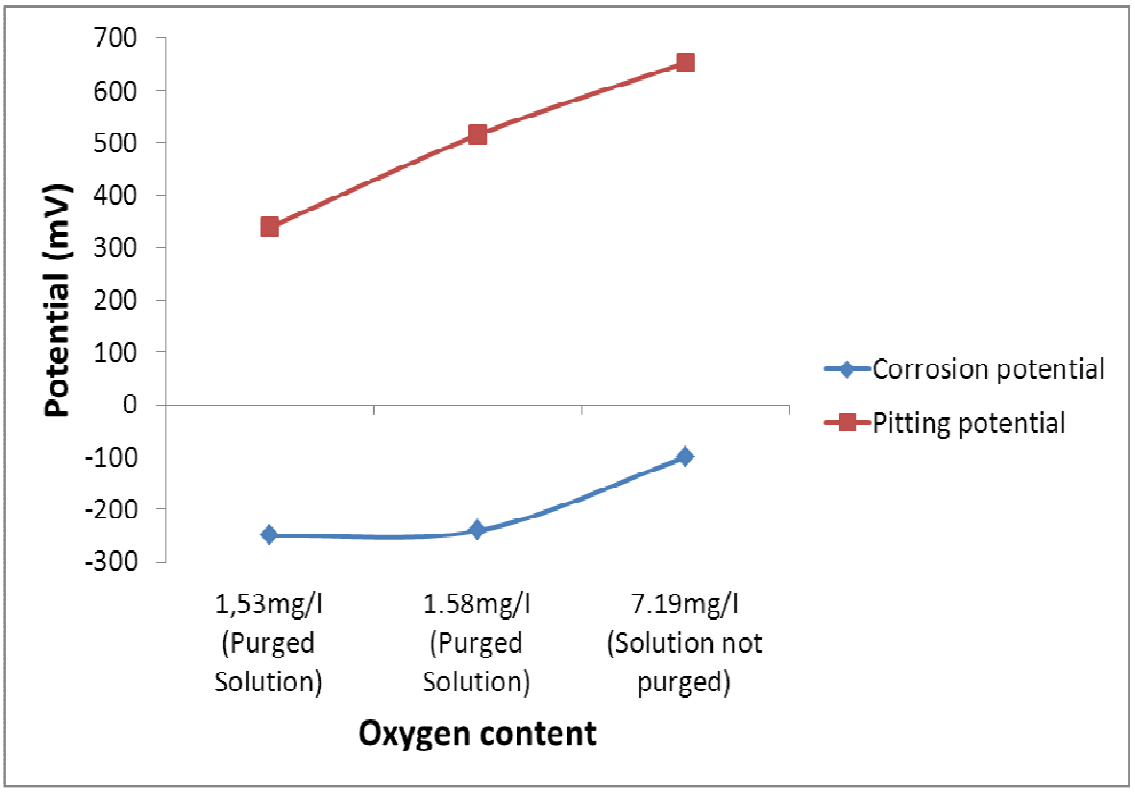

Figure 5.14 Comparison of corrosion and pitting potentials of LDX2101+0.66%wt Ru alloy with different solution oxygen content.

5.5 COMMERCIAL VIABILITY

Another important factor in choosing engineering materials is their commercial viability. Table 5.1 is a summary of the cost analysis that was performed in order to verify the commercial viability of the produced alloys as compared to the gain made in the increase of the alloys pitting corrosion resistance. Based on the analysis, commercial viability of alloys containing ruthenium was less favourable as the benefit ruthenium brought did not offset the cost of adding ruthenium to the alloy. In addition to this, the costs of all alloys with ruthenium were much higher than the cost of 904L which experienced least pitting corrosion during evaluation.

Table 5.1 Commercial viability of the produced alloys as compared to the gain made in the increase of the alloys pitting corrosion resistance.

Control Alloys and Ruthenium				
Alloy/Element	Average alloy Price/ton (USD) (January – December 2012)			
304L	**1935**			
904L	**4967**			
LDX2101	**1029**			
Ruthenium	**3500000**			

Produced Alloys					
Alloy	LDX2101 Required (Ton)	Ru Required (Ton)	Total LDX2101 Cost (USD)	Total Ru Cost (USD)	**Total Alloy Cost (USD)**
LDX2101 +0.66%Ru	0.9934	0.0066	1022	23100	**24122**
LDX2103 + 0.31% Ru	0.9969	0.0031	1026	10850	**11876**
LDX2104 + 0.20% Ru	0.998	0.002	1027	7000	**8027**
LDX2104 + 0.13% Ru	0.9987	0.0013	1028	4550	**5578**

All Alloys				
Alloy	**Price/ton (USD)**	**Pitting Corrosion Potential (mV)**	**Percentage Price Increase due to Ru**	**Percentage Pitting Potential Increase due to Ru***
304L	1935	321	0	0
904L	4967	951	0	0
LDX2101	1029	300	0	0
LDX2101 +0.66%Ru	24122	653	**2244**	**121**
LDX2103 + 0.31% Ru	11876	592	**1054**	**101**
LDX2104 + 0.20% Ru	8027	379	**680**	**27**
LDX2104 + 0.13% Ru	5578	315	**442**	**8**

* Alloy pitting potential / LDX2101 pitting potential

Ideally, for commercially viable alloy, the beneficial effect of alloying LDX2101 stainless steel with ruthenium should offset the cost of adding ruthenium to the LDX2101 stainless steel. However, it is important to note that corrosion is a complex process which is dependent on more than one variable. Hence, there is still a possibility of getting a commercially viable alloy of LDX2101 alloyed with ruthenium in a different reducing media. Further to this, the alloy with 0.66%wt Ru showed a significant improvement for the inhibition of pitting corrosion during all evaluations. Such positive results also suggest a possibility of a better alloy with a little more increase in %wt Ru added to the LDX2101 stainless steel.

5.6 CONCLUSIONS AND RECOMMENDATIONS

The Potentiodynamic polarization test, mostly following ASTM G61-86 procedure, was conducted on control alloys LDX2101, 904L and 304L stainless steels, as well as produced alloys LDX2101+0.13%wt Ru, LDX2101+0.20%wt Ru, LDX2101+0.31%wt Ru and LDX2101+0.66%wt Ru in aerated 3.5% NaCl aqueous solution. Further to these tests, potentiodynamic tests were conducted on LDX2101+0.66%wt Ru in a de-aerated 3.5% NaCl aqueous solution. An XRF Spectrometer was used to verify the chemical composition of produced alloys. Also, the microstructural analysis was conducted on the produced alloys following ASTM932 procedure and the results were compared to the microstructure of LDX2101 stainless steel. Based on the results obtained in this study, the following conclusions could be drawn:

Small additions of ruthenium of up to 0.66%wt Ru to LDX2101 stainless steel will improve the pitting corrosion resistance of the resulting alloy as the pitting potentials of all LDX2101 stainless steel alloys containing ruthenium were shifted to more noble values. Also, if such small additions of ruthenium will not improve the general corrosion of the resulting alloy, it will at least not have any detrimental effect on the resulting alloy as the corrosion potential, corrosion current and corrosion rate of all LDX2101 stainless steel alloys containing ruthenium were equal to or better than that of LDX2101 without ruthenium . The duplex stainless steel microstructure will also be maintained without introducing any detrimental phases as observed through optical microscopy. All LDX2101 containing ruthenium up to 0.66% by weight will have a better pitting corrosion resistance compared to 304L stainless steel but, their pitting corrosion resistance will be inferior compared to 904L stainless steel.

The pitting corrosion resistance of LDX2101 alloys containing ruthenium up to 0.66% by weight will be reduced in chloride containing environment with a depleted oxygen supply. Ruthenium will also lower the current required to maintain the passive state of LDX2101 stainless steel as it was observed that generally, the passive current densities of LDX2101 with up to 66%wt Ru alloys were lower than LDX2101 stainless steel without Ru. In addition to reduced current to maintain the passivity of LDX2101 stainless steel, ruthenium also increased the passive range of LDX2101 stainless steel.

Finally, the resulting alloys from alloying LDX2101 with ruthenium up to 0.66% by weight are not commercially viable as the benefit ruthenium brought did not offset the cost of adding ruthenium to LDX2101stainless steel. Therefore, for economic reasons, should the application demand a duplex stainless steel with a better pitting corrosion resistance than that of LDX2101 stainless steel, it would be recommended to use other duplex stainless steels which will cost less and have better pitting corrosion resistance than LDX2101 stainless steel alloyed with up to 0.66%wt Ru.

The results of this research study on LDX2101 stainless steel alloyed with ruthenium, concurred with the investigations on other duplex stainless steel also alloyed with ruthenium by El-Sayed et al. (2009) and Potgieter et al. (1996) which, also yielded positive results for the inhibition of pitting corrosion as pointed out in the hypothesis.

Following the results of this study, it is recommended that future studies on LDX2101 alloyed with ruthenium should look at the performance of the alloy in other reducing media other than chloride containing media. Also, since the alloy with 0.66%wt Ru showed a significantly higher passive potential range and pitting potential was significantly pushed to more noble values, indicating a significant improvement for the inhibition of pitting corrosion for this alloy in NaCl aqueous solution, it is further recommended that future studies look at alloying LDX2101 stainless steel with relatively higher %wt Ru. Further studies should also adopt better samples production process like using the vacuum furnace and produce larger samples. The samples production process used in these studies where small samples were produced in a button arc furnace resulted in missing of same elements which were contained in feed material, and oxygen contamination.

REFERENCES

Alvarez-Armas, I. 2007. *Duplex Stainless Steels: Brief History and Some Recent Alloys*. Recent Alvarez-Armas, I. 2007. *Duplex Stainless Steels: Brief History and Some Recent Alloys*. Recent Patents on Mechanical Engineering, 2008(1): 51 – 57.

American Society for Metals. 1979. *The metallurgical evolution of stainless steels*. Metals Park, Ohio 44073, USA: American Society for Metals.

Asaduzzaman, M.D., Mustafa, C.M., Islam, M. 2011. *Effects of concentration of sodium chloride solution on the pitting corrosion behavior of AISI-304L austenitic stainless steel*. Chemical Industry & Chemical Engineering Quarterly 17 (4) (2011):477–483.

ASTM Standard A923, 2008, *Standard Test Methods for Detecting Detrimental Inter-metallic Phase in Duplex Austenic/Ferritic Stainless Steels*, ASTM International, West Conshohocken, PA 19428-2959, United States.

ASTM Standard G61, 1986 (1998), *Conducting Cyclic Potentiodynamic Polarisation Measurements for Localised Corrosion Susceptibility of Iron-, Nickel-, or Cobalt-Based Alloys*, ASTM International, West Conshohocken, PA 19428-2959, United States.

ASSDA. 2010. *Pickling and Passivation* [online]. Available at www.assda.asn.au [accessed 16 January 2014]

Baba, H., Kodama, T., Katada, Y. 2002. *Role of nitrogen on the corrosion behavior of austenitic stainless steels*. Corrosion Science, 44 (2002): 2393–2407.

Banas, J., Mazurkiewicz, A. 2000. *The effect of copper on passivity and corrosion behaviour of ferritic and ferritic–austenitic stainless steels.* Materials Science and Engineering , A277 (2000): 183–191.

Barringer, F. 2006. Large oil spill in Alaska went undetected for days. The New York Times [online], March 15. Available at: www.nytimes.com [accessed 26 February 2011].

Berner, M., Liu H., Olsson, C. 2008. *Estimating localised corrosion resistance of low alloy stainless steels: comparison of pitting potentials and critical pitting temperatures measured on lean duplex stainless steel LDX 2101 after sensitization*. Corrosion Engineering, Science and Technology, 43(2): 111 – 116.

British Stainless Steel Association. 2007 -2012. *Selection of 316, 304 and 303 Types of Stainless Steels for Seawater Applications* [Online]. Available at: www.bssa.org.uk [Accessed 19th December 2012]

BP. 2006. *BP to Shutdown Prudhoe Bay Oil Field*. Press release [online]. Available at: http://www.bp.com [Accessed 28 February 2011]

Cox G. L., Roetheli B. E. 1931. *Effect of Oxygen Concentration on Corrosion Rates of Steel and Composition of Corrosion Products Formed in Oxygenated Water.* Industrial & Engineering Chemistry, 23 (9): 1012 – 1016.

Cvijovic´, Z., Radenkovic´, G. 2006. *Microstructure and pitting corrosion resistance of annealed duplex stainless steel*. Corrosion Science, 48 (2006): 3887 – 3906.

Ebrahimi, N., Momeni, M., Moayed, M.H., Davoodi, A. 2010. *Correlation between critical pitting temperature and degree of sensitization on alloy 2205 duplex stainless steel.* Corrosion Science, 53 (2011): 637–644.

Eghbali, F., Moayed, M.H., Davoodi, A., Ebrahimi, N. 2010. *Critical pitting temperature (CPT) assessment of 2205 duplex stainless steel in 0.1 M NaCl at various molybdate concentrations.* Corrosion Science, 53 (2011): 513 – 522.

El-Sayed M., Sherif, E.M., Potgieter, J. H., Comins, J. D., Cornish, L., Olubambi, P. A., Machio, C. N. 2009. *Effects of minor additions of ruthenium on the passivation of duplex stainless-steel corrosion in concentrated hydrochloric acid solutions*. Journal of Applied Electrochemistry, 39(8): 1385 -1392.

Fisher, D.A. 1963. *The epic of steel*. 1st ed. 49 East 33rd Street, New York: Harper & Row Publishers Incorporated.

Fontana, M.G. 1986. *Corrosion engineering*. 3rd ed. United States of America: McGraw-Hill Inc.

Frankenthal, R., Kruger, J. (ed.) 1978. *Passivity of Metals*. Princeton, New Jersey: The Electrochemical Society, Inc.

Fredriksson, W., Edström, K., Olsson C.A. 2010. *XPS analysis of manganese in stainless steel passive films on 1.4432 and the lean duplex 1.4162.* Corrosion Science, 52 (2010): 2505–2510.

Hartt, W. H., Powers, R.G., Leroux, V., Lysogorski, D.K. 2004. *Critical Literature Review of High-Performance Corrosion Reinforcements in Concrete Bridge Applications*. (FHWA- HRT-04-093) [online]. United States. Department of Transport - Federal Highway Administration. Available at: http://www.fhwa.dot.gov [Accessed 12th January 2011].

Higginson, A. 1989. *Passivation of cathodically modified alloys*. British Corrosion Journal, 24(4): 297 – 302.

Ilevbare, G.O., Burstein, G.T. 2001. *The role of alloyed molybdenum in the inhibition of pitting corrosion in stainless steels.* Corrosion Science, 43(2001) 485 – 513.

InvestmentMine. 1990 – 2012. *1 Year Ruthenium Prices and Price Charts* [online]. Available at: http://www.infomine.com/investment/metal-prices/ruthenium/1-year [accessed 19th December 2012]

Jeon, S-H., Kim, S-T., Lee, I-S., Park, J-H., Kim, K-T., Kim, J-S., Park, Y-S. 2011. *Effects of copper addition on the formation of inclusions and the resistance to pitting corrosion of high performance duplex stainless steels.* Corrosion Science, 53 (2011) 1408 – 1416.

Jones, D.A. 1992. *Principles and prevention of corrosion.* 2nd ed. Upper Saddle River, NJ 07458: Prentice-Hall Inc.

Kadry, S. 2008. *Corrosion Analysis of Stainless Steel.* European Journal of Scientific Research, 22 (4): 508 – 516.

Karlberg, G., Wranglen, G. 1971. *On the mechanism of crevice corrosion of stainless Cr steels*. Corrosion Science, 11(7): 499 – 510.

Key to metals. 1999. *Corrosion and Corrosion Properties of Stainless Steels: Part One* [online]. Available at: http://www.keytometals.com [accessed 1st December 2010].

Kovach C.W. 2011. *High-performance stainless steels*. [Online]. Parr Instrument Company. Available at: www.parrinst.com/downloads/Corrosion-Information [Accessed 15th January 2013].

Laycock, N.J., Newman, R.C. 1998. *Temperature dependence of pitting potentials for austenitic stainless steels above their critical pitting temperature*. Corrosion Science, 40 (6) 887–902.

London Metal Exchange. 2003 – 2011. *LME Nickel price graph* [online]. Available at: http://www.lme.com/nickel_graphs.asp [accessed 18th January 2011].

Lothongkum, G., Wongpanya, P., Morito, S., Furuhara, T., Maki, T. 2004. *Effect of nitrogen on corrosion behavior of 28Cr–7Ni duplex and microduplex stainless steels in air-saturated 3.5wt% NaCl solution*. Corrosion Science, 48 (2006) 137–153.

Loubser, M., Verryn, S. 2008. *Reference for preparation of samples and sample analyses: Combining XRF and XRD analyses and sample preparation to solve mineralogical problems*. South African Journal of Geology, 111: 229 – 238.

Lyman, T. (ed.) 1984. *Metals Handbook*. 1984 ed. Cleveland 3, Ohio: The American Society for Metals.

Malik, A.U., Kutty, M., Siddiqi, N.A., Andijani, I. N., Ahmad, S. 1990. *Corrosion studies on SS 316 l in low pH high chloride product water medium* [online]. Available at: www.swcc.gov.sa [accessed 10th January 2013].

Mathiesen, T., Nielsen, T. S., Frantsen, J. E. 2006. *Influence of Various Surface Conditions on Pitting Corrosion Resistance of Stainless Steel Tubes Type EN 1.4404.* NACE Corrosion (06095).

Matter-University of Liverpool. 2000. *Steel making: Removal of impurities* [online]. Available at: http://www.matter.org.uk [accessed 5th January 2011].

McEwan, J.J. (ed.) 2004. Corrosion Control in Southern Africa. 2nd ed. Johannesburg, South Africa: Corrosion Institute of Southern Africa.

McGannon, H.E. (ed.) 1971. *The Making, Shaping and Treating of Steel*. 9th ed. Pittsburg, Pennsylvania, USA: Herbick & Held.

Mcgill, I.R. 1990. Platinum Metals in Stainless Steels: *A Review of Corrosion and Mechanical Properties.* Platinum Metals Review, 34(2): *85-97.*

Mcgill, I.R. 1990. Platinum Metals in Stainless Steels: *A Review of Corrosion and Mechanical Properties Part II*. Platinum Metals Review, 34(3): 144 – 154.

Metrohm Autolab B.V. 2011. *Autolab Application Note COR02:Corrosion Part 2-Measurement of corrosion rates.*[online]. Metrohm Autolab B.V. Available at: www.ecochemie.nl/Applications/ [Accessed 5th December 2011].

Monypenny, J.H. 1951. *Stainless Iron and Steel volume 1, Stainless steels in Industry*. 37 Esses Street, London: Chapman & Hall Ltd.

Mudali, U.K., Shankar, P., Ningshen, S., Dayal, R.K., Khatak, H.S., Raj, B. 2002. *On the pitting corrosion resistance of nitrogen alloyed cold worked austenitic stainless steels*. Corrosion Science, 44 (2002) 2183–2198.

Naoto TAKENO. 2005. *Intercomparison of thermodynamic databases.* (419) [online]. Japan. Geological Survey of Japan. Available at: typhoon.jaea.go.jp [Accessed 5th December 2011].

Outokumpu. 2004. *LDX2101- Duplex Stainless Steel* [online]. Available at: http://www.outokumpu.de/29143.epibrw [accessed 10 May 2011].

Outokumpu. 2008. *A brief history of stainless steel* [online]. Available at: http://www.outokumpu.com [accessed 7 April 2010].

Outokumpu Stainless Steel Oy. 2004. *Outokumpu stainless corrosion handbook*. 9th ed. Finland: Outokumpu Stainless Steel Oy.

Outokumpu Oyj. 2009. *Outokumpu corrosion handbook*. 10th ed. Finland: Outokumpu Oyj.

Outokumpu. 2012. *Pricing/AAF* [online]. Available at: http://www.outokumpu.com/en/Products/Pricing-aaf/Pages/Pricing-AAF.aspx [accessed 20th December 2012]

Parkins, R. (ed.), 1981. *Corrosion Processes*. Ripple Road, Barking, Essex, England: Applied Science Publishers LTD.

Pardo, A., Merino, M.C., Coy, A.E., Viejo, F., Arrabal, R., Matykina, A.E. 2008. Effect of Mo and Mn additions on the corrosion behavior of AISI 304 and 316 stainless steels in H2SO4. *Corrosion Science* [online], 50(2008): 780 – 794. Available at: http://www.sciencedirect.com/science [accessed 5th January 2011].

Pardo, A., Merino, M.C., Coy, A.E., Viejo, F., Arrabal, R., Matykina, A.E. 2008. *Pitting corrosion behaviour of austenitic stainless steels – combining effects of Mn and Mo additions*. Corrosion Science, 50(2008): 1796 – 1806.

Peckner, D., Bernstein, I.M. 1977. *Handbook of Stainless Steels*. New York: McGraw-Hill Book Company.

Peguet, L., Malki, B., Baroux, B. 2006. *Influence of cold working on the pitting corrosion resistance of stainless steels*. Corrosion Science, 49(2007): 1933 – 1948.

Potgieter, J.H. 1991. *Alloys cathodically modified with noble metals*. Journal of Applied Electrochemistry, 21(6): 471 – 482.

Potgieter, J. H., Barnard, W. O., Myburg, G., Varga, K., Baradlai, P., Tomcsanyi, L. 1996. *Corrosion behaviour of duplex stainless steels containing minor ruthenium additions in reducing acid media*. Journal of Applied Electrochemistry, 26(11): 1103 -1110.

Potgieter J. H., Heyns A.M., Skinner W. 1990. *Cathodic modification as a means of improving the corrosion resistance of alloys*. Journal of Applied Electrochemistry, 20: 711 - 715.

Potgieter, J.H., Olubambi, P.A., Cornish, L., Machio, C.N., Sherif, E.M. 2008. *Influence of nickel additions on the corrosion behaviour of low nitrogen 22% Cr series duplex stainless steels*. Corrosion Science, 50(2008): 2572–2579.

Qvarfort, R. 1998. *Some Observations Regarding the Influence of Molybdenum on the Pitting Corrosion Resistance of Stainless Steels*. Corrosion Science, 40(2/3): 215 – 223.

Rollason, E. 1973. *Metallurgy fro engineers*. 4th ed. London: Edward Arnold Publishers.

Scully, J. 1990. *The Fundamentals of Corrosion*. 3rd ed. Headington Hill Hall, Oxford OX3 OBW, England: Pergamon Press plc.

Schmuki, P., Hildebrand H., Friedrich A., Virtanen S. 2004. *The composition of the boundary region of MnS inclusions in stainless steel and its relevance in triggering pitting corrosion*. Corrosion Science, 47(2005): 1239 – 1250.

Schweitzer, P. 2010. Fundamentals of corrosion: mechanism, causes and prevention method. Florida, USA: CRC Press.

Sedriks, A. 1979. *Corrosion of stainless steel*. New York: John Wiley & Sons.

Sheir, L.L. (ed.) 1976. *Corrosion volume 1, metal/environment reactions*. 2nd ed. London: Newnes-Butterworths.

Sherif, E. M., Erasmus, R.M., Comins, J.D. 2010. *In situ Raman spectroscopy and electrochemical techniques for studying corrosion and corrosion inhibition of iron in sodium chloride solutions*. Electrochimica Acta, 55 (2010): 3657–3663.

Sherif, E. M., Potgieter, J. H., Comins, J. D., Cornish, L., Olubambi, P. A., Machio, C. N. 2009. *The beneficial effect of ruthenium additions on the passivation of duplex stainless steel corrosion in sodium chloride solutions*. Corrosion Science, 51 (2009): 1364–1371.

Souzaa, E.C., Rossitti, S.M., Rolloa, J.M. 2009. *Influence of chloride ion concentration and temperature on the electrochemical properties of passive films formed on a superduplex stainless steel.* Materials Characterization, 61 (2010): 240 – 244.

Streicher, M.A. 1977. *Alloying stainless steels with the platinum metals: Increased resistance to corrosion in acids*. Platinum Metal Rev, 21(2): 51 – 55.

Szklarska-Smialowska, Z. 1986. *Pitting Corrosion of Metals*. Houston, Texas 77084: National Association of Corrosion Engineers.

Szummer, A., Janik-Czachor, M., 1993. *Corrosion behaviour of low-manganese Stainless steels*. Corrosion Science, 25(1-4): 317 – 327.

Torres, F., Panyayong, W., Rogers, W., Velasquez-Plata, D., Oshida, Y., Moore, B. 1998. *Corrosion behavior of sensitized duplex stainless steel*. Corrosion Science, 52(3): 950 – 959.

Trepanier C., Pelton A.R. 2006. *Effect of temperature and pH on the corrosion corrosion resistance of nitinol and stainless steel*. Proceddings of SMST-2004: 361-366.

Uhlig, H. 1971. *Corrosion and Corrosion Control: an introduction to corrosion science and engineering*. 2nd ed. New York: John Wiley & Sons Inc.

Ujiro, T., Satoh, S., Staehle, R.W., Smyrl, W.H. 2000. *Effect of alloying Cu on the corrosion resistance of stainless steels in chloride media*. Corrosion Science, 43 (2001) 2185–2200.

Vasilenko, G. V. 2007. *The Effect of Oxygen Concentration on the Corrosion of Heat Supply Networks and Heat Exchangers*. Thermal Engineering 2(54): 156 – 158.

Wolff, I.M. 1999. *New applications for ruthenium: Platinum in South Africa*. South African Journal of Science, 95 (11/12): 539 – 542.

Wrisley, K.L., Duquette, D.J., Steiner, D., Motyka, E.F., Coomer, E.D. 1990. *Corrosion studies of a stainless steel structure for the ITER aqueous lithium salt blanket concept.* Fusion Engineering and Design, 13 (1990): 45 – 52.

Yang, L. (ed.) 2008. *Techniques for corrosion monitoring*. Boca Raton, FL 33487: CRC Press LLC.

Zatkalikova, V., Liptakova, T. 2011. *Pitting Corrosion of Stainless Steel at the Various Surface Treatment.* Materials Engineering - Materiálové inžinierstvo, 18 (2011): 115 – 120.

Zhang, L., Jiang, Y., Deng, B., Zhang, W., Xu, J., Li, J. 2009. *Effect of aging on the corrosion resistance of 2101 lean duplex stainless steel*. Materials Characterization, 60 (2009): 1522–1528.

APPENDICES

APPENDIX A: POTENTIODYNAMIC POLARISATION CURVES

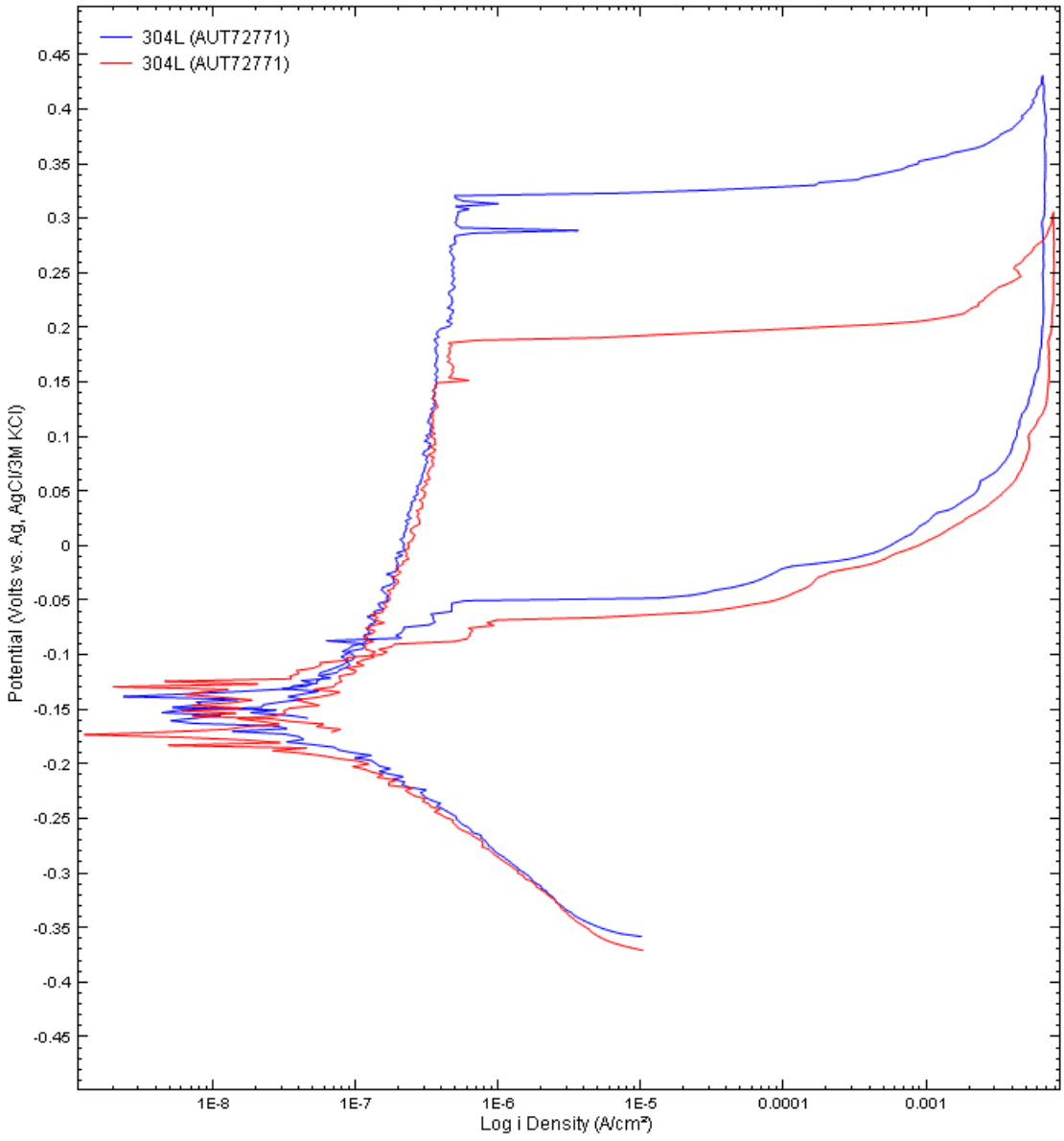

Figure A.1 Comparison of potentiodynamic polarisation curve of two 304L stainless steel samples in 3.5% NaCl aerated solution at 25°C ±1°C

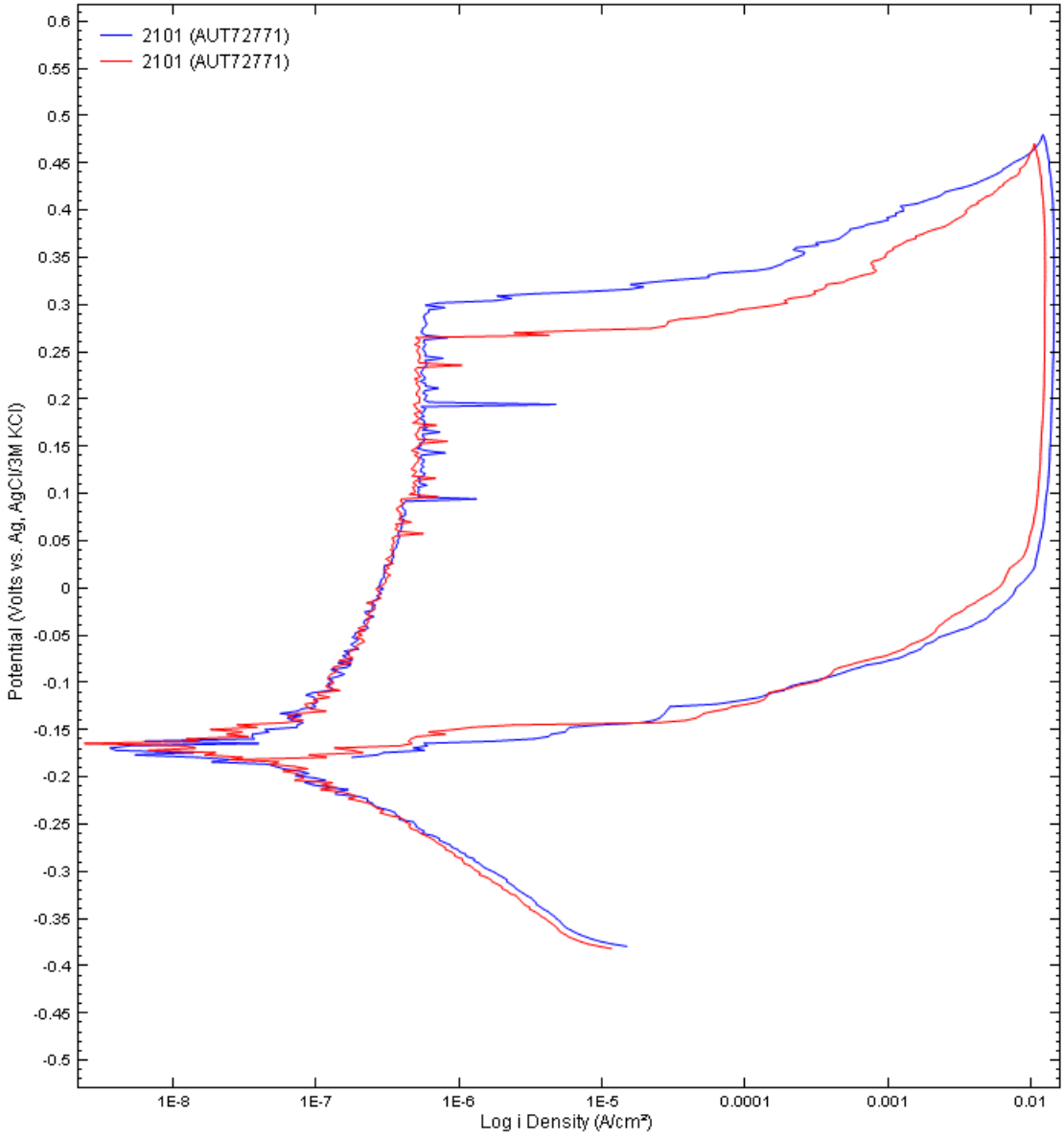

Figure A.2 Comparison of potentiodynamic polarisation curve of two 2101LDX stainless steel samples in 3.5% NaCl aerated solution at 25°C ±1°C

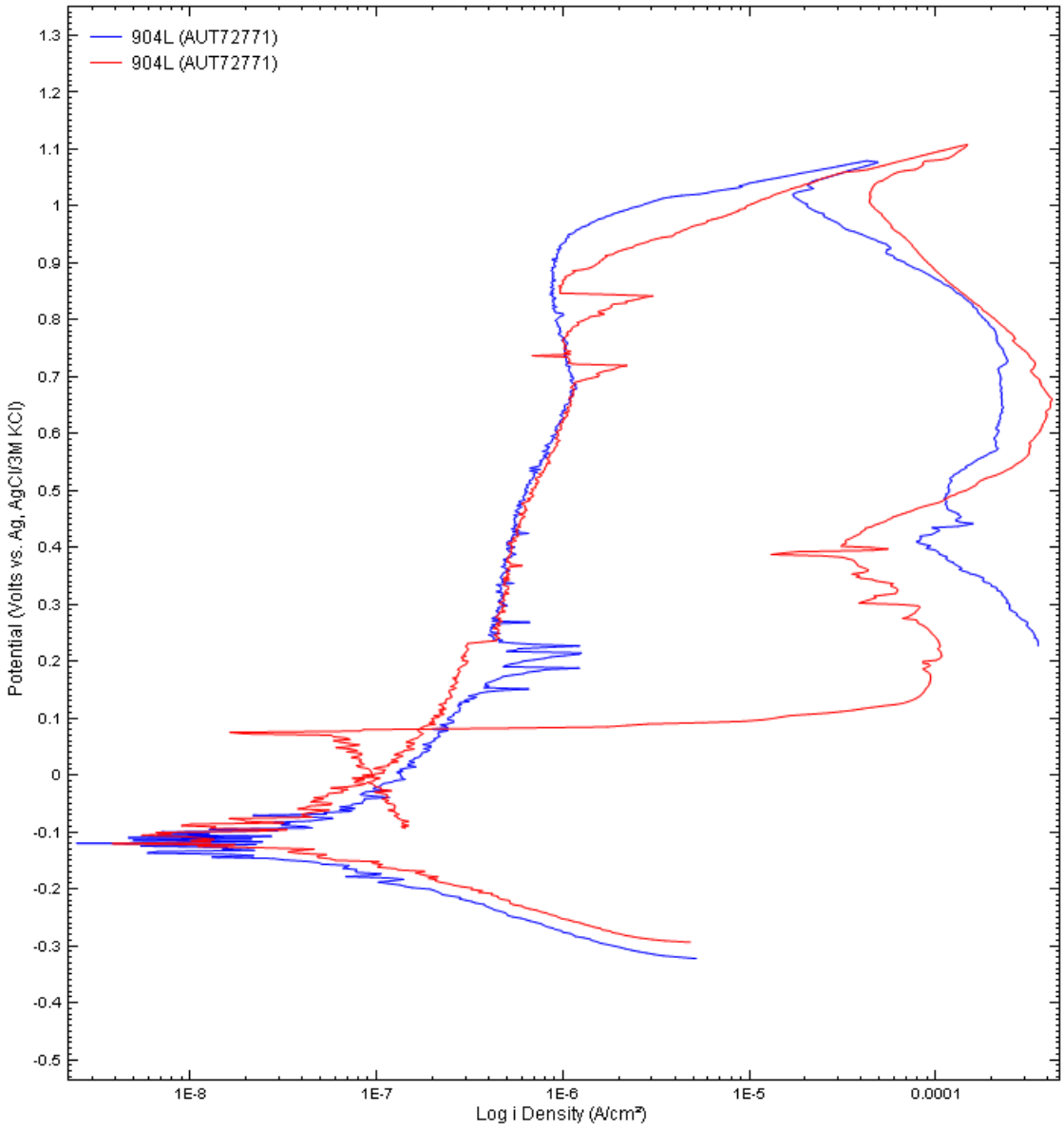

Figure A.3 Comparison of potentiodynamic polarisation curves of two high alloyed austenitic stainless steel 904L samples in 3.5% NaCl aerated solution at 25°C ±1°C

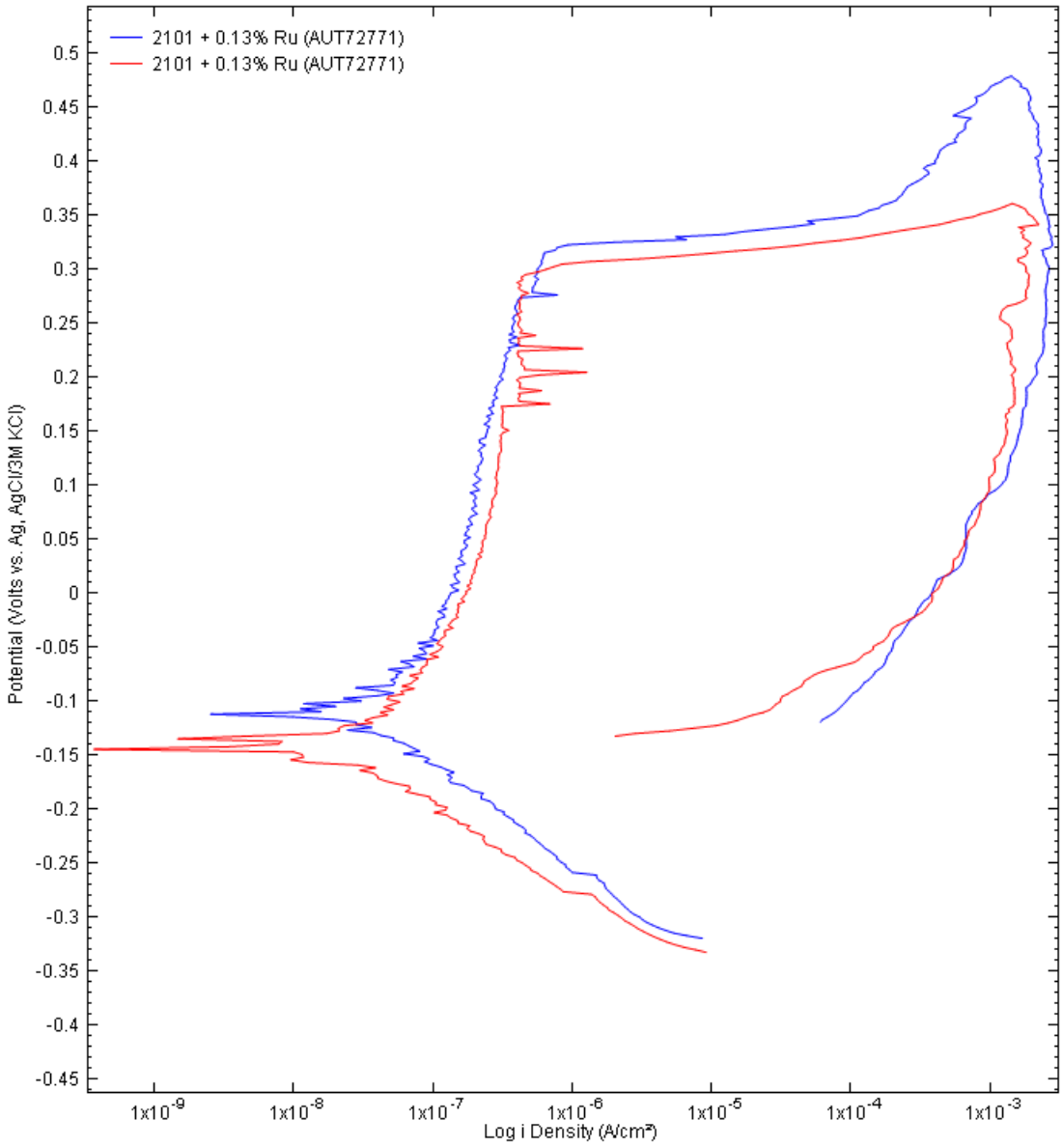

Figure A.4 Comparison of potentiodynamic polarisation curves of two 2101LDX stainless steel samples with 0.13% Ruthenium in 3.5% NaCl aerated solution at 25°C ±1°C

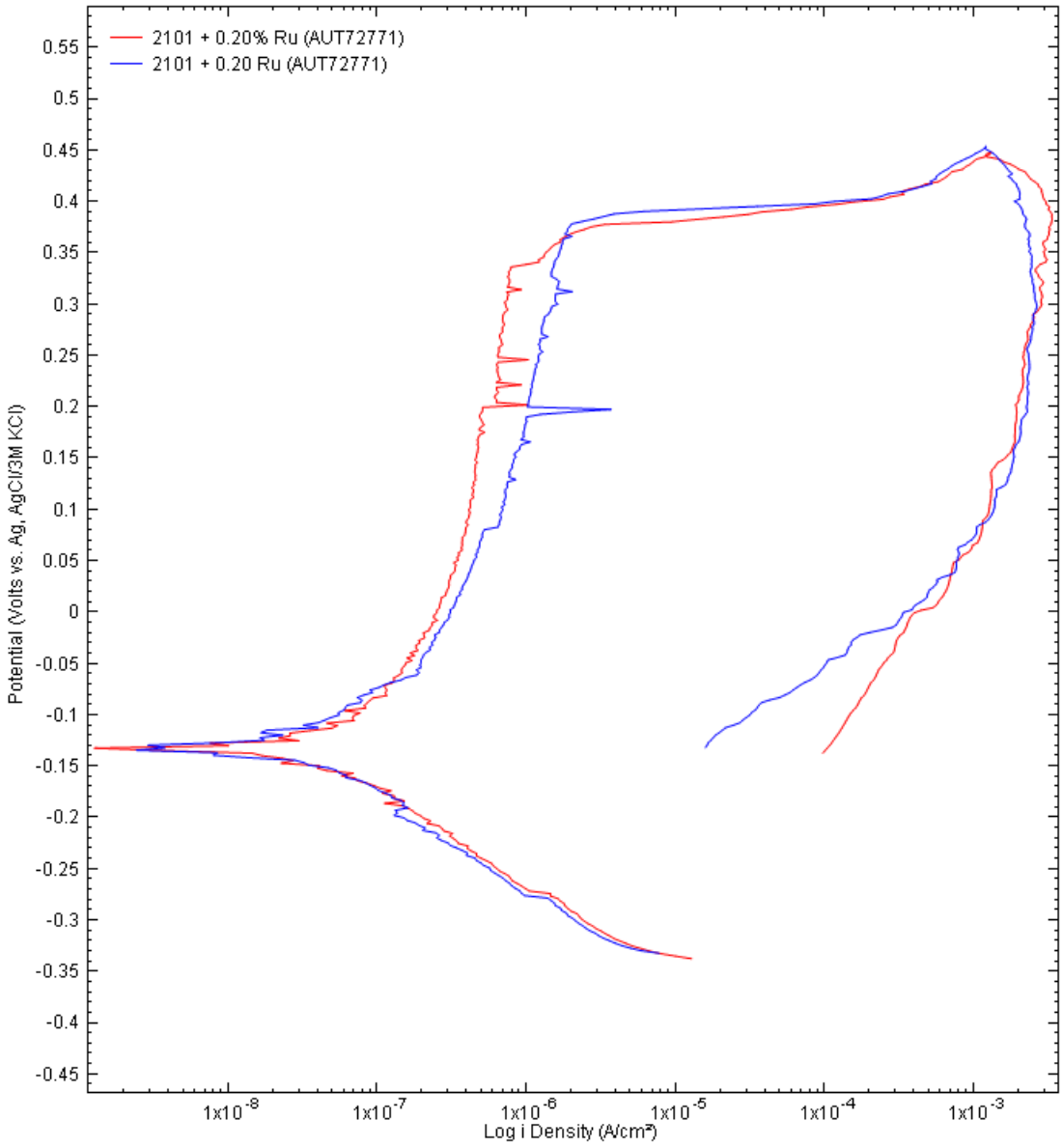

Figure A.5 Comparison of potentiodynamic polarisation curves of two 2101LDX stainless steel samples with 0.20% Ruthenium in 3.5% NaCl aerated solution at 25°C ±1°C

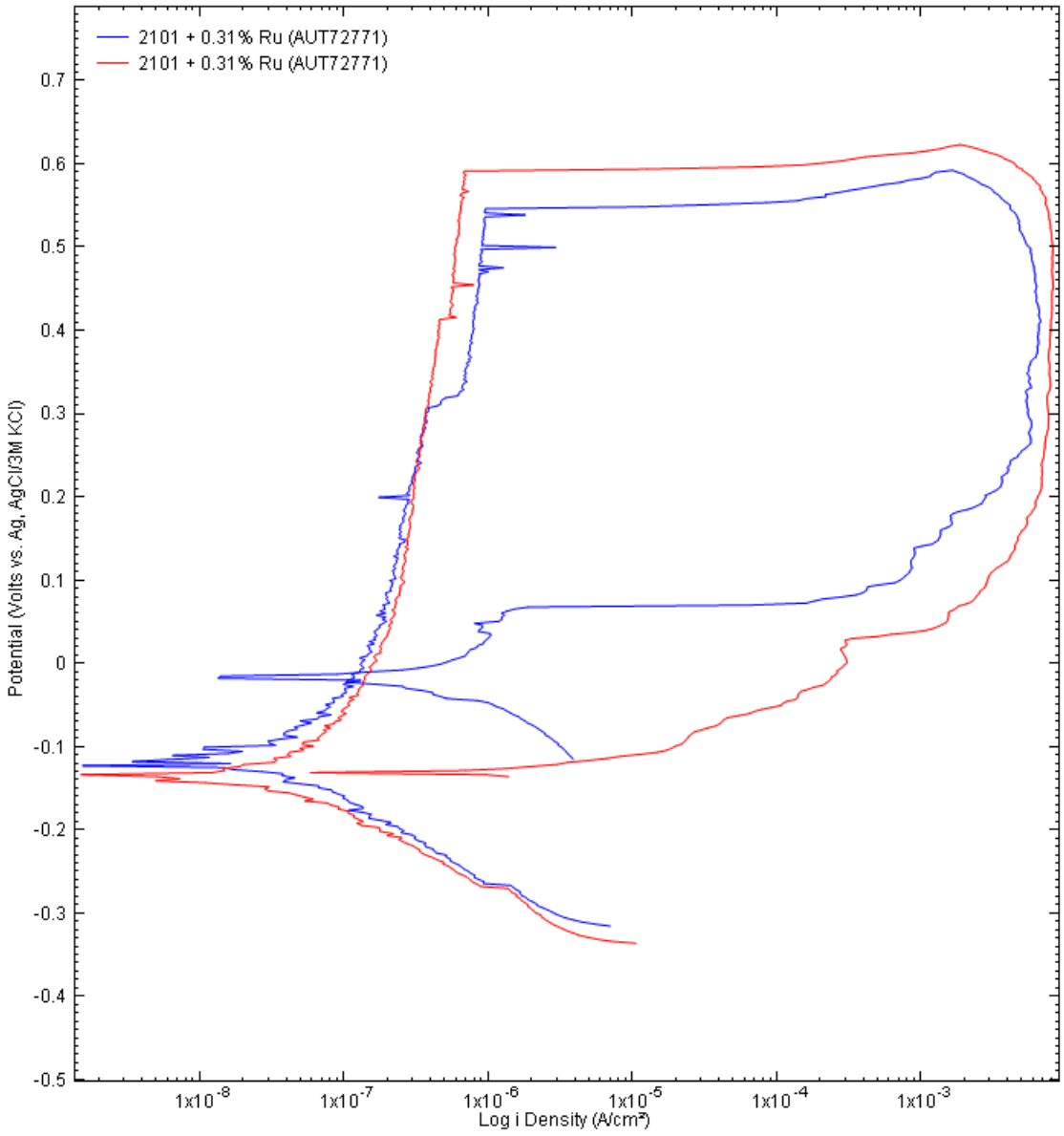

Figure A.6 Comparison of potentiodynamic polarisation curves of two 2101LDX stainless steel samples with 0.31% Ruthenium in 3.5% NaCl aerated solution at 25°C ±1°C

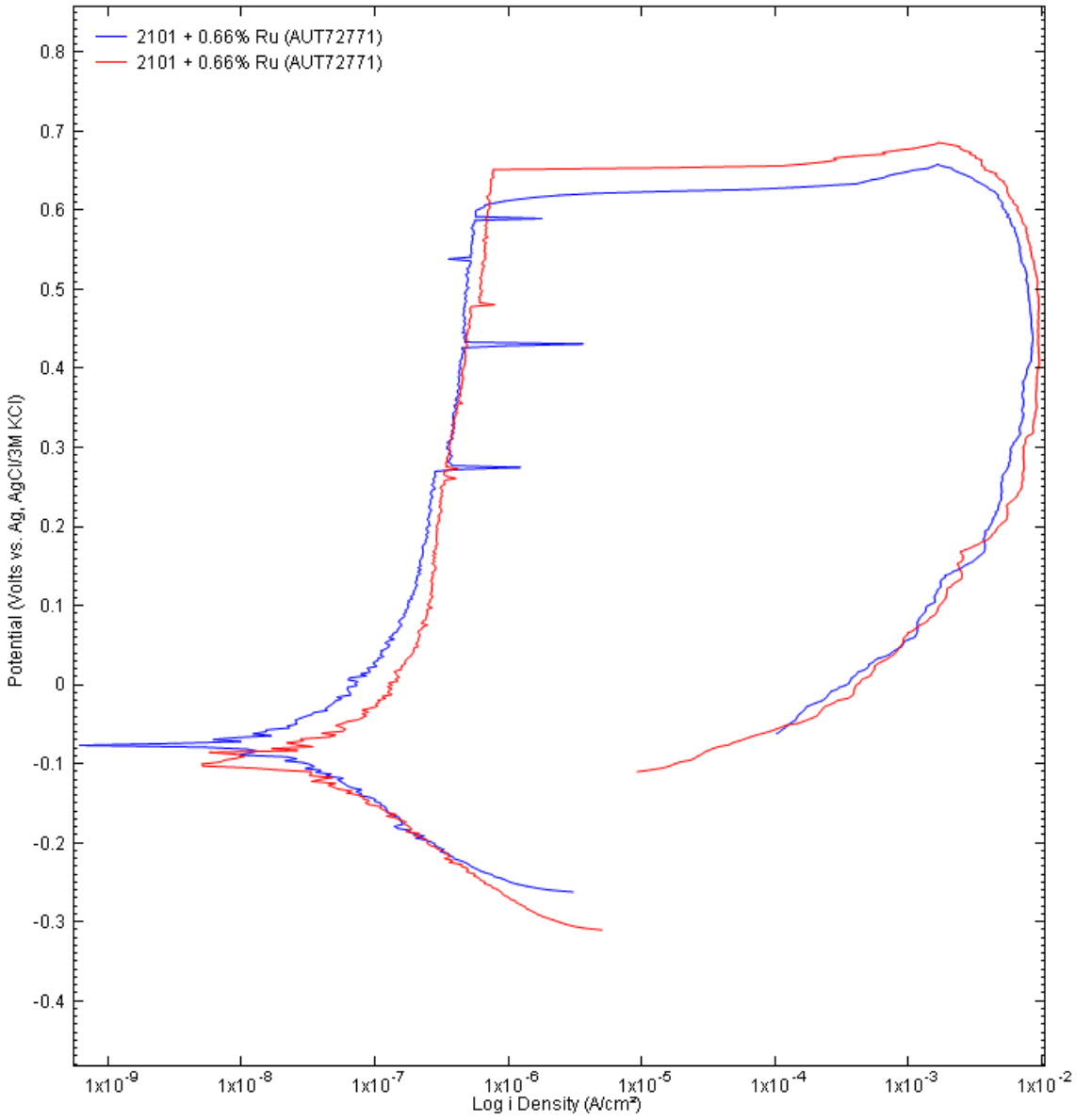

Figure A.7 Comparison of potentiodynamic polarisation curves of two 2101LDX stainless steel samples with 0.66% Ruthenium in 3.5% NaCl aerated solution at 25°C ±1°C

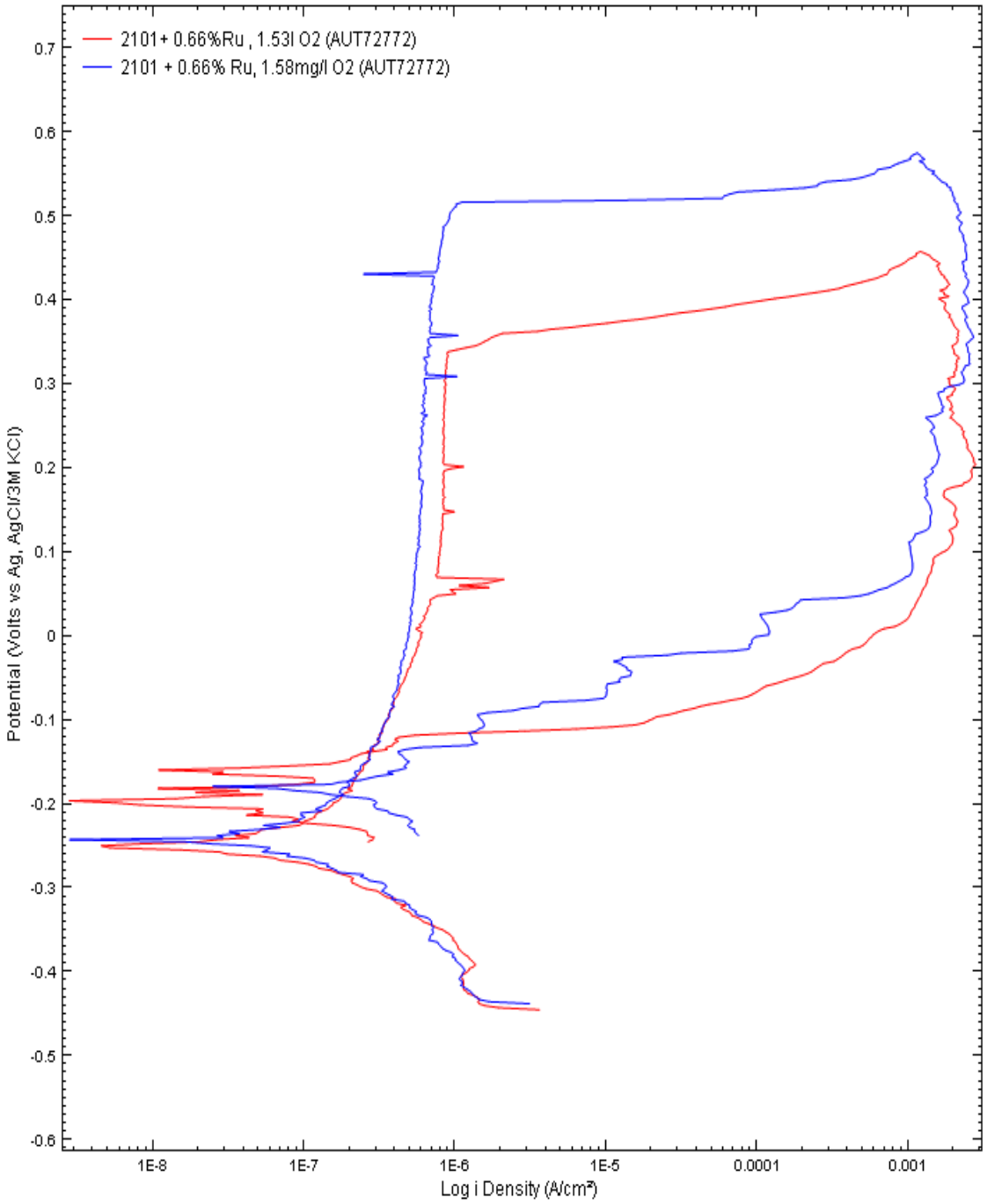

Figure A.8 Comparison of potentiodynamic polarisation curves of two 2101LDX stainless steel samples with 0.66% Ruthenium in 3.5% NaCl de-aerated solution at 25°C ±1°C

APPENDIX B: 2012 PRICES FOR CONTROL ALLOYS AND RUTHENIUM

Table B.1 Summary of 2012 AAF Prices for 304L, 904L and LDX2101 (OUTOKUMP 2012)

Alloy Adjustment Factor USD/Ton													
Alloy	Jan-12	Feb-12	Mar-12	Apr-12	May-12	Jun-12	Jul-12	Aug-12	Sep-12	Oct-12	Nov-12	Dec-12	Average Price
304L	1922	2091	2238	2090	2002	1974	1894	1828	1751	1826	1892	1714	1935
904L	4980	5364	5832	5517	5167	5055	4832	4695	4364	4682	4807	4306	4967
LDX2101	1019	1067	1058	1040	1097	1129	1086	1029	997	997	934	900	1029

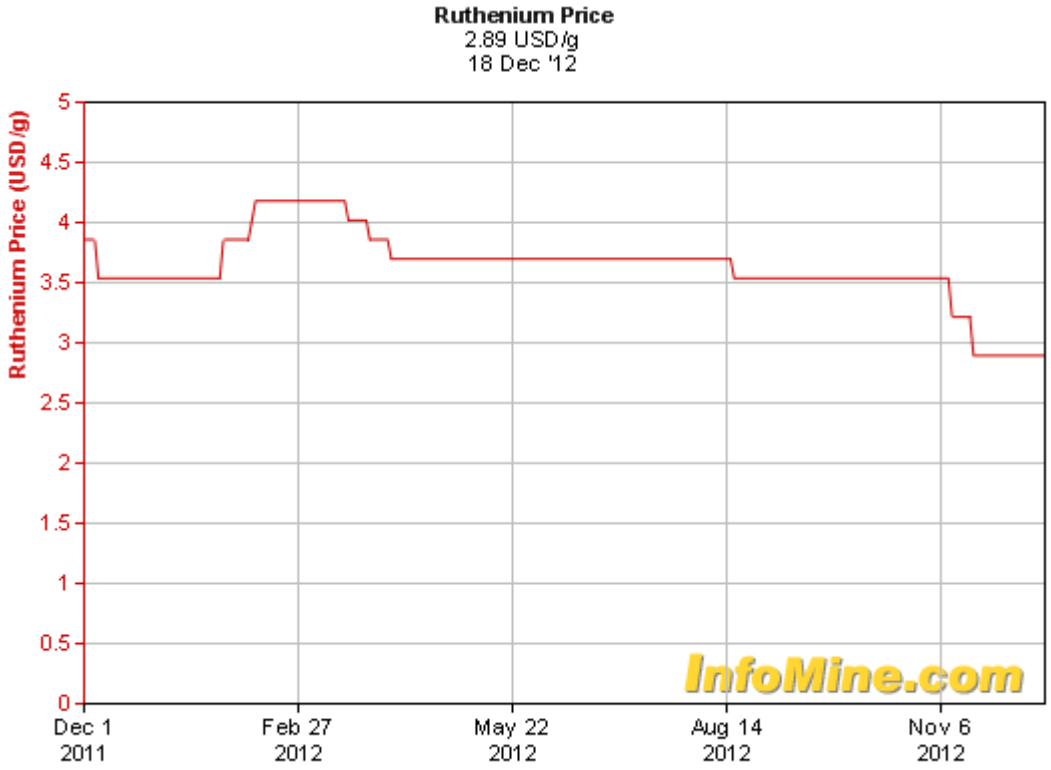

Figure B.1 1 Year Ruthenium Prices and Price Charts (InvestmentMine 1990 – 2012)